ESAIM: M2AN 55 (2021) 2365–2419
https://doi.org/10.1051/m2an/2021055

ESAIM: Mathematical Modelling and Numerical Analysis
www.esaim-m2an.org

EXISTENCE OF SOLUTIONS AND CONTINUOUS AND SEMI-DISCRETE STABILITY ESTIMATES FOR 3D/0D COUPLED SYSTEMS MODELLING AIRFLOWS AND BLOOD FLOWS

Céline Grandmont[1,2,3] and Sébastien Martin[4,*]

Abstract. In this paper we analyse geometric multiscale models arising in the description of physiological flows such as blood flow in arteries or air flow in the bronchial tree. The geometrical complexity of the networks in which air/blood flows lead to a classical decomposition in two areas: a truncated 3D geometry corresponding to the largest contribution of the domain, and a 0D part connected to the 3D part, modelling air/blood flows in smaller airways/vessels. The fluid in the 3D part is described by the Stokes or the Navier–Stokes system which is coupled to 0D models or *so-called* Windkessel models. The resulting Navier–Stokes–Windkessel coupled system involves Neumann non-local boundary conditions that depends on the considered applications. We first show that the different types of Windkessel models share a similar formalism. Next we derive existence results and stability estimates for the continuous coupled Stokes–Windkessel or Navier–Stokes–Windkessel problem as well as stability estimates for the semi-discretized systems with either implicit or explicit treatment of the boundary conditions. In all the calculations, we pay a special attention to the dependency of the various constants and smallness conditions on the data with respect to the physical and numerical parameters. In particular we exhibit different kinds of behavior depending on the considered 0D model. Moreover even if no energy estimates can be derived in energy norms for the Navier–Stokes–Windkessel system, leading to possible and observed numerical instabilities for large applied pressures, we show that stability estimates for both the continuous and semi-discrete problems, can be obtained in appropriate norms for small enough data by introducing a new well chosen Stokes-like operator. These sufficient stability conditions on the data may give a hint on the order of magnitude of the data enabling stable computations without stabilization method for the problem. Numerical simulations illustrate some of the theoretical results.

Mathematics Subject Classification. 76Z05, 76D07, 65M60, 74H15.

Received January 8, 2021. Accepted September 1, 2021.

1. Introduction

In the present work, we focus on the analysis and numerical analysis of geometric multiscale models used either for simulating physiological flows such as airflows in the respiratory tract, see *e.g.* [2, 24, 32, 35, 40, 43, 52]

Keywords and phrases. Stokes, Navier–Stokes, Windkessel models, implicit/explicit schemes, energy estimates, stability analysis, airflows, blood flows.

[1] Sorbonne Université, CNRS, UMR 7598, Laboratoire Jacques-Louis Lions, 4 place Jussieu, 75252 Paris cedex 05, France.

[2] Inria, 2 rue Simone Iff, 75012 Paris, France.

[3] ULB, Faculté des Sciences, Campus de la Plaine - CP 213, Boulevard du Triomphe, 1050 Bruxelles, Belgium.

[4] Université de Paris, MAP5 (CNRS UMR 8145) & FP2M (CNRS FR 2036), 45 rue des Saints-Pères, 75270 Paris Cedex, France.
*Corresponding author: sebastien.martin@parisdescartes.fr

or blood flows in the arterial network, see *e.g.* [17, 19, 28, 44, 45, 51]. We aim, in particular, at giving a general theoretical framework to the models and to numerical observations with respect to numerical stability.

Simulations in patient-specific geometries may provide valuable informations to physicians to improve diagnosis, pulmonary drug delivery [34] or blood surgery [16]. Nevertheless, direct simulations of 3D flows in geometries such as the tracheo-bronchial tree or the arterial network are limited by the following constraints: since the whole respiratory tree and the blood network are very complex, with a lot of bifurcations, and with different scales therein, numerical costs related to a full 3D simulation in the whole domain are prohibitive. Not to mention that the image processing of the complete bronchial tree or blood network is out of reach for the time being. Therefore the whole domain is usually truncated, restricting the computational domain to a smaller part which is considered to be the most significant one in terms of flow description at the global scale: the large bronchi for airflows or the aorta region for blood flows. As a countereffect, the removed part has to be taken into account thanks to suitable reduced models in order to describe the global behaviour of the whole system.

Air and blood are commonly modelled as homogeneous, viscous, Newtonian and incompressible fluids. Thus we consider a system of partial differential equations involving the Navier–Stokes equations, which has to be coupled to reduced models to take into account phenomena in the removed part of the domain. In this work, we focus on *so-called* 0D or Windkessel models that describe how the fluid flux and average pressure on the artificial boundaries is related to the mechanical properties of the truncated part. Note that 1D models (see for instance [18, 20]) can also be considered to describe the reduced part. Here, the existence of solutions and numerical stability of 3D/0D coupled systems is investigated, with special attention brought to applications related to, both, airflows and blood flows modelling, which involve different kinds of 0D models sharing nevertheless a similar formalism. The whole resulting system involves Navier–Stokes equations with nonlocal Neumann-type boundary conditions which depend on the chosen 0D model.

Many authors investigated the difficulties related to this kind of problems. From the theoretical point of view and the numerical point of view, one difficulty comes from the lack of energy estimate when considering the Navier–Stokes system with Neumann boundary conditions and more generally mixed Dirichlet–Neumann boundary conditions. Nevertheless existence of strong solutions (global in time for small data or local in time) has been shown in [31] under the assumption that the out/inlets meet the lateral boundary with a right angle and requiring some strong regularity estimates for the solution of the Stokes problem with mixed boundary conditions (note nevertheless that these regularity results are not satisfied in this case). Additionally, when coupling the Navier–Stokes system with 0D reduced models, we refer to [47] and [2, 26] for the same type of wellposedness results of strong solutions. In particular, in [47], the existence result based on a fixed point strategy, is obtained for the Navier–Stokes system with Robin-type conditions under a smallness assumption on the Robin coefficient modeling the resistive part of the 0D model and under the same regularity assumption required in [31]. In [2] the Navier–Stokes system coupled to the resistive 0D model is considered; the regularity assumption that was previously used in [31] and [47] is dropped as well as the assumption on the resistance of the 0D model needed in [47]. The proof relies on the lower regularity results for the solution of the Stokes system in polygonal domains with mixed boundary conditions, that have been derived in [42] and on the introduction of a well chosen Stokes-like operator, similar but simpler than the one we will introduce in this paper, that takes into account the 0D model. Note that all these results are valid for small data or in small time. Note moreover that concerning 3D/0D models (see [26]) and 3D/1D models (see [7, 18, 20, 46]), coupling conditions based on the total pressure enables to have global energy estimates, allowing to prove global existence of weak solutions as in [26]. From the numerical point of view, the lack of energy estimates for the Navier–Stokes system with Neumann boundary conditions or coupled with 0D model is linked to numerical instabilities as soon as, for a given physical setting, the applied pressure drop reach a threshold. To overcome this difficulty many strategies have been proposed. For general flows, we refer to the early work of [11] that introduces a whole set of boundary conditions that have been further extended and analysed in [12] where existence of weak solutions is proven. For hemodynamic flows, stabilization methods – some of them similar as the one proposed in [12] – have been introduced [1, 3, 4, 28]. These stabilization techniques lead to the modification of the resolved physical system.

We also refer to [21, 31, 40], for reviews on these questions and to [5] where benchmark tests are performed for various stabilization methods.

Concerning the coupling of the Navier–Stokes equations with 0D models (or other reduced models such as 1D models), many strategies have been considered for the theoretical analysis of such problems as for their numerical implementation. For instance, as already stated, the existence result proved in [47] is based on a fixed point theorem, whereas in [2] a global formulation of the coupled system is considered. Moreover, for the modelling of physiological flows, many coupling strategies have been already implemented: the explicit treatment has been used for instance in hemodynamics in [45, 51] or for airflows in [13] for 3D/1D coupling; the implicit coupling with Neumann boundary conditions involving the full traction, achieved thanks to an iterative process has been proposed in [28]. Still in the context of hemodynamics the implicit coupling and the implicit treatment of the convective part of the fluid equations have been achieved by a Newton algorithm [17, 33]; however, in each Newton sub-time-step, the coupling is explicit. The same strategy is used in [43] for mechanical ventilation in a rat bronchial tree. In [37] an iterative procedure is proposed for 3D/0D hydraulic networks. Moreover we refer for instance to [2] in the context of airflow modelling or [6] in the context of blood flows modelling where implicit monolithic coupling schemes are considered. The efficiency of the numerical methods associated to these problems relies on the analysis of two types of numerical difficulties: on the one hand, the explicit/implicit treatment of the nonlocal boundary conditions which couple the 3D and 0D models, which may lead to numerical instabilities and thus possible restrictions on the time-step, even with an implicit treatment of the coupling (when achieved by an iterative procedure). On the other hand, the more intrinsic difficulties coming from the convective term in the Navier–Stokes system which, as already stated, induces a lack of energy estimates and subsequent observed numerical instabilities. When considering full fluid-structure interaction heterogeneous 3D/1D coupled models, the question of the spurious numerical reflexions at the interface is a crucial one and is investigated in [38], for instance, in which an iterative implicit coupling scheme is proposed.

Thus this paper is concerned with the analysis and numerical analysis of the coupled 3D/0D models arising in blood flows in large arteries as well as airflows in the bronchial tree. Here we derive energy or stability estimates for continuous and semi-discrete Stokes or Navier–Stokes system coupled to typical Windkessel models for explicit and implicit couplings, with a special emphasis to the dependance with respect to the physical parameters. These estimates enable to justify the existence of solutions and in the discrete case, the aim is to quantify, depending on the application field, the stability restrictions on the time step or on the data that are sufficient to ensure stability estimates. Note that this paper improves and generalizes partial results that can be found in [22, 23]. The outline of this article is as follows: in Section 2 we introduce the coupled fluid-Windkessel models under study. We choose standard 0D models used in blood flow or airflow and we embed them in a similar formalism. We also present the semi-discretized in time schemes considered for the coupled fluid-Windkessel models, whose stability analysis will be performed in the next sections. Next, in Section 3, we derive energy or stability estimates for the continuous or semi-discretized in time Stokes–Windkessel coupled system. Implicit and explicit treatments of the boundary conditions are considered. We exhibit different type of results depending on the considered 0D model. Note that the derived estimates leads to the existence of weak solutions. Finally in Section 4 we study the Navier–Stokes–Windkessel coupled system. We prove stability estimates both in the continuous case and two semi-discrete cases with either explicit or implicit coupling. Since no energy estimate can be derived, we prove estimates in stronger norms linked to the domain of a new well-chosen Stokes-like operator adapted to the coupled system. Once again the derived estimates enable to prove existence of strong solutions locally in time or for small enough data and we exhibit different types of behavior depending on the considered 0D model as well as on the coupling strategy. The final section is devoted to some numerical illustrations of the physical and stability behavior of the considered model and schemes. In particular we emphasize the difference between the different 0D models, exhibit restrictions on the time step when considering an explicit strategy or on the applied data when considering the Navier–Stokes system.

2. Reduced models in airflows and blood flows

2.1. Models

In this section, we describe different types of models associated to physiological flows, such as air through the bronchial tree or blood in the arterial network. The bronchial tree and the blood network have a complex structure which can be described as an assembly of tubes in which the biological fluid (air or blood) flows. For instance, the human respiratory tract is a dyadic tree of about 23 generations. The first generation (the trachea) has a length of about 10 cm, while the last one is about 1 mm. Until the 15th generation, the flow is convective whereas it is mainly diffusive in the acinar region. Moreover, the medical imaging and image processing techniques allow to obtain a good segmented surface and an associated mesh only up to the 6th or 7th generation. In the same way, the arterial network can be described as tube network.

In this context the complexity of the geometries makes it difficult to address direct simulations over the whole domain which then have to be truncated. Nevertheless, the removed parts corresponding to the smaller scales have to be taken into account in the global modelling: this can be done by defining appropriate reduced models. After truncation of the whole domain, we get a domain $\Omega \subset \mathbb{R}^3$ involving artificial boundaries which are denoted Γ_i, with $i \in \{0, \cdots, \mathcal{N}\}$, $\mathcal{N}+1$ being the number of in/outlets. The lateral walls of the respiratory tree or of the aorta are denoted Γ_ℓ. In these 3D domains, we assume that the velocity $\mathbf{u}$ and the pressure p of the fluid satisfy the following incompressible Stokes or Navier–Stokes system (corresponding respectively to $\varepsilon = 0$ and $\varepsilon = 1$):

$$\begin{cases} \rho(\partial_t \mathbf{u} + \varepsilon(\mathbf{u}\cdot\nabla)\mathbf{u}) - \mu\Delta\mathbf{u} + \nabla p = 0 & \text{in } \Omega, \\ \operatorname{div}(\mathbf{u}) = 0 & \text{in } \Omega, \\ \mathbf{u} = 0 & \text{on } \Gamma_\ell, \\ \mathbf{u}(0,\cdot) = \mathbf{u}_0 & \text{in } \Omega, \end{cases}$$

with $\mathbf{u}_0$ the initial velocity, $\mathbf{n}$ the outward unit vector on every part of the boundary $\partial\Omega$ and ρ and μ the density and the viscosity of the fluid respectively. In order to model the whole system, *i.e.* the whole respiratory tree or the whole blood network, taking into account the fluid flow in the removed part, the 3D model has to be completed with a well-chosen reduced model. For instance, the removed part can be condensed into a 0D model (0D in the sense that it does not depend on a space variable) coupled to the 3D model at each outlet Γ_i. Here we choose to consider some classical 0D models (also referred to as Windkessel models), used in blood or air flow modelling, but sharing the same formalism. We refer the reader to [48] for a review on geometric multiscale modeling in the context of cardiovascular systems. The coupling between the 3D and the 0D parts can be written as

$$\mu\nabla\mathbf{u}\cdot\mathbf{n} - p\mathbf{n} = -p_i\mathbf{n}, \quad \text{on } \Gamma_i,\ i = 0, \ldots, \mathcal{N},$$

where p_i is a constant in space interface pressure that depends on the considered 0D model. In all the studied cases, the 0D pressure is a function of the 0D fluid flux Q_i, namely

$$p_i(t) = F_i(Q_i(s),\ 0 \le s \le t).$$

Moreover the mass conservation at the interface Γ_i writes

$$Q_i(s) := \int_{\Gamma_i} \mathbf{u}(s,\cdot)\cdot\mathbf{n}.$$

As a consequence the coupled system is Stokes or Navier–Stokes system with a generalized Neumann boundary conditions based upon the modelling of phenomena in the truncated part:

$$\begin{cases} \rho(\partial_t \mathbf{u} + \varepsilon(\mathbf{u}\cdot\nabla)\mathbf{u}) - \mu\Delta\mathbf{u} + \nabla p = 0 & \text{in } \Omega, \\ \operatorname{div}(\mathbf{u}) = 0 & \text{in } \Omega, \\ \mathbf{u} = 0 & \text{on } \Gamma_\ell, \\ \mu\nabla\mathbf{u}\cdot\mathbf{n} - p\mathbf{n} = -F_i\left(\int_{\Gamma_i}\mathbf{u}\cdot\mathbf{n}\right)\mathbf{n} & \text{on } \Gamma_i,\ i = 0, \ldots, \mathcal{N}, \\ \mathbf{u}(0,\cdot) = \mathbf{u}_0 & \text{in } \Omega, \end{cases} \tag{2.1}$$

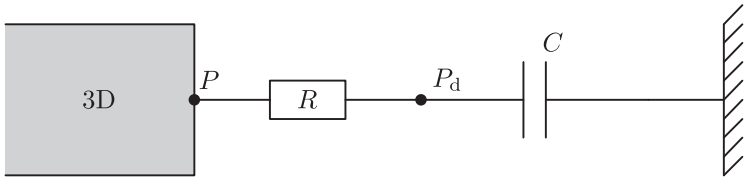

FIGURE 1. Reduced 0D model: the RC model for air flows.

Note that, as they involve the velocity flux at the artificial boundary, the boundary conditions are *nonlocal*. Note also that we have implicitly made a choice: we consider the 3D system with Neumann boundary conditions, in particular when we the 0D model is treated explicitly. Thus the splitting strategy will involve a Navier–Stokes system solved with a prescribed pressure. Another choice could be to consider the continuity of the flux, which leads to defective boundary conditions [39, 50]. In this paper we do not address this splitting strategy. Many other coupling strategies have been developed for 3D/1D coupling, see for instance [9, 36] and also [8] for a theoretical analysis of a simplified coupled problem. The choice of function F_i depends on the application field as it is designed to mimic the behaviour of the truncated subtree. For instance in the context of blood networks models, *so-called* RCR and LRCR models are used whereas, in the context of airflows in the bronchial tree, a *so-called* RC model is used. These models will be discussed thereafter.

Remark 2.1. *In this work, several choice have been made:*

- *We express the Neumann condition by using the non-symmetric tensor* $\boldsymbol{\sigma} := \mu\nabla\mathbf{u} - p\mathbb{I}$. *This choice can be justified by the fact that this quantity is continuous on cross section boundary in a Poiseuille flow in a cylindrical domain. Another choice could be based on the physical symmetric stress tensor* $\boldsymbol{\sigma}_{\mathrm{symm.}} := \mu(\nabla\mathbf{u} + \nabla\mathbf{u}^{\mathrm{t}}) - p\mathbb{I}$ *and we refer to [21, 31] for numerical comparisons between the two versions. Note nevertheless that the analysis performed hereafter remains unchanged when considering the full fluid strain tensor.*
- *Lateral walls in the 3D part are assumed to be fully rigid and, consequently, we impose the fluid velocity to be equal to zero on* Γ_ℓ. *This assumption is valid in the context of air flows, at least for normal breathing. In the context of blood flow modelling, the models should be enriched in order to take into account deformable walls: we refer to [25, 48] for more sophisticated models involving a deformable domain.*

Let us give some details on the considered reduced models.

- **The RC model for air flows** consists in reducing the truncated subtree into a resistive contribution and a compliant contribution plugged in series at each outlet of the 3D domain, see Figure 1: therefore we introduce a resistance R related to the resistance of the distal network (bronchial subtrees) and a compliance C describing the elasticity property of the surrounding tissues (lung parenchyma). The outlet pressure p_i is associated to the current pressure P and the model reduces to the following ODE:

$$\begin{cases} P = RQ + P_{\mathrm{d}}, \\ Q = C\dfrac{\mathrm{d}P_{\mathrm{d}}}{\mathrm{d}t}. \end{cases} \tag{2.2}$$

As a straightforward consequence,

$$P(t) = RQ(t) + (P(0) - RQ(0)) + C^{-1}\int_0^t Q(s)\,\mathrm{d}s. \tag{2.3}$$

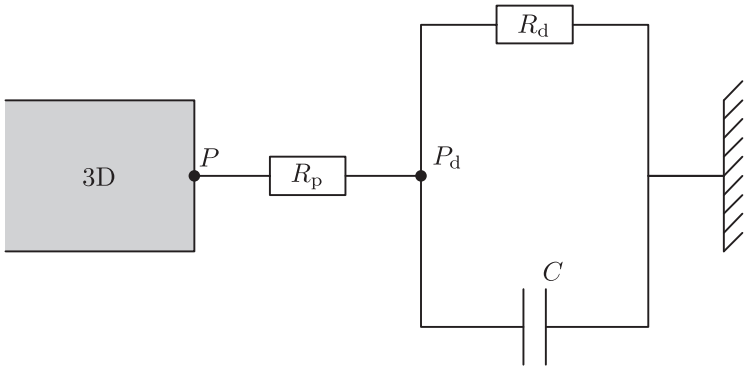

FIGURE 2. Reduced 0D model: the RCR model for blood flows.

- **The RCR model for blood flows** consists in reducing the truncated subtree into a proximal part which is mainly resistive and a distal part which is resistive and compliant. The two parts are plugged in series at each outlet of the 3D domain, see Figure 2. Therefore we introduce a proximal resistance R_{p}, a distal resistance R_{d} and a compliance C, the latter representing the wall elasticity of the blood vessels. The outlet pressure p_i is the current pressure P and the model reduces to the following ODE:

$$\begin{cases} P = R_{\mathrm{p}} Q + P_{\mathrm{d}}, \\ Q = C \dfrac{\mathrm{d}P_{\mathrm{d}}}{\mathrm{d}t} + \dfrac{P_{\mathrm{d}}}{R_{\mathrm{d}}}. \end{cases}$$

As a straightforward consequence,

$$P(t) = P(0)\mathrm{e}^{-\frac{t}{R_{\mathrm{d}}C}} + R_{\mathrm{p}}\left(Q(t) - \mathrm{e}^{-\frac{t}{R_{\mathrm{d}}C}} Q(0)\right) + C^{-1}\int_0^t Q(s)\,\mathrm{e}^{-\frac{t-s}{R_{\mathrm{d}}C}}\,\mathrm{d}s. \tag{2.4}$$

- **The LRCR model** consists in considering inductive properties plugged in series with the previous RCR model, see Figure 3. The corresponding set of equations is

$$\begin{cases} P &= R_{\mathrm{p}} Q + P_{\mathrm{d}}, \\ Q &= C \dfrac{\mathrm{d}}{\mathrm{d}t}(P_{\mathrm{d}} - P_{\mathrm{L}}) + \dfrac{P_{\mathrm{d}} - P_{\mathrm{L}}}{R_{\mathrm{d}}}, \\ P_{\mathrm{L}} &= L \dfrac{\mathrm{d}Q}{\mathrm{d}t}. \end{cases}$$

As a straightforward consequence,

$$P(t) = P(0)\mathrm{e}^{-\frac{t}{R_{\mathrm{d}}C}} + L\left(\frac{\mathrm{d}Q}{\mathrm{d}t}(t) - \mathrm{e}^{-\frac{t}{R_{\mathrm{d}}C}}\frac{\mathrm{d}Q}{\mathrm{d}t}(0)\right) + R_{\mathrm{p}}\left(Q(t) - \mathrm{e}^{-\frac{t}{R_{\mathrm{d}}C}} Q(0)\right) + C^{-1}\int_0^t Q(s)\,\mathrm{e}^{-\frac{t-s}{R_{\mathrm{d}}C}}\,\mathrm{d}s.$$

In all these cases, it can be noticed that the proximal pressure that connects the 3D domain to the truncated 0D model only depends on the flux Q_i so that function $F_i(\cdot)$ takes the following general form:

$$F_i(Q_i(s),\, 0 \le s \le t) = \alpha_i Q_i(t) + \beta_i \frac{\mathrm{d}Q_i}{\mathrm{d}t}(t) + \gamma_i \int_0^t \mathrm{e}^{-\frac{t-s}{\tau_i}} Q_i(s)\,\mathrm{d}s + \mathcal{P}_i(t), \tag{2.5}$$

where coefficients $\alpha_i \ge 0$, $\beta_i \ge 0$, $\gamma_i \ge 0$ and characteristic time $\tau_i \in (0, +\infty)$ are associated to corresponding models, and $t \mapsto \mathcal{P}_i(t)$ is a source term which also depends on the models. The coefficients α_i model

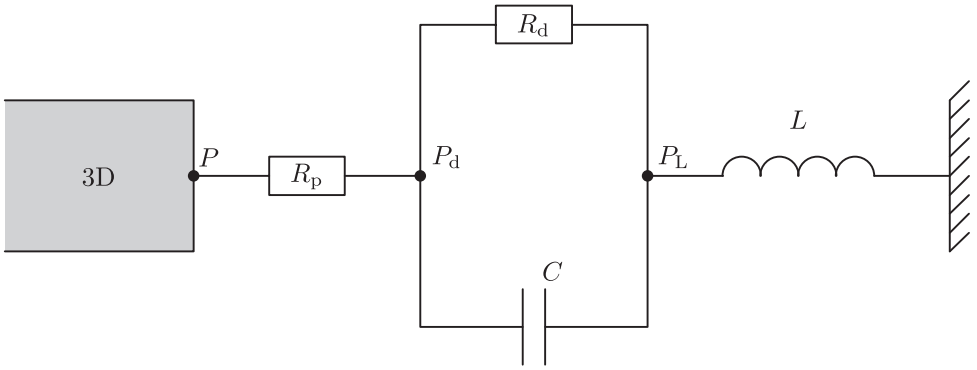

FIGURE 3. Reduced 0D model: the RCRL model.

TABLE 1. Model parameters.

	α	β	γ	τ	$\mathcal{P}(t)$
R	R	0	0	$+\infty$	0
RC	R_{p}	0	C^{-1}	$+\infty$	$P(0) - RQ(0)$
RCR	R_{p}	0	C^{-1}	$R_{\mathrm{d}}C$	$(P(0) - R_{\mathrm{p}}Q(0))\mathrm{e}^{-\frac{t}{R_{\mathrm{d}}C}}$
RCL	R_{p}	L	C^{-1}	$+\infty$	$(P(0) - R_{\mathrm{p}}Q(0) - L\frac{\mathrm{d}Q}{\mathrm{d}t}(0))$
RCRL	R_{p}	L	C^{-1}	$R_{\mathrm{d}}C$	$(P(0) - R_{\mathrm{p}}Q(0) - L\frac{\mathrm{d}Q}{\mathrm{d}t}(0))\mathrm{e}^{-\frac{t}{R_{\mathrm{d}}C}}$

dissipation of the flux, β_i represent inertia, γ_i represent elastance of the 0D models with an associated relaxation time τ_i. In particular, Table 1 summarizes the possible choices for these parameters related to the previous described models:

Remark 2.2. *The link between the different models can be described as follows*

- *The four-element RCRL model with* $R_{\mathrm{d}} = +\infty$ *leads to a* so-called *RCL model.*
- *The four-element RCRL model with* $L = 0$ *leads to the RCR model.*
- *The RCR model with* $R_{\mathrm{d}} = +\infty$ *allows us to get the RC model with* $R = R_{\mathrm{p}}$.
- *The RC model with* $C = +\infty$ *allows us to get the R model.*

Remark 2.3. *The compliance parameter in the RCR and LRCR represent the wall elasticity whereas we choose to consider rigid wall for the 3D part. We refer to [25, 48] for more sophisticated models involving a deformable domain.*

2.2. Variational formulation of the coupled system

Let us now write the variational formulation associated to the coupled problem. Define the following functional spaces

$$H^1_{0,\Gamma_\ell}(\Omega) = \{\mathbf{v} \in (H^1(\Omega))^3,\ \mathbf{v} = 0 \text{ on } \Gamma_\ell\}, \quad \mathbf{V} = \{\mathbf{v} \in H^1_{0,\Gamma_\ell}(\Omega),\ \mathrm{div}(\mathbf{v}) = 0\}.$$

Multiplying the first equation of system (2.1) by $\mathbf{v} \in \mathbf{V}$, integrating over the whole domain Ω and using integrations by parts with boundary conditions (2.5), we get:

$$\begin{aligned}\rho \int_\Omega \partial_t \mathbf{u}(t,\cdot)\cdot\mathbf{v} + \varepsilon\rho \int_\Omega (\mathbf{u}(t,\cdot)\nabla)\mathbf{u}(t,\cdot)\,\mathbf{v} + \mu \int_\Omega \nabla\mathbf{u}(t,\cdot):\nabla\mathbf{v} + \sum_{i=0}^{\mathcal{N}} \alpha_i \left(\int_{\Gamma_i} \mathbf{u}(t,\cdot)\cdot\mathbf{n}\right)\left(\int_{\Gamma_i} \mathbf{v}\cdot\mathbf{n}\right) \\ + \sum_{i=0}^{\mathcal{N}} \beta_i \left(\int_{\Gamma_i} \partial_t\mathbf{u}(t,\cdot)\cdot\mathbf{n}\right)\left(\int_{\Gamma_i} \mathbf{v}\cdot\mathbf{n}\right) + \sum_{i=0}^{\mathcal{N}} \gamma_i \left(\int_0^t \mathrm{e}^{-\frac{t-s}{\tau_i}} \left(\int_{\Gamma_i} \mathbf{u}(s,\cdot)\cdot\mathbf{n}\right) \mathrm{d}s\right)\left(\int_{\Gamma_i} \mathbf{v}\cdot\mathbf{n}\right) \\ = -\sum_{i=0}^{\mathcal{N}} \mathcal{P}_i \left(\int_{\Gamma_i} \mathbf{v}\cdot\mathbf{n}\right).\end{aligned}$$

Notice that $\varepsilon = 1$ includes the full Navier–Stokes system whereas $\varepsilon = 0$ allows us to deal with the linear Stokes system. The variational formulation is essential for the derivation of energy estimates (see the forthcoming subsections) which may be obtained by considering $\mathbf{v} = \mathbf{u}$. The estimates are easily derived in the linear case but difficulties emerge in the nonlinear case because of the inertial effects. This difficulty is partially overcome by using several tools: first the construction of a suitable operator (see Definition 4.1, page 2384) associated to a normed space which is deeply related to the inertia of the system and, second, a bilinear form that takes into account the fluid dissipation along with its 0D counterpart, namely the flux dissipation of 0D model. Let us moreover introduce a useful functional space and related property:

$$\mathbf{H} := \overline{\mathbf{V}}^{L^2} = \{\mathbf{v} \in L^2(\Omega),\ \mathrm{div}(\mathbf{v}) = 0,\ \mathbf{v}\cdot\mathbf{n} = 0 \text{ on } \Gamma_\ell\}.$$

In this space the following lemma holds true:

Lemma 2.4. *There exists $\kappa > 0$ such that,*

$$\left|\int_{\Gamma_i} \mathbf{v}\cdot\mathbf{n}\right| \le \kappa \|\mathbf{v}\|_{L^2(\Omega)},\ \forall \mathbf{v} \in \mathbf{H}, \quad \forall i \in \{0,\dots,\mathcal{N}\}.$$

We refer the reader to [2] for the proof of this lemma. Note that this estimate is deeply based on the divergence-free property and on the fact that $\overline{\Gamma_i} \cup \overline{\Gamma_j} = \emptyset$ for all $i \neq j$. Note that, for all $\mathbf{v} \in \mathbf{H}$, the flux $\int_{\Gamma_i} \mathbf{v}\cdot\mathbf{n}$ has to be understood in a weak way: indeed it can be defined by means of duality:

$$\int_{\Gamma_i} \mathbf{v}\cdot\mathbf{n} := \langle \mathbf{v}\cdot\mathbf{n}, 1\rangle_{H^{-\frac{1}{2}}(\Gamma_i), H^{\frac{1}{2}}(\Gamma_i)} = \langle \mathbf{v}\cdot\mathbf{n}, g_i\rangle_{H^{-\frac{1}{2}}(\partial\Omega), H^{\frac{1}{2}}(\partial\Omega)} = \int_\Omega \mathbf{v}\cdot\nabla g_i,$$

where g_i is a function in $H^1(\Omega)$ such that $g_i = 1$ on Γ_i and $g_i = 0$ on Γ_j, $j \neq i$. Note that such functions exist as the boundaries Γ_i are not in contact. Finally, if $\mathbf{v} \in \mathbf{V}$, the classical flux formula is recovered. Let us also introduce the following inequality, that can be deduced from the trace inequality: there exists $C_\Gamma > 0$ such that

$$\left|\int_{\Gamma_i} \mathbf{v}\cdot\mathbf{n}\right| \le C_\Gamma \|\nabla\mathbf{v}\|_{L^2(\Omega)}, \qquad \forall \mathbf{v} \in \mathbf{V}, \quad \forall i \in \{0,\dots,\mathcal{N}\}. \tag{2.6}$$

In what follows, for the sake of simplicity (and without loss of generality for the mathematical analysis), we will consider two artificial boundaries:

- one "inlet" Γ_0 with standard Neumann boundary condition, *i.e.*

$$\alpha_0 = 0, \quad \beta_0 = 0, \quad \gamma_0 = 0, \quad \mathcal{P}_0 := p_0,$$

  where $t \mapsto p_0(t)$ is a prescribed pressure.
- one "outlet" Γ_1 which is renamed Γ_W (with a subscript which stands for Windkessel boundary condition) coupled with a generic Windkessel model. For that reason we rename $\alpha_1, \beta_1, \gamma_1, \tau_1$ as $\alpha, \beta, \gamma, \tau$.

Moreover note that the non-homogeneous Neumann boundary condition on Γ_0 can be reduced to homogeneous Neumann boundary condition by defining a new unknown pressure $p - p_0$ (which will be still denoted p) and a new Windkessel source term $\mathcal{P} - p_0$ (which will be still denoted $\mathcal{P}$). Thus we will consider $p_0 = 0$, since the pressure drop is taken into account in the Windkessel source term $\mathcal{P}$. Consequently we consider the following problem:

$$\left\{\begin{array}{l} \text{Find } \mathbf{u}(t,\cdot) \in \mathbf{V} \text{ such that, for all } \mathbf{v} \in \mathbf{V}, \\ \rho \displaystyle\int_\Omega \partial_t \mathbf{u}(t,\cdot)\cdot\mathbf{v} + \varepsilon\rho \int_\Omega (\mathbf{u}(t,\cdot)\nabla)\mathbf{u}(t,\cdot)\,\mathbf{v} + \mu \int_\Omega \nabla\mathbf{u}(t,\cdot):\nabla\mathbf{v} + \alpha \left(\displaystyle\int_{\Gamma_W} \mathbf{u}(t,\cdot)\cdot\mathbf{n}\right)\left(\int_{\Gamma_W} \mathbf{v}\cdot\mathbf{n}\right) \\ \qquad +\beta \left(\displaystyle\int_{\Gamma_W} \partial_t\mathbf{u}(t,\cdot)\cdot\mathbf{n}\right)\left(\int_{\Gamma_W} \mathbf{v}\cdot\mathbf{n}\right) + \gamma \left(\int_0^t \mathrm{e}^{-\frac{t-s}{\tau}} \left(\int_{\Gamma_W} \mathbf{u}(s,\cdot)\cdot\mathbf{n}\right) \mathrm{d}s\right)\left(\int_{\Gamma_W} \mathbf{v}\cdot\mathbf{n}\right) \\ \qquad\qquad = -\mathcal{P}(t)\left(\displaystyle\int_{\Gamma_W} \mathbf{v}\cdot\mathbf{n}\right). \end{array}\right. \tag{2.7}$$

Remark 2.5. *In the whole paper we consider Neumann boundary conditions at the outlets for the 3D parts. We could have considered* $\mathbf{u}\cdot\boldsymbol{\tau} = 0$ *and* $(\boldsymbol{\sigma}\cdot\mathbf{n})\cdot\mathbf{n} = F_i(Q_i)$ *instead. The analysis that follows would be essentially unchanged except for some regularity properties associated to the Stokes-like operator we introduce for the Navier–Stokes–Windkessel system, see Remark 4.5.*

2.3. Discretization schemes

We investigate the numerical stability of various coupling strategies between the Stokes or Navier–Stokes system and the 0D models. In particular, we aim at deriving stability estimates on the solution of the discretized-in-time and pay attention to the sensitivity of the stability constants or possible smallness conditions with respect to the physiological and numerical parameters.

In what follows, discretized-in-time systems will be referred as semi-discretized systems. Let $\Delta t > 0$ be the time step and $t^n = n\Delta t$, $n \in \{0,\dots,N\}$, with $N\Delta t = T$. We denote by $(\mathbf{u}^n, p^n)$ the approximated solution at time t^n of the continuous velocity and pressure fields $t \mapsto (\mathbf{u}(t,\cdot), p(t,\cdot))$. If we discretize in time the strong formulation of system (2.7), using the first order backward Euler scheme for the time derivative, the approximated velocity and pressure $\mathbf{u}^{n+1}$ and p^{n+1} satisfy:

$$\left\{\begin{array}{r} \rho\left(\dfrac{\mathbf{u}^{n+1}-\mathbf{u}^n}{\Delta t} + \varepsilon\mathbf{u}^{n+I}\cdot\nabla\mathbf{u}^{n+1}\right) - \mu\Delta\mathbf{u}^{n+1} + \nabla p^{n+1} = 0, \text{ in } \Omega, \\ \operatorname{div}(\mathbf{u}^{n+1}) = 0, \text{ in } \Omega, \\ \mathbf{u}^{n+1} = 0, \text{ on } \Gamma_\ell, \\ \mu\nabla\mathbf{u}^{n+1}\cdot\mathbf{n} - p^{n+1}\mathbf{n} = 0, \text{ on } \Gamma_0, \\ \mu\nabla\mathbf{u}^{n+1}\cdot\mathbf{n} - p^{n+1}\mathbf{n} = -F_{\Delta t}((Q^k)_{0\le k\le m}), \text{ on } \Gamma_W, \\ \mathbf{u}^0 = \mathbf{u}_0, \text{ in } \Omega, \end{array}\right. \tag{2.8}$$

where the choice $I \in \{0,1\}$ corresponds to a semi-implicit or an implicit treatment of the convection term. Function $F_{\Delta t}$ is a time approximation of F, where F is defined by (2.5). It depends on the approximations $(Q^k)_{0\le k\le m}$ of the fluxes $(Q(t^k))_{0\le k\le m}$. Note that we may consider either explicit treatment of the boundary conditions with $m = n$ or implicit treatment with $m = n+1$. The approximate function is chosen as:

$$F_{\Delta t}((Q^k)_{0\le k\le m}) = \alpha Q^m + \beta\frac{Q^{n+1}-Q^n}{\Delta t} + \gamma\Delta t \sum_{k=m-n}^{m} \left(\frac{\tau}{\tau+\Delta t}\right)^{m+1-k} Q^k + \mathcal{P}(t^m). \tag{2.9}$$

Note that, here, the inertance term will be always treated in an implicit way. Indeed an explicit treatment of this added mass term leads to possibly unconditionally unstable schemes, see Section 5.3.1, as it has been observed and analyzed in [15] in the context of blood flows. In what follows we investigate the case $\beta = 0$ and the case $\beta \neq 0$ in order to understand the stabilization effect of the inertance on the scheme.

Remark 2.6. *The Definition* (2.9) *of the approximate function modelling the 0D model is built upon the approximation of the RC and RCR models which leads us to the following quadrature formula*

$$\gamma \int_0^{t_m} \mathrm{e}^{-\frac{t_m-s}{\tau}} Q(s)\,\mathrm{d}s \simeq \gamma \Delta t \sum_{k=m-n}^{m} \left(\frac{\tau}{\tau+\Delta t}\right)^{m+1-k} Q^k.$$

Indeed in the case of the RC model ($\alpha > 0$, $\beta = 0$, $\gamma > 0$, $\tau = +\infty$), the integral $\int_0^t Q(s)\,\mathrm{d}s$ is approximated by the classical rectangle rule whereas for the RCR model ($\alpha > 0$, $\beta = 0$, $\gamma > 0$, $\tau < +\infty$), Equation (2.9) *corresponds to the following discretization of system* (2.2)

$$\begin{cases} F_{\Delta t}((Q^k)_{0\le k\le m}) := P^{n+1} = R_{\mathrm{p}} Q^m + P_{\mathrm{d}}^{n+1}, \\ C\dfrac{P_{\mathrm{d}}^{n+1} - P_{\mathrm{d}}^n}{\Delta t} + \dfrac{P_{\mathrm{d}}^{n+1}}{R_{\mathrm{d}}} = Q^m. \end{cases} \tag{2.10}$$

We aim at studying the stability of the coupling schemes in both Stokes and Navier–Stokes regimes. In particular we focus on the derivation of stability conditions for the implicit and explicit schemes. The goal is to quantify the possible restrictions on the data and numerical parameters with respect to the physiological parameters and investigate the differences that can be encountered for various 0D models corresponding to blood flows and respiratory flows. Consequently since our aim is to differentiate the behaviour of typical models used either in blood flows or in air flows, we focus on the case $\gamma > 0$ in the forthcoming theorems. Note that the case $\gamma = 0$ will be treated in remarks pointing out the possible simplifications. In any case, the variational formulation of System (2.8) writes:

$$\begin{cases} \text{Find } \mathbf{u}^{n+1} \in \mathbf{V} \text{ such that, for all } \mathbf{v} \in \mathbf{V}, \\ \rho \displaystyle\int_\Omega (\mathbf{u}^{n+1} - \mathbf{u}^n)\cdot\mathbf{v} + \varepsilon\,\rho\Delta t \int_\Omega (\mathbf{u}^{n+I}\nabla)\mathbf{u}^{n+1}\,\mathbf{v} + \mu\,\Delta t \int_\Omega \nabla\mathbf{u}^{n+1}\cdot\nabla\mathbf{v} + \alpha\,\Delta t \left(\int_{\Gamma_W} \mathbf{u}^m\cdot\mathbf{n}\right)\left(\int_{\Gamma_W}\mathbf{v}\cdot\mathbf{n}\right) \\ +\beta\left(\displaystyle\int_{\Gamma_W}\mathbf{u}^{n+1}\cdot\mathbf{n} - \int_{\Gamma_W}\mathbf{u}^n\cdot\mathbf{n}\right)\left(\int_{\Gamma_W}\mathbf{v}\cdot\mathbf{n}\right) + \gamma\Delta t^2\left(\sum_{k=m-n}^{m}\left(\frac{\tau}{\tau+\Delta t}\right)^{m+1-k}\int_{\Gamma_W}\mathbf{u}^k\cdot\mathbf{n}\right)\left(\int_{\Gamma_W}\mathbf{v}\cdot\mathbf{n}\right) \\ \qquad = -\mathcal{P}^m\,\Delta t\left(\displaystyle\int_{\Gamma_W}\mathbf{v}\cdot\mathbf{n}\right), \end{cases} \tag{2.11}$$

where $\mathcal{P}^m = \mathcal{P}(t^m)$. In the above formulation, the choice of ε allows us to discuss the Stokes ($\varepsilon = 0$) and Navier–Stokes ($\varepsilon = 1$) cases; the index I corresponds to the implicit ($I = 1$) or semi-implicit ($I = 0$) treatment of the convection term; finally the index m allows us to describe an explicit ($m = n$) or implicit ($m = n+1$) coupling between 3D and 0D models.

3. Study of the Stokes–Windkessel coupled system

3.1. Energy estimates for the continuous system

Let us now derive the energy estimates related to Problem (2.7) with $\varepsilon = 0$. This property is an important issue of the analysis of the numerical strategies which are built upon similar principles at the discrete level and is a key ingredient to prove existence of weak solutions. In particular, all the following calculations can be justified thanks to a Galerkin approximation, leading to a rigorous derivation of the existence of weak solution.

Theorem 3.1 (Energy estimates for the Stokes system)**.** *Let $T > 0$ and $\mu > 0$. Assume that $\alpha \ge 0$, $\beta \ge 0$, $\gamma > 0$ and $0 < \tau \le +\infty$. Any weak solution $\mathbf{u}$ of the Problem* (2.7) *with $\varepsilon = 0$ satisfies, for $0 \le t \le T$:*

$$\begin{aligned} \frac{\rho}{2}\|\mathbf{u}(t,\cdot)\|_{L^2(\Omega)}^2 + \frac{\mu}{2}\int_0^t \|\nabla\mathbf{u}(s,\cdot)\|_{L^2(\Omega)}^2\,\mathrm{d}s + \frac{\beta}{2}Q^2(t) + \alpha\int_0^t Q^2(s)\,\mathrm{d}s + \frac{\gamma}{2}V^2(t) + \frac{\gamma}{\tau}\int_0^t V^2(s)\mathrm{d}s \\ \le \frac{\rho}{2}\|\mathbf{u}_0\|_{L^2(\Omega)}^2 + \frac{\beta}{2}Q^2(0) + \frac{C_\Gamma^2}{2\mu}\int_0^t (\mathcal{P}(s))^2\,\mathrm{d}s, \end{aligned} \tag{3.1}$$

where $Q(s) = \int_{\Gamma_W} \mathbf{u}(s,\cdot)\cdot\mathbf{n}$ *and* $V(t) = \int_0^t \mathrm{e}^{-\frac{t-s}{\tau}} Q(s)\mathrm{d}s$.

Proof. Taking $\mathbf{v} = \mathbf{u}(t,\cdot)$ in the variational formulation (2.7) we get

$$\frac{\rho}{2}\frac{\mathrm{d}}{\mathrm{d}t}\|\mathbf{u}(t,\cdot)\|^2_{L^2(\Omega)} + \mu\|\nabla\mathbf{u}(t,\cdot)\|^2_{L^2(\Omega)} + \alpha Q^2(t) + \beta\frac{\mathrm{d}Q^2}{\mathrm{d}t}(t) + \gamma Q(t)\int_0^t \mathrm{e}^{-\frac{t-s}{\tau}} Q(s)\,\mathrm{d}s + \mathcal{P}(t)Q(t) = 0.$$

Introducing the auxiliary volume

$$V(t) = \int_0^t \mathrm{e}^{-\frac{t-s}{\tau}} Q(s)\mathrm{d}s, \tag{3.2}$$

we obtain easily that V satisfies the following ODE

$$\frac{\mathrm{d}V}{\mathrm{d}t}(t) + \frac{1}{\tau}V(t) = Q(t). \tag{3.3}$$

Note that the previous ODE (3.3) is also valid for $\tau = +\infty$ since, in this case, $V(t) = \int_0^t Q(s)\,\mathrm{d}s$. From equations (3.2) and (3.3), we get

$$\gamma Q(t)\int_0^t \mathrm{e}^{-\frac{t-s}{\tau}} Q(s)\,\mathrm{d}s = \gamma\left(\frac{\mathrm{d}V}{\mathrm{d}t}(t) + \frac{1}{\tau}V(t)\right)V(t) = \frac{\gamma}{2}\frac{\mathrm{d}V^2}{\mathrm{d}t}(t) + \frac{\gamma}{\tau}V^2(t).$$

Then we obtain

$$\frac{\rho}{2}\frac{\mathrm{d}}{\mathrm{d}t}\|\mathbf{u}(t,\cdot)\|^2_{L^2(\Omega)} + \mu\|\nabla\mathbf{u}(t,\cdot)\|^2_{L^2(\Omega)} + \frac{\beta}{2}\frac{\mathrm{d}}{\mathrm{d}t}Q^2(t) + \alpha Q^2(t) + \frac{\gamma}{2}\frac{\mathrm{d}}{\mathrm{d}t}V^2(t) + \frac{\gamma}{\tau}V^2(t) = -\mathcal{P}(t)\int_{\Gamma_W}\mathbf{u}(t,\cdot)\cdot\mathbf{n}. \tag{3.4}$$

Using a trace inequality and Young's inequality, the term $\mathcal{P}(t)\int_{\Gamma_W}\mathbf{u}(t,\cdot)\cdot\mathbf{n}$ can be controlled by:

$$\left|\mathcal{P}(t)\int_{\Gamma_W}\mathbf{u}(t,\cdot)\cdot\mathbf{n}\right| \le \frac{\mu}{2}\|\nabla\mathbf{u}(t,\cdot)\|^2_{L^2(\Omega)} + \frac{C_\Gamma^2}{2\mu}\mathcal{P}^2(t). \tag{3.5}$$

Finally using (3.5) to bound the right hand side of (3.4), we obtain

$$\frac{\rho}{2}\frac{\mathrm{d}}{\mathrm{d}t}\|\mathbf{u}(t,\cdot)\|^2_{L^2(\Omega)} + \frac{\mu}{2}\|\nabla\mathbf{u}(t,\cdot)\|^2_{L^2(\Omega)} + \frac{\beta}{2}\frac{\mathrm{d}}{\mathrm{d}t}Q^2(t) + \alpha Q^2(t) + \frac{\gamma}{2}\frac{\mathrm{d}}{\mathrm{d}t}V^2(t) + \frac{\gamma}{\tau}V^2(t) \le \frac{C_\Gamma^2}{2\mu}\mathcal{P}^2(t). \tag{3.6}$$

We conclude by a simple time integration and remembering that $V(0) = 0$. □

Remark 3.2 (Case $\gamma = 0$)**.** *In this case, the introduction of the auxiliary volume V is not necessary and the estimate (3.1) is still valid with $\gamma = 0$.*

Remark 3.3. *Note that other energy estimates can be derived. For instance, assume that $\alpha \neq 0$. Then the estimate of the source term can be replaced by*

$$\left|\mathcal{P}(t)\int_{\Gamma_W}\mathbf{u}(t,\cdot)\cdot\mathbf{n}\right| \le \frac{\alpha}{2}Q^2(t) + \frac{1}{2\alpha}\mathcal{P}^2(t). \tag{3.7}$$

As a consequence (3.6) can be replaced by

$$\frac{\rho}{2}\frac{\mathrm{d}}{\mathrm{d}t}\|\mathbf{u}(t,\cdot)\|^2_{L^2(\Omega)} + \mu\|\nabla\mathbf{u}(t,\cdot)\|^2_{L^2(\Omega)} + \frac{\beta}{2}\frac{\mathrm{d}}{\mathrm{d}t}Q^2(t) + \frac{\alpha}{2}Q^2(t) + \frac{\gamma}{2}\frac{\mathrm{d}}{\mathrm{d}t}V^2(t) + \frac{\gamma}{\tau}V^2(t) \le \frac{1}{\alpha}\mathcal{P}^2(t).$$

It leads to

$$\frac{\rho}{2}\|\mathbf{u}(t,\cdot)\|^2_{L^2(\Omega)} + \mu\int_0^t \|\nabla\mathbf{u}(s,\cdot)\|^2_{L^2(\Omega)}\,\mathrm{d}s + \frac{\beta}{2}Q^2(t) + \frac{\alpha}{2}\int_0^t Q^2(s)\,\mathrm{d}s + \frac{\gamma}{2}V^2(t) + \frac{\gamma}{\tau}\int_0^t V^2(s)\,\mathrm{d}s \\ \leq \frac{\rho}{2}\|\mathbf{u}_0\|^2_{L^2(\Omega)} + \frac{\beta}{2}Q^2(0) + \frac{1}{2\alpha}\int_0^t \mathcal{P}^2(s)\,\mathrm{d}s. \tag{3.8}$$

Note moreover that different estimates can be obtained for other cases:

- *If $\mu = 0$ and $\alpha = 0$, then the source term can be bounded as*

$$\left|\mathcal{P}(t)\int_{\Gamma_W}\mathbf{u}(t,\cdot)\cdot\mathbf{n}\right| \leq \kappa\,|\mathcal{P}(t)|\,\|\mathbf{u}(t,\cdot)\|_{L^2(\Omega)} \leq \kappa^2\frac{\mathcal{P}^2(t)}{2\rho} + \frac{\rho}{2}\,\|\mathbf{u}(t,\cdot)\|^2_{L^2(\Omega)}\,. \tag{3.9}$$

  by Lemma 2.4 and Young's inequality.
- *If $\beta \neq 0$,*

$$\left|\mathcal{P}(t)\int_{\Gamma_W}\mathbf{u}(t,\cdot)\cdot\mathbf{n}\right| \leq |\mathcal{P}(t)|\,|Q(t)| \leq \frac{\mathcal{P}^2(t)}{2\beta} + \frac{\beta}{2}Q^2(t). \tag{3.10}$$

Nevertheless, with the previous inequalities (3.9) and (3.10), the energy estimate obtained by Gronwall lemma involves an exponential growth that behaves as e^t. Indeed if we denote $\mathcal{U}(t)$ as the left-hand side of (3.1), we use (3.4) and (3.9) to obtain: $\mathcal{U}'(t) \leq \kappa^2\frac{\mathcal{P}^2(t)}{2\rho} + \mathcal{U}(t)$ and by Gronwall lemma,

$$\mathcal{U}(t) \leq \left\{\frac{\kappa^2}{2\rho}\int_0^t \mathcal{P}^2(s)\,\mathrm{d}s + \mathcal{U}(0)\right\}\mathrm{e}^t.$$

A very similar argument leads to a similar estimate if we use (3.10) instead of (3.9).

To summarize, when $\gamma > 0$ and $\tau < +\infty$, in the case where the system is dissipative in $\mathbf{u}$ ($\mu > 0$) or Q ($\alpha > 0$) then, for zero applied pressures, the energy of the system is decreasing. When $\mu = \alpha = 0$ then the energy of the system is also bounded but with a bound that behaves as e^T.

Remark 3.4. *Note that when $\gamma > 0$ and $\tau < +\infty$, the auxiliary volume V defined by (3.2) is "dissipated" by the model. In particular, in that respect, the RCR model ($\tau < +\infty$) and the RC model ($\tau = +\infty$) used respectively in blood flow simulations and air flow simulations behave in a different way, the auxiliary volume V being dissipated in the RCR case whereas it is not in the RC case.*

This energy estimate enable to obtain the following existence theorem:

Theorem 3.5. *Let $T > 0$, $\mathbf{u}_0 \in H$, $\mathcal{P} \in L^2(0,T)$. There exists a unique $\mathbf{u} \in L^\infty(0,T;H) \cap L^2(0,T;V)$ weak solution of (2.7) with $\varepsilon = 0$ satisfying (3.6).*

Proof. The proof is standard and based on a Galerkin approximation. □

3.2. Energy estimates for the semi-discretized system

In this subsection, we establish energy estimates for the solution of the semi-discretized Stokes system with implicit treatment of the boundary conditions (see Thm. 3.6) or explicit treatment (see Thm. 3.9). Taking $\mathbf{u}^{n+1}$ as a test function in the variational formulation (2.11) with $\varepsilon = 0$ provides the following equality:

$$\rho\left\|\mathbf{u}^{n+1}\right\|^2_{L^2(\Omega)} - \rho\int_\Omega \mathbf{u}^n\cdot\mathbf{u}^{n+1} + \mu\Delta t\left\|\nabla\mathbf{u}^{n+1}\right\|^2_{L^2(\Omega)} + \alpha\Delta t Q^m Q^{n+1} + \beta((Q^{n+1})^2 - Q^nQ^{n+1}) \\ +\gamma\Delta t^2\sum_{k=m-n}^{m}\left(\frac{\tau}{\tau+\Delta t}\right)^{m+1-k}Q^kQ^{n+1} + \Delta t\mathcal{P}^mQ^{n+1} = 0.$$

We have

$$\rho \left\|\mathbf{u}^{n+1}\right\|^2_{L^2(\Omega)} - \rho \int_\Omega \mathbf{u}^n \cdot \mathbf{u}^{n+1} = \frac{\rho}{2} \left\|\mathbf{u}^{n+1}\right\|^2_{L^2(\Omega)} - \frac{\rho}{2} \left\|\mathbf{u}^{n}\right\|^2_{L^2(\Omega)} + \frac{\rho}{2} \left\|\mathbf{u}^{n+1} - \mathbf{u}^n\right\|^2_{L^2(\Omega)}$$

and

$$(Q^{n+1})^2 - Q^n Q^{n+1} = \frac{(Q^{n+1})^2}{2} - \frac{(Q^n)^2}{2} + \frac{(Q^{n+1} - Q^n)^2}{2}.$$

The discrete energy balance thus writes:

$$\begin{aligned}\frac{\rho}{2} \left\|\mathbf{u}^{n+1}\right\|^2_{L^2(\Omega)} - \frac{\rho}{2} \left\|\mathbf{u}^{n}\right\|^2_{L^2(\Omega)} + \frac{\rho}{2} \left\|\mathbf{u}^{n+1} - \mathbf{u}^n\right\|^2_{L^2(\Omega)} + \mu \Delta t \left\|\nabla \mathbf{u}^{n+1}\right\|^2_{L^2(\Omega)} + \alpha \Delta t Q^m Q^{n+1} \\ + \frac{\beta}{2}(Q^{n+1})^2 - \frac{\beta}{2}(Q^n)^2 + \frac{\beta}{2}(Q^{n+1} - Q^n)^2 + \gamma \Delta t V^{n+1,m} Q^{n+1} + \Delta t \mathcal{P}^m Q^{n+1} = 0, \quad (3.11)\end{aligned}$$

where

$$V^{n+1,m} := \begin{cases} \Delta t \displaystyle\sum_{k=1}^{n+1} \left(\frac{\tau}{\tau + \Delta t}\right)^{n+2-k} Q^k, & \text{if } m = n+1, \\ \Delta t \displaystyle\sum_{k=0}^{n} \left(\frac{\tau}{\tau + \Delta t}\right)^{n+1-k} Q^k, & \text{if } m = n. \end{cases}$$

Defining the dimensionless parameter

$$\delta_{\Delta t} := \frac{\tau}{\tau + \Delta t}, \quad (3.12)$$

note that the discrete volume $V^{n+1,n+1}$ (resp. $V^{n+1,n}$) is obtained by the rectangle rule with top–right (resp. top–left) corner approximation of the volume $V(t^{n+1})$:

$$V^{n+1,m} = \begin{cases} \Delta t \delta_{\Delta t} \displaystyle\sum_{k=1}^{n+1} \left(\frac{\tau}{\tau + \Delta t}\right)^{n+1-k} Q^k =: V^{n+1}_{\text{imp}}, & \text{if } m = n+1, \\ \Delta t \delta_{\Delta t} \displaystyle\sum_{k=0}^{n} \left(\frac{\tau}{\tau + \Delta t}\right)^{n-k} Q^k =: V^{n+1}_{\text{exp}}, & \text{if } m = n. \end{cases} \quad (3.13)$$

We now distinguish the implicit and explicit cases in the following (resp. $m = n+1$ and $m = n$).

3.2.1. Implicit coupling

Let us first consider the implicit case, namely $m = n+1$. In the case of implicit coupling the analysis is nearly the same as in the continuous framework. More precisely the implicit coupling of the Stokes system with any 0D model leads to unconditionally stable schemes in standard energy norms. Denoting $V^k_{\text{imp}} = V^{k,k}$, see (3.13), we easily verify that

$$Q^{n+1} = \frac{V^{n+1}_{\text{imp}} - V^n_{\text{imp}}}{\Delta t} + \frac{1}{\tau} V^{n+1}_{\text{imp}},$$

which corresponds to the time discretization of Equation (3.3) by a backward Euler scheme. Here we choose to analyse the standard backward Euler scheme; nevertheless alternate time discretization schemes may be considered, based on Crank–Nicolson method for instance. In this case the analysis should be quite similar since the dissipative property of the backward Euler scheme is not used in the forthcoming derivation of the stability estimates.

Theorem 3.6 (Implicit coupling with the Stokes system)**.** *Let $\mu > 0$ and $T > 0$. Assume that $\alpha \geq 0$, $\beta \geq 0$, $\gamma > 0$ and $0 < \tau \leq +\infty$. Let $\Delta t > 0$ be the time step and $t^n = n\Delta t$, $n \in \{0, \ldots, N\}$, with $N\Delta t = T$. The*

discrete solution $\mathbf{u}^{n+1}$ *of Problem* (2.11) *with* $\varepsilon = 0$ *satisfies the estimate*

$$\frac{\rho}{2}\|\mathbf{u}^{n+1}\|^2_{L^2(\Omega)} + \frac{\mu}{2}\Delta t\sum_{k=1}^{n+1}\|\nabla \mathbf{u}^k\|^2_{L^2(\Omega)} + \frac{\beta}{2}(Q^{n+1})^2 + \alpha\Delta t\sum_{k=1}^{n+1}(Q^k)^2 + \frac{\gamma}{2}(V_{\text{imp}}^{n+1})^2 + \frac{\gamma\Delta t}{\tau}\sum_{k=1}^{n+1}(V_{\text{imp}}^k)^2 \quad (3.14)$$
$$\leq \frac{\rho}{2}\|\mathbf{u}^0\|^2_{L^2(\Omega)} + \frac{\beta}{2}(Q^0)^2 + \frac{C_\Gamma^2}{2\mu}\Delta t\sum_{k=1}^{n+1}(\mathcal{P}^k)^2.$$

Proof. The proof is a straightforward adaptation of the proof of Theorem 3.1. □

Remark 3.7 (Case $\gamma = 0$)**.** *As for the continuous case, the same kind of discrete energy estimate for* $\gamma = 0$ *may be derived without introducing the discrete auxiliary volume.*

Remark 3.8. *Note that Theorem 3.6 can be extended to the fully-discretized system, using a standard Lagrange finite element approximation. Moreover different estimates of the source term as the estimates* (3.7) *and* (3.10) *obtained in Remark 3.3, can be adapted to the semi-discrete and fully-discrete frameworks with straightforward consequences on the global estimate* (3.14)*. Furthermore in the semi-discrete framework, the estimate* (3.9) *is still true, and, in the fully-discrete framework, it is still valid but under some assumptions on the discrete finite element spaces, ensuring that Lemma 2.4 holds at the discrete finite element level. In particular, Lemma 2.4 will be satisfied for any* $\mathbf{v}_h \in \mathbf{V}_h = \{\mathbf{v}_h \in \mathbf{X}_h,\ \int_\Omega \text{div}(\mathbf{v}_h)q_h = 0,\ \forall q_h \in M_h\}$ *provided that* $\mathbf{X}_h$ *is a conformal Lagrange finite element approximation of* $H^1_{0,\Gamma_\ell}(\Omega)$ *and* M_h *contains an internal approximation space of* $H^1(\Omega)$*. In particular we cannot consider finite element spaces involving discontinuous pressures. For instance if we consider* P_2–P_1 *continuous Lagrange discretizations, any* $\mathbf{v}_h \in \mathbf{V}_h$ *satisfies*

$$\left|\int_{\Gamma_i}\mathbf{v}_h\cdot\mathbf{n}\right| \leq \kappa\|\mathbf{v}_h\|_{L^2(\Omega)}, \quad \forall i \in \{0,\dots,\mathcal{N}\}.$$

Indeed to prove Lemma 2.4 in the discrete setting, we need to build a discrete lifting g_h *such that*

- $g_h = 1$ *on* Γ_i *and* $g_h = 0$ *on* Γ_j, $j \neq i$*;*
- $g_h \in H^1(\Omega)$ *with* $\|g_h\|_{H^1} \leq C$ *where* C *does not depend on* h*;*
- g_h *has to belong to* M_h *so that*
$$\int_\Omega \text{div}(\mathbf{v}_h)g_h = 0, \quad \forall \mathbf{v}_h \in \mathbf{V}_h.$$

3.2.2. Explicit coupling

We recall that the β-term that accounts for the 0D model inertia is treated in an implicit way. Using the definition of the auxiliary volume, and denoting $V_{\text{exp}}^k := V^{k,k-1}$, see (3.13), we can derive discrete equations relating the flow to the discrete auxiliary volume:

$$\frac{V_{\text{exp}}^{n+1} - V_{\text{exp}}^n}{\Delta t} + \frac{1}{\tau}V_{\text{exp}}^{n+1} = Q^n, \quad (3.15)$$

$$\frac{1}{\delta_{\Delta t}}\frac{V_{\text{exp}}^{n+1} - V_{\text{exp}}^n}{\Delta t} + \frac{1}{\tau}V_{\text{exp}}^n = Q^n, \quad (3.16)$$

where $\delta_{\Delta t}$ is defined by (3.12).

These are the key ingredients to prove:

Theorem 3.9 (Explicit coupling with the Stokes system)**.** *Let* $\mu > 0$ *and* $T > 0$*. Assume that* $\alpha \geq 0$, $\beta \geq 0$, $\gamma > 0$ *and* $0 < \tau \leq +\infty$*. Let* $\Delta t > 0$ *be the time step and* $t^n = n\Delta t$, $n \in \{0,\dots,N\}$*, with* $N\Delta t = T$*. The discrete solution* $\mathbf{u}^{n+1}$ *of Problem* (2.11) *with* $\varepsilon = 0$ *and* $m = n$ *satisfies the following stability estimate*

- *Under the condition*

$$0 < \Delta t < \lambda_1 := \frac{\alpha}{4\gamma}\left(\sqrt{1+\frac{8\rho\gamma}{\kappa^2\alpha^2}}-1\right),$$

we have

$$\frac{\rho}{2}\left\|\mathbf{u}^{n+1}\right\|^2_{L^2(\Omega)} + \frac{\mu\Delta t}{2}\sum_{k=1}^{n+1}\|\nabla\mathbf{u}^k\|^2_{L^2(\Omega)} + \frac{\gamma\Delta t}{\tau}\sum_{k=1}^{n+1}(V^k_{\exp})^2 + \frac{\beta}{2}(Q^{n+1})^2 + \frac{\gamma}{2\delta_{\Delta t}}(V^{n+2}_{\exp})^2 \leq \mathrm{e}^{C^{\mathrm{S}}_{\Delta t}T}\mathrm{e}^{\frac{T}{\lambda_1-\Delta t}}\left(E^0 + \frac{C^2_\Gamma}{2\mu}\Delta t\sum_{k=0}^{N}(\mathcal{P}^k)^2\right),$$

where E^0 is a constant that only depends on the energy norm of the initial conditions and

$$C^{\mathrm{S}}_{\Delta t} := \frac{\alpha\kappa^2}{\rho} + \frac{2\Delta t}{\tau^2}.$$

- *Assume furthermore that $\beta > 0$. Then, under the condition*

$$0 \leq \Delta t < \tilde{\lambda}_1 := \frac{\alpha}{4\gamma}\left(\sqrt{1+\frac{8\beta\gamma}{\alpha^2}}-1\right),$$

we have

$$\frac{\rho}{2}\left\|\mathbf{u}^{n+1}\right\|^2_{L^2(\Omega)} + \frac{\mu\Delta t}{2}\sum_{k=1}^{n+1}\|\nabla\mathbf{u}^k\|^2_{L^2(\Omega)} + \frac{\gamma\Delta t}{\tau}\sum_{k=1}^{n+1}(V^k_{\exp})^2 + \frac{\beta}{2}(Q^{n+1})^2 + \frac{\gamma}{2\delta_{\Delta t}}(V^{n+2}_{\exp})^2 \leq \mathrm{e}^{\tilde{C}^{\mathrm{S}}_{\Delta t}T}\mathrm{e}^{\frac{T}{\lambda_1-\Delta t}}\left(E^0 + \frac{C^2_\Gamma}{2\mu}\Delta t\sum_{k=0}^{N}(\mathcal{P}^k)^2\right),$$

where E^0 is a constant that only depends on the energy norm of the initial conditions and

$$\tilde{C}^{\mathrm{S}}_{\Delta t} := \frac{\alpha}{\beta} + \frac{2\Delta t}{\tau^2}.$$

Proof. Considering the energy equality (3.11), with $m = n$, we obtain

$$\frac{\rho}{2}\left\|\mathbf{u}^{n+1}\right\|^2_{L^2(\Omega)} - \frac{\rho}{2}\left\|\mathbf{u}^{n}\right\|^2_{L^2(\Omega)} + \frac{\rho}{2}\left\|\mathbf{u}^{n+1}-\mathbf{u}^{n}\right\|^2_{L^2(\Omega)} + \mu\Delta t\left\|\nabla\mathbf{u}^{n+1}\right\|^2_{L^2(\Omega)} + \alpha\Delta t\,Q^nQ^{n+1} + \frac{\beta}{2}(Q^{n+1})^2 - \frac{\beta}{2}(Q^n)^2 + \frac{\beta}{2}(Q^{n+1}-Q^n)^2 + \gamma\Delta t\,V^{n+1}_{\exp}Q^{n+1} + \Delta t\,\mathcal{P}^nQ^{n+1} = 0. \tag{3.17}$$

Let us deal with the explicit terms. The first one can be bounded simply as follows

$$\left|\alpha\Delta t\,Q^nQ^{n+1}\right| \leq \frac{\alpha\Delta t}{2}(Q^n)^2 + \frac{\alpha\Delta t}{2}(Q^{n+1})^2.$$

The second one, involving the discrete auxiliary volume $V^{n+1}_{\exp}$, can be rewritten as follows, using Equation (3.16)

$$\begin{aligned}\gamma\Delta t\,V^{n+1}_{\exp}Q^{n+1} &= \gamma\Delta t\left(\frac{1}{\delta_{\Delta t}}\frac{V^{n+2}_{\exp}-V^{n+1}_{\exp}}{\Delta t} + \frac{1}{\tau}V^{n+1}_{\exp}\right)V^{n+1}_{\exp}\\ &= \frac{\gamma}{\delta_{\Delta t}}\left(\frac{(V^{n+2}_{\exp})^2}{2} - \frac{(V^{n+1}_{\exp})^2}{2} - \frac{(V^{n+2}_{\exp}-V^{n+1}_{\exp})^2}{2}\right) + \frac{\gamma\Delta t}{\tau}(V^{n+1}_{\exp})^2,\end{aligned}$$

and we get

$$\begin{aligned}\frac{\rho}{2}\left\|\mathbf{u}^{n+1}\right\|^2_{L^2(\Omega)} + \mu\Delta t\|\nabla\mathbf{u}^{n+1}\|^2_{L^2(\Omega)} + \frac{\beta}{2}(Q^{n+1})^2 + \frac{\gamma}{\delta_{\Delta t}}\frac{(V_{\rm exp}^{n+2})^2}{2} + \frac{\gamma\Delta t}{\tau}(V_{\rm exp}^{n+1})^2 \\ \leq \frac{\rho}{2}\left\|\mathbf{u}^{n}\right\|^2_{L^2(\Omega)} + \frac{\beta}{2}(Q^{n})^2 + \frac{\alpha\Delta t}{2}(Q^{n})^2 + \frac{\alpha\Delta t}{2}(Q^{n+1})^2 + \frac{\gamma}{\delta_{\Delta t}}\frac{(V_{\rm exp}^{n+1})^2}{2} + \frac{\gamma}{\delta_{\Delta t}}\frac{(V_{\rm exp}^{n+2}-V_{\rm exp}^{n+1})^2}{2} \\ + \frac{C_\Gamma^2}{2\mu}\Delta t(\mathcal{P}^n)^2 + \frac{\mu\Delta t}{2}\|\nabla\mathbf{u}^{n+1}\|^2_{L^2(\Omega)},\end{aligned}$$

where we have used an estimate similar to (3.5) to bound the source term. The stability estimate is built upon the control of the following extra terms:

$$\frac{\alpha\Delta t}{2}(Q^n)^2 + \frac{\alpha\Delta t}{2}(Q^{n+1})^2, \qquad \frac{\gamma}{\delta_{\Delta t}}\frac{(V_{\rm exp}^{n+2}-V_{\rm exp}^{n+1})^2}{2}.$$

Thanks to (3.16) we have

$$\frac{\gamma}{\delta_{\Delta t}}\frac{(V_{\rm exp}^{n+2}-V_{\rm exp}^{n+1})^2}{2} \leq \frac{\gamma}{\delta_{\Delta t}}\left(\Delta t^2\delta^2_{\Delta t}(Q^{n+1})^2 + \frac{\Delta t^2}{\tau^2}\delta^2_{\Delta t}(V_{\rm exp}^{n+1})^2\right).$$

Consequently we obtain

$$\begin{aligned}\frac{\rho}{2}\|\mathbf{u}^{n+1}\|^2_{L^2(\Omega)} + \frac{\mu\Delta t}{2}\|\nabla\mathbf{u}^{n+1}\|^2_{L^2(\Omega)} + \frac{\beta}{2}(Q^{n+1})^2 + \frac{\gamma}{\delta_{\Delta t}}\frac{(V_{\rm exp}^{n+2})^2}{2} + \frac{\gamma\Delta t}{\tau}(V_{\rm exp}^{n+1})^2 \\ \leq \frac{\rho}{2}\|\mathbf{u}^{n}\|^2_{L^2(\Omega)} + \frac{\beta}{2}(Q^{n})^2 + \frac{\alpha\Delta t}{2}(Q^{n})^2 + \frac{\alpha\Delta t}{2}(Q^{n+1})^2 + \frac{\gamma}{\delta_{\Delta t}}\frac{(V_{\rm exp}^{n+1})^2}{2} \\ + \frac{\gamma}{\delta_{\Delta t}}\left(\Delta t^2\delta^2_{\Delta t}(Q^{n+1})^2 + \frac{\Delta t^2}{\tau^2}\delta^2_{\Delta t}(V_{\rm exp}^{n+1})^2\right) + \frac{C_\Gamma^2}{2\mu}\Delta t(\mathcal{P}^n)^2.\end{aligned}$$

and since $\delta_{\Delta t} < 1$, we obtain

$$\begin{aligned}\frac{\rho}{2}\|\mathbf{u}^{n+1}\|^2_{L^2(\Omega)} + \frac{\mu\Delta t}{2}\|\nabla\mathbf{u}^{n+1}\|^2_{L^2(\Omega)} + \frac{\beta}{2}(Q^{n+1})^2 + \frac{\gamma}{\delta_{\Delta t}}\frac{(V_{\rm exp}^{n+2})^2}{2} + \frac{\gamma\Delta t}{\tau}(V_{\rm exp}^{n+1})^2 \\ \leq \frac{\rho}{2}\|\mathbf{u}^{n}\|^2_{L^2(\Omega)} + \frac{\beta}{2}(Q^{n})^2 + \frac{\alpha\Delta t}{2}(Q^{n})^2 + \frac{\alpha\Delta t}{2}(Q^{n+1})^2 + \frac{\gamma}{\delta_{\Delta t}}\frac{(V_{\rm exp}^{n+1})^2}{2} \\ + \frac{\gamma}{\delta_{\Delta t}}\left(\Delta t^2(Q^{n+1})^2 + \frac{\Delta t^2}{\tau^2}(V_{\rm exp}^{n+1})^2\right) + \frac{C_\Gamma^2}{2\mu}\Delta t(\mathcal{P}^n)^2. \qquad (3.18)\end{aligned}$$

Now we discuss two different cases: $\beta \geq 0$ (general case), $\beta > 0$ (0D inertial case).

• In the general case $\beta \geq 0$, and in particular if $\beta = 0$, the terms

$$\frac{\alpha\Delta t}{2}(Q^n)^2, \qquad \frac{\alpha\Delta t}{2}(Q^{n+1})^2, \qquad \frac{\gamma}{\delta_{\Delta t}}\Delta t^2(Q^{n+1})^2,$$

in the right-hand side of (3.18) cannot be controlled by the inertia of the 0D model. However they can be controlled by the inertial term of the fluid. Indeed by Lemma 2.4,

$$(Q^k)^2 \leq \kappa^2\left\|\mathbf{u}^k\right\|^2_{L^2(\Omega)},$$

and, as a consequence, we deduce from (3.18) and the above inequality that

$$\begin{aligned}\frac{\rho}{2}\left(1 - \frac{\alpha\kappa^2}{\rho}\Delta t - \frac{2\gamma\kappa^2}{\rho}\Delta t^2\right)\|\mathbf{u}^{n+1}\|^2_{L^2(\Omega)} + \frac{\mu\Delta t}{2}\|\nabla\mathbf{u}^{n+1}\|^2_{L^2(\Omega)} + \frac{\gamma}{\delta_{\Delta t}}\frac{(V_{\rm exp}^{n+2})^2}{2} + \frac{\gamma\Delta t}{\tau}(V_{\rm exp}^{n+1})^2 + \frac{\beta}{2}(Q^{n+1})^2 \\ \leq \frac{\rho}{2}\left(1 + \frac{\alpha\kappa^2}{\rho}\Delta t\right)\|\mathbf{u}^{n}\|^2_{L^2(\Omega)} + \frac{\gamma}{\delta_{\Delta t}}\left(1 + \frac{2\Delta t^2}{\tau^2}\right)\frac{(V_{\rm exp}^{n+1})^2}{2} \\ + \frac{\beta}{2}(Q^n)^2 + \frac{C_\Gamma^2}{2\mu}\Delta t(\mathcal{P}^n)^2.\end{aligned}$$

Defining

$$P(\Delta t) := 1 - \frac{\alpha\kappa^2}{\rho}\Delta t - \frac{2\gamma\kappa^2}{\rho}\Delta t^2, \tag{3.19}$$

we introduce the roots of this polynomial

$$\lambda_1 := \frac{\alpha}{4\gamma}\left(\sqrt{1+\frac{8\rho\gamma}{\kappa^2\alpha^2}}-1\right), \qquad -\lambda_2 := -\frac{\alpha}{4\gamma}\left(\sqrt{1+\frac{8\rho\gamma}{\kappa^2\alpha^2}}+1\right) \tag{3.20}$$

with, for the sake of convenience, $\lambda_i > 0$. Then we get

$$P(\Delta t) = \frac{2\gamma\kappa^2}{\rho}(\lambda_1 - \Delta t)(\lambda_2 + \Delta t) \geq 1 - \frac{\Delta t}{\lambda_1}. \tag{3.21}$$

As a consequence, we obtain

$$\begin{aligned}\frac{\rho}{2}\left(1-\frac{\Delta t}{\lambda_1}\right)\|\mathbf{u}^{n+1}\|^2_{L^2(\Omega)} + \frac{\mu\Delta t}{2}\|\nabla\mathbf{u}^{n+1}\|^2_{L^2(\Omega)} + \frac{\gamma}{\delta_{\Delta t}}\frac{(V^{n+2}_{\exp})^2}{2} + \frac{\gamma\Delta t}{\tau}(V^{n+1}_{\exp})^2 + \frac{\beta}{2}(Q^{n+1})^2 \\ \leq \frac{\rho}{2}\left(1+\frac{\alpha\kappa^2}{\rho}\Delta t\right)\|\mathbf{u}^n\|^2_{L^2(\Omega)} + \frac{\gamma}{\delta_{\Delta t}}\left(1+\frac{2\Delta t^2}{\tau^2}\right)\frac{(V^{n+1}_{\exp})^2}{2} + \frac{\beta}{2}(Q^n)^2 + \frac{C_\Gamma^2}{2\mu}\Delta t(\mathcal{P}^n)^2.\end{aligned}$$

Using the discrete Gronwall lemma [30] and under the condition $0 < \Delta t < \lambda_1$, this provides the following stability estimate

$$\begin{aligned}\frac{\rho}{2}\left\|\mathbf{u}^{n+1}\right\|^2_{L^2(\Omega)} + \frac{\mu\Delta t}{2}\sum_{k=1}^{n+1}\|\nabla\mathbf{u}^k\|^2_{L^2(\Omega)} + \frac{\gamma\Delta t}{\tau}\sum_{k=1}^{n+1}(V^k_{\exp})^2 + \frac{\beta}{2}(Q^{n+1})^2 + \frac{\gamma}{2\delta_{\Delta t}}(V^{n+2}_{\exp})^2 \\ \leq \mathrm{e}^{C^{\mathrm{S}}_{\Delta t}T}\mathrm{e}^{\frac{T}{\lambda_1-\Delta t}}\left(E^0 + \frac{C_\Gamma^2}{2\mu}\Delta t\sum_{k=0}^{N}(\mathcal{P}^k)^2\right),\end{aligned}$$

where E^0 is a constant that only depends on the energy norm of the initial conditions and

$$C^{\mathrm{S}}_{\Delta t} = \frac{\alpha\kappa^2}{\rho} + \frac{2\Delta t}{\tau^2}.$$

• Assume now that $\beta > 0$. In that case the terms

$$\frac{\alpha\Delta t}{2}(Q^n)^2, \qquad \frac{\alpha\Delta t}{2}(Q^{n+1})^2, \qquad \frac{\gamma}{\delta_{\Delta t}}\Delta t^2\delta^2_{\Delta t}(Q^{n+1})^2$$

in the right-hand side of (3.18) can be controlled by the inertia of the 0D model. The estimate (3.18) yields

$$\begin{aligned}\frac{\rho}{2}\|\mathbf{u}^{n+1}\|^2_{L^2(\Omega)} + \frac{\mu\Delta t}{2}\|\nabla\mathbf{u}^{n+1}\|^2_{L^2(\Omega)} + \frac{\beta}{2}\left(1-\frac{\alpha}{\beta}\Delta t - \frac{2\gamma}{\beta}\Delta t^2\right)(Q^{n+1})^2 + \frac{\gamma}{\delta_{\Delta t}}\frac{(V^{n+2}_{\exp})^2}{2} + \frac{\gamma\Delta t}{\tau}(V^{n+1}_{\exp})^2 \\ \leq \frac{\rho}{2}\|\mathbf{u}^n\|^2_{L^2(\Omega)} + \frac{\beta}{2}\left(1+\frac{\alpha}{\beta}\Delta t\right)(Q^n)^2 + \frac{\gamma}{\delta_{\Delta t}}\left(1+\frac{2\Delta t^2}{\tau^2}\right)\frac{(V^{n+1}_{\exp})^2}{2} + \frac{C_\Gamma^2}{2\mu}\Delta t(\mathcal{P}^n)^2.\end{aligned}$$

Defining $\tilde{P}(\Delta t) := 1 - \frac{\alpha}{\beta}\Delta t - \frac{2\gamma}{\beta}\Delta t^2$, we introduce the roots of this polynomial

$$\tilde{\lambda}_1 := \frac{\alpha}{4\gamma}\left(\sqrt{1+\frac{8\beta\gamma}{\alpha^2}}-1\right), \qquad -\tilde{\lambda}_2 := -\frac{\alpha}{4\gamma}\left(\sqrt{1+\frac{8\beta\gamma}{\alpha^2}}+1\right),$$

with, for the sake of convenience, $\tilde{\lambda}_i > 0$. Then we get

$$\tilde{P}(\Delta t) = \frac{2\gamma}{\beta}(\tilde{\lambda}_1 - \Delta t)(\tilde{\lambda}_2 + \Delta t) \geq 1 - \frac{\Delta t}{\tilde{\lambda}_1}.$$

As a consequence, we obtain

$$\begin{aligned}\frac{\rho}{2}\|\mathbf{u}^{n+1}\|^2_{L^2(\Omega)} + \frac{\mu\Delta t}{2}\|\nabla\mathbf{u}^{n+1}\|^2_{L^2(\Omega)} + \frac{\beta}{2}\left(1 - \frac{\Delta t}{\tilde{\lambda}_1}\right)(Q^{n+1})^2 + \frac{\gamma}{\delta_{\Delta t}}\frac{(V_{\text{exp}}^{n+2})^2}{2} + \frac{\gamma\Delta t}{\tau}(V_{\text{exp}}^{n+1})^2 \\ \leq \frac{\rho}{2}\|\mathbf{u}^{n}\|^2_{L^2(\Omega)} + \frac{\beta}{2}\left(1 + \frac{\alpha}{\beta}\Delta t\right)(Q^{n})^2 + \frac{\gamma}{\delta_{\Delta t}}\left(1 + \frac{2\Delta t^2}{\tau^2}\right)\frac{(V_{\text{exp}}^{n+1})^2}{2} + \frac{C_\Gamma^2}{2\mu}\Delta t(\mathcal{P}^n)^2.\end{aligned}$$

Under the condition $0 < \Delta t < \tilde{\lambda}_1$, the discrete Gronwall lemma [30], implies that

$$\begin{aligned}\frac{\rho}{2}\left\|\mathbf{u}^{n+1}\right\|^2_{L^2(\Omega)} + \frac{\mu\Delta t}{2}\sum_{k=1}^{n+1}\|\nabla\mathbf{u}^{k}\|^2_{L^2(\Omega)} + \frac{\gamma\Delta t}{\tau}\sum_{k=1}^{n+1}(V_{\text{exp}}^{k})^2 + \frac{\beta}{2}(Q^{n+1})^2 + \frac{\gamma}{2\delta_{\Delta t}}(V_{\text{exp}}^{n+2})^2 \\ \leq \mathrm{e}^{\tilde{C}^{\mathrm{S}}_{\Delta t}T}\mathrm{e}^{\frac{T}{\tilde{\lambda}_1 - \Delta t}}\left(E^0 + \frac{C_\Gamma^2}{2\mu}\Delta t\sum_{k=0}^{N}(\mathcal{P}^k)^2\right),\end{aligned}$$

where E^0 is a constant that only depends on the energy norm of the initial conditions and

$$\tilde{C}^{\mathrm{S}}_{\Delta t} = \frac{\alpha}{\beta} + \frac{2\Delta t}{\tau^2}.$$

Note that alternate estimates can be derived following the continuous case that have been developed in Remark 3.3. □

Remark 3.10 (Case $\gamma = 0$)**.** *In this case, no auxiliary volume is required to derive discrete energy estimates. The sufficient conditions that guarantee the stability of the explicit scheme become:*

$$\Delta t \leq \frac{\max\left(\frac{\rho}{\kappa^2}, \beta\right)}{\alpha}.$$

This condition involves the ratio of the inertance of the 3D or 0D system to the resistance of the 0D model. Moreover the exponential growth constants are modified as follows:

$$C^{\mathrm{S}}_{\Delta t} := \frac{\alpha\kappa^2}{\rho}, \qquad \tilde{C}^{\mathrm{S}}_{\Delta t} = \frac{\alpha}{\beta}.$$

Remark 3.11 (Influence of the inertia)**.** *When the inertia parameters of the problem, namely ρ and β, tend to $+\infty$, so do the critical times λ_1 and $\tilde{\lambda}_1$ which implies that in practice no condition on the time step is required to ensure stability. Moreover, the exponential growth remains bounded. Let us discuss the influence of the inertance parameter β on the critical time $\tilde{\lambda}_1$:*

$$\tilde{\lambda}_1 \sim_{\beta\to+\infty} \sqrt{\frac{\beta}{2\gamma}}, \qquad \tilde{C}^{\mathrm{S}}_{\Delta t} \sim_{\beta\to+\infty} \frac{2\Delta t}{\tau^2},$$

and

$$\tilde{\lambda}_1 \sim_{\beta\to 0} \frac{\beta}{\alpha}, \qquad \tilde{C}^{\mathrm{S}}_{\Delta t} \sim_{\beta\to 0} \frac{\alpha}{\beta}.$$

When the inertance of the 0D model is small, so is the critical time $\tilde{\lambda}_1$; nevertheless in this case it is sufficient to impose $\Delta t \leq \lambda_1$ that may be less restrictive to ensure the stability of the explicit scheme.

Remark 3.12. *Let us discuss the influence of the characteristic relaxation time τ on the obtained stability estimates and smallness assumption on the time step:*

- *the sufficient conditions on the time step do not depend on the parameter τ.*
- *when $\tau \to +\infty$, the contribution $\mathrm{e}^{2\Delta t T/\tau^2}$ to the exponential growth goes to 1 and thus is uniformly bounded.*
- *when $\tau \ll T$, the exponential bound $\mathrm{e}^{2\Delta t T/\tau^2}$ hides an effective restriction on the time-step. Indeed in order to obtain a uniform bound of the exponential growth, this requires a severe restriction on the time step by choosing Δt such that $\Delta t T/\tau^2 = \mathcal{O}(1)$, namely $\Delta t = \mathcal{O}(\frac{\tau^2}{T})$.*

Remark 3.13 (Influence of the resistance parameter α)**.** *When α becomes large then the critical times λ_1 and $\tilde{\lambda}_1$ behave as*

$$\lambda_1 \sim_{\alpha\to+\infty} \frac{\rho}{\kappa^2\alpha}, \qquad \tilde{\lambda}_1 \sim_{\alpha\to+\infty} \frac{\beta}{\alpha}.$$

Thus the larger α is (which corresponds to the resistive parameter of the 0D model), the more severe is the constraint on the time step together with the exponential growth.

4. Study of the Navier–Stokes–Windkessel coupled system

4.1. Estimates for the continuous system

Let us consider the Navier–Stokes system and underline the standard difficulties met when one is interested in analyzing the energy balance when adding nonlinearities to the problem. Note that the estimates we will derive hereafter lead to the existence of strong solution for small time or for small enough data. Let us first review the difficulties coming from the convection term. To fix the idea we consider the Navier–Stokes system (2.7) coupled with a R model ($F(Q(s), 0 \le s \le t) = \alpha Q(t)$). Proceeding as in the linear case, we derive the following energy equality:

$$\frac{\rho}{2}\frac{\mathrm{d}}{\mathrm{d}t}\int_\Omega |\mathbf{u}|^2 + \rho\int_{\Gamma_0\cup\Gamma_W} \frac{|\mathbf{u}|^2}{2}\mathbf{u}\cdot\mathbf{n} + \mu\int_\Omega |\nabla\mathbf{u}|^2 + \alpha\left(\int_{\Gamma_W}\mathbf{u}\cdot\mathbf{n}\right)^2 = \mathcal{P}(t)\int_{\Gamma_W}\mathbf{u}\cdot\mathbf{n}.$$

Here we are considering the coupling with the R model only and have used the divergence free property of the fluid velocity. We see a term $\rho\int_{\Gamma_W}\frac{|\mathbf{u}|^2}{2}\mathbf{u}\cdot\mathbf{n}$ that represents the flux of kinetic energy at the artificial boundary, whose sign is not known *a priori*. Consequently unlike for the Stokes system one can not derive easily an energy estimate. To obtain a satisfactory energy estimate and existence theorems, one has to be able to control this kinetic energy flux at the interface where Neumann boundary conditions are prescribed. Note that in dimension three we can prove the following bound (see [31])

$$\left|\rho\int_{\Gamma_W}\frac{|\mathbf{u}|^2}{2}\mathbf{u}\cdot\mathbf{n}\right| \le C\|\mathbf{u}\|^{5/2}_{L^2(\Omega)}\|\nabla\mathbf{u}\|^{1/2}_{L^2(\Omega)},$$

which does not allow to obtain an energy estimate. Nevertheless existence of a unique strong solution can be proven. In particular, in [2], the existence of a unique strong solution (locally in time or for small data) is derived, based on the same ideas developped in [31] and on regularity results of the solution of the stationary Stokes system with mixed Dirichlet–Neumann boundary conditions in polyhedral domains [41].

Regarding the existence of solutions for the Navier–Stokes system with mixed Dirichlet–Neumann boundary conditions, we refer to [31]: the authors prove the existence of a unique smooth solution which is local in time; under an additional assumption on the smallness of the data, the smooth solution is proven to be global-in-time. Note that the existence of global weak solutions can be derived by choosing appropriate outflow boundary conditions that control the flux of incoming kinetic energy and thus stabilize the system [12]. The case of Robin-type boundary conditions which involve the modelling of a local-in-space resistive contribution is analyzed in [47]: existence of a strong solution is obtained under the assumption that the resistance is small enough. In [2]

a RC-like model is studied: the existence of a unique local-in-time strong solution for any data is proven; the particular case of a single R model is also investigated, leading to the existence and uniqueness of a global-in-time smooth solution for small data even if the resistance is large. Finally in [47], existence of a local-in-time strong solution for the RCR model is proven for small data. Proofs of the above results are all based upon Galerkin approximations with special bases. Note moreover that they all require that in/outlet meet the lateral boundary with right angles. This framework will be used in the analysis of the semi-discretized Navier–Stokes systems. We point out that the main difficulty in the above references relies on the estimate of the convective term of the Navier–Stokes system.

Let us now focus on the more general 0D model we study here and introduce key tools for the derivation of suitable estimates of the solution of the coupled system. In particular we introduce a new Stokes-like operator adapted to our coupled Navier–Stokes–Windkessel model.

Definition 4.1 (Stokes operator)**.** *The space* $\mathbf{H}$ *is endowed with the scalar product*

$$(\mathbf{v},\mathbf{w})_{\rho,\beta} := \rho\int_\Omega \mathbf{v}\cdot\mathbf{w} + \beta\left(\int_{\Gamma_W}\mathbf{v}\cdot\mathbf{n}\right)\left(\int_{\Gamma_W}\mathbf{w}\cdot\mathbf{n}\right),$$

and we denote $\|\cdot\|_{\rho,\beta}$ *the norm associated to this scalar product. Then we define the bilinear form* $a_{\mu,\alpha}$ *as*

$$\begin{aligned} a_{\mu,\alpha} : \mathbf{V}\times\mathbf{V} &\to \mathbb{R}\\ (\mathbf{v},\mathbf{w}) &\mapsto \mu\int_\Omega \nabla\mathbf{v}\cdot\nabla\mathbf{w} + \alpha\left(\int_{\Gamma_W}\mathbf{v}\cdot\mathbf{n}\right)\left(\int_{\Gamma_W}\mathbf{w}\cdot\mathbf{n}\right). \end{aligned}$$

Finally we introduce the operator $A_{\mu,\alpha} : \mathcal{D}(A_{\mu,\alpha}) \to \mathbf{H}$ *associated to the bilinear form* $a_{\mu,\alpha}$ *by*

$$(A_{\mu,\alpha}\mathbf{v},\mathbf{w})_{\rho,\beta} = a_{\mu,\alpha}(\mathbf{v},\mathbf{w})$$

with

$$\mathcal{D}(A_{\mu,\alpha}) = \{\mathbf{u}\in\mathbf{V},\ |a_{\mu,\alpha}(\mathbf{u},\mathbf{v})| \le C\,\|\mathbf{v}\|_{\mathbf{H}},\ \forall\mathbf{v}\in\mathbf{V}\}.$$

Proposition 4.2 (Properties of the Stokes operator)**.** *The operator* $A_{\mu,\alpha}$ *has the following properties:*

- $A_{\mu,\alpha}\in\mathcal{L}(\mathcal{D}(A_{\mu,\alpha}),\mathbf{H})$ *is invertible and its inverse is compact on* $\mathbf{H}$*;*
- $A_{\mu,\alpha}$ *is self-adjoint.*

As a consequence, $A_{\mu,\alpha}$ *admits a family of eigenfunctions* $\{\phi_j\}$

$$A_{\mu,\alpha}\phi_j = \nu_j\phi_j, \quad \text{with} \quad 0<\nu_1\le\nu_2\le\ldots\le\nu_j\to_{j\to+\infty}+\infty$$

which is complete and orthogonal in both $\mathbf{H}$ *and* $\mathbf{V}$*.*

Proof. The proof of this proposition relies on classical arguments, see for instance [10] for general arguments and [27] for a direct proof in a similar context. □

Lemma 4.3. *The following estimates hold:*

1. *There exists* $\mathcal{L}>0$ *such that*

$$\forall\mathbf{v}\in\mathcal{D}(A_{\mu,\alpha}),\quad \|\nabla\mathbf{v}\|_{L^2(\Omega)} \le \mathcal{L}\,\|A_{\mu,\alpha}\mathbf{v}\|_{L^2(\Omega)}. \tag{4.1}$$

The constant $\mathcal{L}$ *depends on the parameters as* $\mathcal{L} := C_P\dfrac{\rho+\beta\kappa^2}{\mu}$*, where* C_P *denotes the Poincaré constant.*

2. *If furthermore the artificial boundaries* Γ_0 *and* Γ_W *meet the lateral boundaries* Γ_ℓ *at angle* $\frac{\pi}{2}$ *and each boundary is smooth enough, then there exist* $\epsilon > 0$ *and* $\mathcal{M} > 0$*, such that*

$$\forall \mathbf{v} \in \mathcal{D}(A_{\mu,\alpha}), \quad \|\mathbf{v}\|_{H^{\frac{3}{2}+\epsilon}(\Omega)} \leq \mathcal{M} \|A_{\mu,\alpha}\mathbf{v}\|_{L^2(\Omega)}. \tag{4.2}$$

The constant $\mathcal{M}$ *depends on the parameters as:*

$$\mathcal{M} := C_\Omega^{(2)} \left(\frac{\rho}{\mu} + C_\Omega^{(1)} \kappa \frac{\beta}{\mu} + C_\Omega^{(1)} C_\Gamma \frac{\alpha}{\mu} \mathcal{L} \right), \tag{4.3}$$

where $C_\Omega^{(i)}$ *are constants which only depend on the domain.*

Remark 4.4. *Both constants* $\mathcal{L}$ *and* $\mathcal{M}$ *are proportional to the ratio of a density to a viscosity.*

Proof. Both estimates rely on the properties of the Stokes operator. Using the definition of the scalar product on $\mathbf{H}$, we obtain

$$\begin{aligned}
(A_{\mu,\alpha}\mathbf{v}, \mathbf{v})_{\rho,\beta} &= \rho \int_\Omega A_{\mu,\alpha}\mathbf{v} \cdot \mathbf{v} + \beta \left(\int_{\Gamma_W} A_{\mu,\alpha}\mathbf{v} \cdot \mathbf{n} \right) \left(\int_{\Gamma_W} \mathbf{v} \cdot \mathbf{n} \right) \\
&\leq \rho \|A_{\mu,\alpha}\mathbf{v}\|_{L^2(\Omega)} \|\mathbf{v}\|_{L^2(\Omega)} + \beta\kappa^2 \|\mathbf{v}\|_{L^2(\Omega)} \|A_{\mu,\alpha}\mathbf{v}\|_{L^2(\Omega)} \\
&\leq C_P(\rho + \beta\kappa^2) \|A_{\mu,\alpha}\mathbf{v}\|_{L^2(\Omega)} \|\nabla\mathbf{v}\|_{L^2(\Omega)},
\end{aligned}$$

where we have used Lemma 2.4 and Poincaré inequality. Besides, by definition of the operator $A_{\mu,\alpha}$, we have

$$(A_{\mu,\alpha}\mathbf{v}, \mathbf{v})_{\rho,\beta} = a_{\mu,\alpha}(\mathbf{v}, \mathbf{v}) = \mu \|\nabla\mathbf{v}\|_{L^2(\Omega)}^2 + \alpha \left(\int_{\Gamma_W} \mathbf{v} \cdot \mathbf{n} \right)^2 \geq \mu \|\nabla\mathbf{v}\|_{L^2(\Omega)}^2,$$

thus

$$\mu \|\nabla\mathbf{v}\|_{L^2(\Omega)}^2 \leq C_P(\rho + \beta\kappa^2) \|A_{\mu,\alpha}\mathbf{v}\|_{L^2(\Omega)} \|\nabla\mathbf{v}\|_{L^2(\Omega)},$$

which, by simplification, concludes the proof of (4.1). The proof of estimate (4.2) is based upon a regularity result for the Stokes problem with homogeneous mixed boundary conditions, see [41], for which we need the geometric angular assumption. The problem $A_{\mu,\alpha}\mathbf{v} = \mathbf{f} \in \mathbf{H}$ can be rewritten as

$$\begin{cases}
-\Delta\mathbf{v} + \nabla\left(\frac{p}{\mu}\right) = \frac{\rho}{\mu}\mathbf{f}, & \text{in } \Omega, \\
\operatorname{div}(\mathbf{v}) = 0, & \text{in } \Omega, \\
\mathbf{v} = 0, & \text{on } \Gamma_\ell, \\
\nabla\mathbf{v} \cdot \mathbf{n} - \frac{p}{\mu}\mathbf{n} = 0, & \text{on } \Gamma_0, \\
\nabla\mathbf{v} \cdot \mathbf{n} - \frac{p}{\mu}\mathbf{n} = -\frac{\beta}{\mu}\left(\int_{\Gamma_W} \mathbf{f} \cdot \mathbf{n} \right)\mathbf{n} - \frac{\alpha}{\mu}\left(\int_{\Gamma_W} \mathbf{v} \cdot \mathbf{n} \right)\mathbf{n}, & \text{on } \Gamma_W.
\end{cases} \tag{4.4}$$

We consider the auxiliary pressure defined by

$$\begin{cases}
-\Delta\tilde{p} = 0, & \text{in } \Omega, \\
\nabla\tilde{p} \cdot \mathbf{n} = 0, & \text{on } \Gamma_\ell, \\
\tilde{p} = 0, & \text{on } \Gamma_0, \\
\tilde{p} = -\beta\left(\int_{\Gamma_W} \mathbf{f} \cdot \mathbf{n} \right) - \alpha\left(\int_{\Gamma_W} \mathbf{v} \cdot \mathbf{n} \right), & \text{on } \Gamma_W.
\end{cases}$$

By standard arguments and using Lemma 2.4 and Equation (2.6), we have

$$\|\nabla\tilde{p}\|_{L^2(\Omega)} \leq C_\Omega^{(1)} \left(\alpha C_\Gamma \|\nabla\mathbf{v}\|_{L^2(\Omega)} + \beta\kappa \|\mathbf{f}\|_{L^2(\Omega)} \right), \tag{4.5}$$

where $C_\Omega^{(1)}$ is a constant which only depends on Ω. Using this auxiliary pressure, the problem defined by (4.4) can be rewritten as

$$\begin{cases} -\Delta \mathbf{v} + \nabla\left(\dfrac{p-\tilde{p}}{\mu}\right) = \dfrac{\rho}{\mu}\mathbf{f} - \dfrac{\nabla\tilde{p}}{\mu}, & \text{in } \Omega, \\ \operatorname{div}(\mathbf{v}) = 0, & \text{in } \Omega, \\ \mathbf{v} = 0, & \text{on } \Gamma_\ell, \\ \nabla\mathbf{v}\cdot\mathbf{n} - \dfrac{p-\tilde{p}}{\mu}\mathbf{n} = 0, & \text{on } \Gamma_0, \\ \nabla\mathbf{v}\cdot\mathbf{n} - \dfrac{p-\tilde{p}}{\mu}\mathbf{n} = 0, & \text{on } \Gamma_W. \end{cases}$$

As a consequence, from regularity results that can be found in [41] in the case of right angles, there exists $\epsilon > 0$ such that

$$\|\mathbf{v}\|_{H^{\frac{3}{2}+\epsilon}(\Omega)} \leq C_\Omega^{(2)}\left(\frac{\rho}{\mu}\|\mathbf{f}\|_{L^2(\Omega)} + \frac{\|\nabla\tilde{p}\|_{L^2(\Omega)}}{\mu}\right),$$

where $C_\Omega^{(2)}$ is a constant which only depends on Ω. Using estimate (4.5), we get

$$\|\mathbf{v}\|_{H^{\frac{3}{2}+\epsilon}(\Omega)} \leq C_\Omega^{(2)}\left(\frac{\rho}{\mu} + C_\Omega^{(1)}\kappa\frac{\beta}{\mu}\right)\|\mathbf{f}\|_{L^2(\Omega)} + C_\Omega^{(2)}C_\Omega^{(1)}C_\Gamma\frac{\alpha}{\mu}\|\nabla\mathbf{v}\|_{L^2(\Omega)}.$$

By (4.1) and since $\mathbf{f} = A_{\mu,\alpha}\mathbf{v}$, we obtain

$$\|\mathbf{v}\|_{H^{\frac{3}{2}+\epsilon}(\Omega)} \leq \left[C_\Omega^{(2)}\left(\frac{\rho}{\mu} + C_\Omega^{(1)}\kappa\frac{\beta}{\mu}\right) + C_\Omega^{(2)}C_\Omega^{(1)}C_\Gamma\frac{\alpha}{\mu}\mathfrak{L}\right]\|A_{\mu,\alpha}\mathbf{v}\|_{L^2(\Omega)},$$

which concludes the proof of (4.2). □

Remark 4.5. *If we impose only the normal component of the velocity to be free, namely* $\mathbf{u}\cdot\boldsymbol{\tau} = 0$ *and* $(\boldsymbol{\sigma}\cdot\mathbf{n})\cdot\mathbf{n} = 0$*, then the Stokes-like operator has to be slightly adapted and it will be defined on* $\mathbf{H}_{\boldsymbol{\tau}} = \overline{\mathbf{V}_{\boldsymbol{\tau}}}^{L^2}$ *with*

$$\mathbf{V}_{\boldsymbol{\tau}} = \{\mathbf{v} \in L^2(\Omega),\ \operatorname{div}(\mathbf{v}) = 0,\ \mathbf{v}\cdot\mathbf{n} = 0 \text{ on } \Gamma_\ell,\ \mathbf{v}\cdot\boldsymbol{\tau} = 0 \text{ on } \Gamma_0\cup\Gamma_W\}.$$

The only difference concerns Lemma 4.3 and lies in the regularity properties associated to this operator. In particular in this case, due to the symmetry properties of the Stokes solution, $\mathcal{D}(A_{\mu,\alpha}) \subset H^2(\Omega)$ *and not only in* $H^{\frac{3}{2}+\epsilon}(\Omega)$*. Consequently the solution velocity* $\mathbf{u}$ *will then belong to* $L^2(0,T;\mathcal{D}(A_{\mu,\alpha})) \subset L^2(0,T;H^2(\Omega))$*.*

Now that we have introduced an appropriate Stokes-like operator adapted to our coupled Navier–Stokes–Windkessel system we can derive estimates in suitable norms for this system. The idea relies on the formal choice of $\mathbf{u}$ and $A_{\mu,\alpha}\mathbf{u}$ as test functions and then a linear combination of the obtained inequalities. We will consider two cases.

- the *so-called general case* for which we prove an estimate valid for small time;
- the *so-called dissipative case*, with $\tau < +\infty$, for which we prove that, if the initial data and applied pressures are small enough, an "energy" decrease can be established.

Theorem 4.6 (Estimates for the Navier–Stokes system)**.** *Let* $\mu > 0$*. Assume that the artificial boundaries* Γ_0 *and* Γ_W *meet the lateral boundaries* Γ_ℓ *at angle* $\frac{\pi}{2}$ *and that each boundary is smooth enough. Assume that* $\alpha \geq 0$*,* $\beta \geq 0$*,* $\gamma > 0$*.*

- **General case: local-in-time "energy" bound for any data**. *Assume that* $0 < \tau \leq +\infty$*. For any smooth solution* $\mathbf{u}$ *of the Problem (2.7), there exists* $T^* > 0$ *and* $t \mapsto G_r(t)$ *which depend on the data such that, for*

all $t \in (0, T^*)$*:*

$$\frac{\rho}{2}\|\mathbf{u}(t,\cdot)\|^2_{L^2(\Omega)} + \frac{\mu}{4}\int_0^t \|\nabla\mathbf{u}(s,\cdot)\|^2_{L^2(\Omega)}\,\mathrm{d}s + \frac{\beta}{2}Q^2(t) + \alpha\int_0^t Q^2(s)\,\mathrm{d}s + \frac{\gamma}{2}V^2(t) + \frac{\gamma}{\tau}\int_0^t V^2(s)\,\mathrm{d}s$$
$$+ra_{\mu,\alpha}(\mathbf{u}(t,\cdot),\mathbf{u}(t,\cdot)) + \frac{r}{2}\int_0^t \|A_{\mu,\alpha}\mathbf{u}(s,\cdot)\|^2_{\rho,\beta}\,\mathrm{d}s \le G_r(t), \quad (4.6)$$

where r *is any positive homogeneity constant.*

- **Dissipative case: global-in-time "energy" bound for small data.** *Assume furthermore that* $\tau < +\infty$*. Let* $\delta > 0$ *and* $\eta > 0$ *such that*

$$\delta + \frac{\kappa^2\tau\gamma}{2\rho}\eta = \frac{1}{2}.$$

Define

$$H(t) := \left(\frac{C_\Gamma^2}{2\mu} + \frac{\eta\kappa^2}{4\delta\rho}\right)\mathcal{P}^2(t).$$

There exists a dissipation parameter $\mathcal{D} > 0$ *(defined by (4.28)) such that, if the initial data and external forces are small enough, namely*

$$\frac{\rho}{2}\|\mathbf{u}_0\|^2_{L^2(\Omega)} + \frac{\eta\mu}{2}\|\nabla\mathbf{u}_0\|^2_{L^2(\Omega)} + \frac{\eta\alpha+\beta}{2}Q^2(0) \le \mathcal{E} := \frac{\mu\eta^3}{32\left(\eta\mathcal{M} + C_\Omega^{(3)}\mathcal{L}^2\right)^2},$$

and

$$\|H\|_\infty \le \mathcal{D}\mathcal{E},$$

then the solution satisfies a stability estimate:

$$\frac{\rho}{2}\|\mathbf{u}(t,\cdot)\|^2_{L^2(\Omega)} + \frac{\eta\mu}{2}\|\nabla\mathbf{u}(t,\cdot)\|^2_{L^2(\Omega)} + \frac{\eta\alpha+\beta}{2}Q^2(t) + \frac{\gamma}{2}V^2(t) \le \mathcal{E}. \quad (4.7)$$

Moreover $t \mapsto \int_0^t \|A_{\mu,\alpha}\mathbf{u}(s,\cdot)\|^2_{\rho,\beta}\,\mathrm{d}s$ *is also bounded on any time interval* $[0,T]$*.*

Proof. Let us derive the estimates in the general case, then in the *so-called* dissipative case. Note that all the following formal calculations can be justified by using Galerkin approximation with a special basis associated to the eigenfunctions of the operator $A_{\mu,\alpha}$, see Proposition 4.2.

General case. Taking $\mathbf{u}$ as a test function in the variational formulation (2.7), we proceed as for the Stokes–Windkessel system and obtain estimate (3.6) with an additional term $\rho\int_\Omega(\mathbf{u}\nabla)\mathbf{u}\,\mathbf{u}$ that we bound as follows:

$$\left|\rho\int_\Omega[(\mathbf{u}\cdot\nabla)\mathbf{u}]\cdot\mathbf{u}\right| \le \rho\|\nabla\mathbf{u}\|_{L^2(\Omega)}\|\mathbf{u}\|^2_{L^4(\Omega)} \le C_\Omega^{(3)}\rho\|\nabla\mathbf{u}\|^3_{L^2(\Omega)}, \quad (4.8)$$

where $C_\Omega^{(3)}$ is a constant related to the continuous embedding of $H^1(\Omega)$ onto $L^4(\Omega)$. The estimate writes

$$\frac{\rho}{2}\frac{\mathrm{d}}{\mathrm{d}t}\|\mathbf{u}(t,\cdot)\|^2_{L^2(\Omega)} + \frac{\mu}{2}\|\nabla\mathbf{u}(t,\cdot)\|^2_{L^2(\Omega)} + \frac{\beta}{2}\frac{\mathrm{d}}{\mathrm{d}t}Q^2(t) + \alpha Q^2(t) + \frac{\gamma}{2}\frac{\mathrm{d}}{\mathrm{d}t}V^2(t) + \frac{\gamma}{\tau}V^2(t)$$
$$\le \frac{C_\Gamma^2}{2\mu}\mathcal{P}^2(t) + C_\Omega^{(3)}\rho\|\nabla\mathbf{u}(t,\cdot)\|^3_{L^2(\Omega)}. \quad (4.9)$$

To control the last term in (4.9), we need to control $\mathbf{u}$ in $L^\infty(0,T;H^1(\Omega))$. Thus we take $A_{\mu,\alpha}\mathbf{u}$ as a test function in the variational formulation (2.7). By definition of the operator $A_{\mu,\alpha}$, see Definition 4.1, we have

$$\frac{1}{2}\frac{\mathrm{d}}{\mathrm{d}t}a_{\mu,\alpha}(\mathbf{u}(t,\cdot),\mathbf{u}(t,\cdot)) + \|A_{\mu,\alpha}\mathbf{u}(t,\cdot)\|^2_{\rho,\beta}$$
$$= -\rho\int_\Omega(\mathbf{u}\nabla)\mathbf{u}(t,\cdot)\,A_{\mu,\alpha}\mathbf{u}(t,\cdot) - \gamma V(t)\left(\int_{\Gamma_W}A_{\mu,\alpha}\mathbf{u}(t,\cdot)\cdot\mathbf{n}\right) - \mathcal{P}(t)\int_{\Gamma_W}A_{\mu,\alpha}\mathbf{u}(t,\cdot)\cdot\mathbf{n}. \quad (4.10)$$

The convection term can be estimated as follows

$$\left|\rho\int_\Omega (\mathbf{u}\nabla)\mathbf{u}\, A_{\mu,\alpha}\mathbf{u}\right| \le \rho\,\|\mathbf{u}\|_{L^\infty(\Omega)}\,\|\nabla\mathbf{u}\|_{L^2(\Omega)}\,\|A_{\mu,\alpha}\mathbf{u}\|_{L^2(\Omega)}\,.$$

Thanks to the continuous embedding of $H^{\frac{3}{2}+\epsilon'}(\Omega)$ in $L^\infty(\Omega)$, we have, for every $\epsilon'>0$,

$$\|\mathbf{u}\|_{L^\infty(\Omega)} \le C_\Omega^{(4)}\,\|\mathbf{u}\|_{H^{\frac{3}{2}+\epsilon'}(\Omega)}\,.$$

Then, choosing $\epsilon'<\epsilon$ where ϵ is defined in Lemma 4.3, by a Hilbert interpolation combined with Lemma 4.3 there exists $\theta\in(0,1)$ such that

$$\|\mathbf{u}\|_{L^\infty(\Omega)} \le C_\Omega^{(5)}\mathcal{M}^{1-\theta}\,\|A_{\mu,\alpha}\mathbf{u}\|_{L^2(\Omega)}^{1-\theta}\,\|\nabla\mathbf{u}\|_{L^2(\Omega)}^{\theta}\,.$$

Consequently,

$$\left|\rho\int_\Omega (\mathbf{u}\nabla)\mathbf{u}\, A_{\mu,\alpha}\mathbf{u}\right| \le C_\Omega^{(5)}\rho\mathcal{M}^{1-\theta}\,\|A_{\mu,\alpha}\mathbf{u}\|_{L^2(\Omega)}^{2-\theta}\,\|\nabla\mathbf{u}\|_{L^2(\Omega)}^{1+\theta}\,.$$

Using Young's inequality, we get

$$\begin{aligned}\left|\rho\int_\Omega (\mathbf{u}\nabla)\mathbf{u}\, A_{\mu,\alpha}\mathbf{u}\right| &\le \delta\rho\,\|A_{\mu,\alpha}\mathbf{u}\|_{L^2(\Omega)}^2 + C_{\Omega,\delta}\rho\mathcal{M}^{\frac{2(1-\theta)}{\theta}}\,\|\nabla\mathbf{u}\|_{L^2(\Omega)}^{\frac{2(1+\theta)}{\theta}}\\ &\le \delta\,\|A_{\mu,\alpha}\mathbf{u}\|_{\rho,\beta}^2 + C_{\Omega,\delta}\rho\mathcal{M}^{\frac{2(1-\theta)}{\theta}}\,\|\nabla\mathbf{u}\|_{L^2(\Omega)}^{\frac{2(1+\theta)}{\theta}}\,,\end{aligned} \tag{4.11}$$

where $\delta>0$ will be chosen later on and $C_{\Omega,\delta}$ is a constant which depends on δ^{-1} and Ω only. Let us now deal with terms like $\gamma V(t)(\int_{\Gamma_W} A_{\mu,\alpha}\mathbf{u}(t,\cdot)\cdot\mathbf{n})$, for which we need a control of the auxiliary volume V defined by (3.2). This control will be provided by estimate (4.9). By using Lemma 2.4, the definition of $\|\cdot\|_{\rho,\beta}$ and Young's inequality, we have

$$\left|\gamma V\int_{\Gamma_W} A_{\mu,\alpha}\mathbf{u}\cdot\mathbf{n}\right| \le \frac{\kappa\,|\gamma V|}{\sqrt{\rho}}\,\|A_{\mu,\alpha}\mathbf{u}\|_{\rho,\beta} \le \frac{\kappa^2}{4\delta\rho}(\gamma V)^2 + \delta\,\|A_{\mu,\alpha}\mathbf{u}\|_{\rho,\beta}^2\,. \tag{4.12}$$

The linear forcing terms can be treated similarly:

$$\left|\mathcal{P}\int_{\Gamma_W} A_{\mu,\alpha}\mathbf{u}\cdot\mathbf{n}\right| \le \frac{\kappa\,|\mathcal{P}|}{\sqrt{\rho}}\,\|A_{\mu,\alpha}\mathbf{u}\|_{\rho,\beta} \le \frac{\kappa^2}{4\delta\rho}\mathcal{P}^2 + \delta\,\|A_{\mu,\alpha}\mathbf{u}\|_{\rho,\beta}^2\,. \tag{4.13}$$

Thus, from (4.10) and thanks the previous estimates (4.11), (4.12), (4.13), we obtain

$$\frac{1}{2}\frac{\mathrm{d}}{\mathrm{d}t}a_{\mu,\alpha}(\mathbf{u}(t,\cdot),\mathbf{u}(t,\cdot))+(1-3\delta)\,\|A_{\mu,\alpha}\mathbf{u}(t,\cdot)\|_{\rho,\beta}^2 \le C_{\Omega,\delta}\rho\mathcal{M}^{\frac{2(1-\theta)}{\theta}}\,\|\nabla\mathbf{u}(t,\cdot)\|_{L^2(\Omega)}^{\frac{2(1+\theta)}{\theta}}+\frac{\kappa^2}{4\delta\rho}(\gamma V)^2(t)+\frac{\kappa^2}{4\delta\rho}\mathcal{P}^2(t). \tag{4.14}$$

We next choose $\delta>0$ such that $1-3\delta>0$, for instance

$$1-3\delta=\frac{1}{2}, \tag{4.15}$$

i.e. $\delta=\frac{1}{6}$ and we denote $C_\Omega^{(6)}:=C_{\Omega,\frac{1}{6}}$. Using (4.15), we add (4.9) and (4.14) that has been multiplied by a positive homogeneity constant r to obtain:

$$\begin{aligned}&\frac{\rho}{2}\frac{\mathrm{d}}{\mathrm{d}t}\|\mathbf{u}(t,\cdot)\|_{L^2(\Omega)}^2+\frac{\mu}{2}\|\nabla\mathbf{u}(t,\cdot)\|_{L^2(\Omega)}^2+\frac{\beta}{2}\frac{\mathrm{d}}{\mathrm{d}t}Q^2(t)+\alpha Q^2(t)+\frac{\gamma}{2}\frac{\mathrm{d}}{\mathrm{d}t}V^2(t)+\frac{\gamma}{\tau}V^2(t)\\ &\qquad+\frac{r}{2}\frac{\mathrm{d}}{\mathrm{d}t}a_{\mu,\alpha}(\mathbf{u}(t,\cdot),\mathbf{u}(t,\cdot))+\frac{r}{2}\,\|A_{\mu,\alpha}\mathbf{u}(t,\cdot)\|_{\rho,\beta}^2\\ &\le\left(\frac{C_\Gamma^2}{2\mu}+\frac{3r\kappa^2}{2\rho}\right)\mathcal{P}^2(t)+C_\Omega^{(3)}\rho\,\|\nabla\mathbf{u}(t,\cdot)\|_{L^2(\Omega)}^3+rC_\Omega^{(6)}\rho\mathcal{M}^{\frac{2(1-\theta)}{\theta}}\,\|\nabla\mathbf{u}(t,\cdot)\|_{L^2(\Omega)}^{\frac{2(1+\theta)}{\theta}}+\frac{3r\kappa^2}{2\rho}(\gamma V)^2(t).\end{aligned} \tag{4.16}$$

Thus we can apply a nonlinear Gronwall lemma by setting

$$\varphi(t) = \frac{\rho}{2}\|\mathbf{u}(t,\cdot)\|^2_{L^2(\Omega)} + \frac{\beta}{2}Q^2(t) + \frac{\gamma}{2}V^2(t) + \frac{r}{2}a_{\mu,\alpha}(\mathbf{u}(t,\cdot),\mathbf{u}(t,\cdot)),$$

which, by (4.16) and since $\|\nabla\mathbf{u}(t,\cdot)\|^2_{L^2(\Omega)} \le \frac{1}{\mu}a_{\mu,\alpha}(\mathbf{u}(t,\cdot),\mathbf{u}(t,\cdot))$, satisfies the following inequality:

$$\frac{\mathrm{d}}{\mathrm{d}t}\varphi(t) \le F(t) + \frac{3\kappa^2\gamma}{\rho r}\varphi(t) + C_\Omega^{(3)}\frac{2^{\frac{3}{2}}\rho}{(r\mu)^{\frac{3}{2}}}\varphi^{3/2}(t) + C_\Omega^{(6)}\frac{2^{\frac{1+\theta}{\theta}}\rho}{r^{\frac{1}{\theta}}\mu^{\frac{(1+\theta)}{\theta}}}\mathcal{M}^{\frac{2(1-\theta)}{\theta}}\varphi^{\frac{(1+\theta)}{\theta}}(t),$$

with

$$F(t) = \left(\frac{C_\Gamma^2}{2\mu} + \frac{3r\kappa^2}{2\rho}\right)\mathcal{P}^2(t).$$

Consequently, we obtain a stability estimate at least for a small time T^* (depending on the data of the problem). From this bound on φ one can deduce that

$$\int_0^t \|A_{\mu,\alpha}\mathbf{u}(s,\cdot)\|^2_{\rho,\beta}\,\mathrm{d}s$$

is also bounded on $(0,T^*)$.

- **Dissipative case** $\tau < +\infty$.

Next we further investigate the case $\tau < +\infty$. In this case, as already underlined for the Stokes system, the auxiliary volume V, defined by (3.2), is dissipated by the system. We take advantage of this to derive a stability estimate for any time but for small enough data. When taking $\mathbf{u}$ as a test function in the variational formulation (2.7), we bound the convective term in a coarser way than we did previously: using inequality (4.1) in Lemma 4.3 and the definition of $\|\cdot\|_{\rho,\beta}$ we get

$$\begin{aligned}\left|\rho\int_\Omega(\mathbf{u}\nabla)\mathbf{u}\,\mathbf{u}\right| &\le \rho\,\|\nabla\mathbf{u}\|_{L^2(\Omega)}\,\|\mathbf{u}\|^2_{L^4(\Omega)}\\ &\le C_\Omega^{(3)}\rho\mathcal{L}^2\,\|A_{\mu,\alpha}\mathbf{u}\|^2_{L^2(\Omega)}\,\|\nabla\mathbf{u}\|_{L^2(\Omega)}\\ &\le C_\Omega^{(3)}\mathcal{L}^2\,\|A_{\mu,\alpha}\mathbf{u}\|^2_{\rho,\beta}\,\|\nabla\mathbf{u}\|_{L^2(\Omega)},\end{aligned} \tag{4.17}$$

where, as in inequality (4.8), constant $C_\Omega^{(3)}$ is related to the continuous embedding of $H^1(\Omega)$ onto $L^4(\Omega)$. The estimate now writes

$$\begin{aligned}&\frac{\rho}{2}\frac{\mathrm{d}}{\mathrm{d}t}\|\mathbf{u}(t,\cdot)\|^2_{L^2(\Omega)} + \frac{\mu}{2}\|\nabla\mathbf{u}(t,\cdot)\|^2_{L^2(\Omega)} + \frac{\beta}{2}\frac{\mathrm{d}}{\mathrm{d}t}Q^2(t) + \alpha Q^2(t) + \frac{\gamma}{2}\frac{\mathrm{d}}{\mathrm{d}t}V^2(t) + \frac{\gamma}{\tau}V^2(t)\\ &\qquad\le \frac{C_\Gamma^2}{2\mu}\mathcal{P}^2(t) + C_\Omega^{(3)}\mathcal{L}^2\,\|A_{\mu,\alpha}\mathbf{u}(t,\cdot)\|^2_{\rho,\beta}\,\|\nabla\mathbf{u}(t,\cdot)\|_{L^2(\Omega)}.\end{aligned} \tag{4.18}$$

Next we take $A_{\mu,\alpha}\mathbf{u}$ as a test function in the variational formulation (2.7). First the convective term can be bounded as follows

$$\begin{aligned}\left|\rho\int_\Omega(\mathbf{u}\nabla)\mathbf{u}\,A_{\mu,\alpha}\mathbf{u}\right| \le \rho\,\|\mathbf{u}\|_{L^\infty(\Omega)}\,\|\nabla\mathbf{u}\|_{L^2(\Omega)}\,\|A_{\mu,\alpha}\mathbf{u}\|_{L^2(\Omega)} &\le \rho\mathcal{M}\,\|A_{\mu,\alpha}\mathbf{u}\|^2_{L^2(\Omega)}\,\|\nabla\mathbf{u}\|_{L^2(\Omega)}\\ &\le \mathcal{M}\,\|A_{\mu,\alpha}\mathbf{u}\|^2_{\rho,\beta}\,\|\nabla\mathbf{u}\|_{L^2(\Omega)},\end{aligned} \tag{4.19}$$

where we have used the continuity of the embedding $H^{\frac{3}{2}+\epsilon}(\Omega) \hookrightarrow L^\infty(\Omega)$ together with estimate (4.2) of Lemma 4.3 and the definition of $\|\cdot\|_{\rho,\beta}$. Let us now deal with the term $\gamma V(\int_{\Gamma_W} A_{\mu,\alpha}\mathbf{u}\cdot\mathbf{n})$. Using Lemma 2.4, Young's inequality and the definition of $\|\cdot\|_{\rho,\beta}$, and taking advantage of $\tau < +\infty$, leads to

$$\gamma\left|V\left(\int_{\Gamma_W} A_{\mu,\alpha}\mathbf{u}\cdot\mathbf{n}\right)\right| \le \gamma\kappa\,|V|\,\|A_{\mu,\alpha}\mathbf{u}\|_{L^2(\Omega)} \le \frac{1}{2}\frac{\gamma}{\eta\tau}V^2 + \frac{\eta\tau\kappa^2}{2}\gamma\,\|A_{\mu,\alpha}\mathbf{u}\|^2_{L^2(\Omega)}$$
$$\le \frac{\gamma}{2\eta\tau}V^2 + \frac{\tau\kappa^2\gamma}{2\rho}\eta\,\|A_{\mu,\alpha}\mathbf{u}\|^2_{\rho,\beta}\,, \tag{4.20}$$

where $\eta > 0$ will be chosen later on. The linear forcing terms are bounded as in the general case, see (4.13). Thus, by (4.10), (4.19), (4.20) and (4.13), we obtain

$$\frac{1}{2}\frac{\mathrm{d}}{\mathrm{d}t}a_{\mu,\alpha}(\mathbf{u}(t,\cdot),\mathbf{u}(t,\cdot)) + \|A_{\mu,\alpha}\mathbf{u}(t,\cdot)\|^2_{\rho,\beta}$$
$$\le \mathcal{M}\,\|A_{\mu,\alpha}\mathbf{u}(t,\cdot)\|^2_{\rho,\beta}\,\|\nabla\mathbf{u}(t,\cdot)\|_{L^2(\Omega)} + \frac{\gamma}{2\eta\tau}V^2(t) + \frac{\kappa^2}{4\delta\rho}\mathcal{P}^2(t) + \left(\delta + \frac{\kappa^2\tau\gamma}{2\rho}\eta\right)\|A_{\mu,\alpha}\mathbf{u}(t,\cdot)\|^2_{\rho,\beta}\,. \tag{4.21}$$

By choosing δ and η sufficiently small such that

$$\delta + \frac{\kappa^2\tau\gamma}{2\rho}\eta = \frac{1}{2}, \tag{4.22}$$

we obtain

$$\frac{1}{2}\frac{\mathrm{d}}{\mathrm{d}t}a_{\mu,\alpha}(\mathbf{u}(t,\cdot),\mathbf{u}(t,\cdot)) + \frac{1}{2}\|A_{\mu,\alpha}\mathbf{u}(t,\cdot)\|^2_{\rho,\beta}$$
$$\le \mathcal{M}\,\|A_{\mu,\alpha}\mathbf{u}(t,\cdot)\|^2_{\rho,\beta}\,\|\nabla\mathbf{u}(t,\cdot)\|_{L^2(\Omega)} + \frac{\gamma}{2\eta\tau}V^2(t) + \frac{\kappa^2}{4\delta\rho}\mathcal{P}^2(t). \tag{4.23}$$

We multiply (4.23) by η and add (4.18) to obtain:

$$\frac{\mathrm{d}}{\mathrm{d}t}\left(\frac{\rho}{2}\|\mathbf{u}(t,\cdot)\|^2_{L^2(\Omega)} + \frac{\eta}{2}a_{\mu,\alpha}(\mathbf{u}(t,\cdot),\mathbf{u}(t,\cdot)) + \frac{\beta}{2}Q^2(t) + \frac{\gamma}{2}V^2(t)\right) + \frac{\mu}{2}\|\nabla\mathbf{u}(t,\cdot)\|^2_{L^2(\Omega)} + \alpha Q^2(t) + \frac{\gamma}{2\tau}V^2(t)$$
$$+ \left(\frac{\eta}{2} - (\eta\mathcal{M} + C_\Omega^{(3)}\mathcal{L}^2)\,\|\nabla\mathbf{u}(t,\cdot)\|_{L^2(\Omega)}\right)\|A_{\mu,\alpha}\mathbf{u}(t,\cdot)\|^2_{\rho,\beta} \le \left(\frac{C_\Gamma^2}{2\mu} + \frac{\eta\kappa^2}{4\delta\rho}\right)\mathcal{P}^2(t).$$

Recalling the definition of $a_{\mu,\alpha}(\cdot,\cdot)$ (see Def. 4.1) we get

$$\frac{\mathrm{d}}{\mathrm{d}t}\left(\frac{\rho}{2}\|\mathbf{u}(t,\cdot)\|^2_{L^2(\Omega)} + \frac{\eta\mu}{2}\|\nabla\mathbf{u}(t,\cdot)\|^2_{L^2(\Omega)} + \frac{\eta\alpha+\beta}{2}Q^2(t) + \frac{\gamma}{2}V^2(t)\right) + \frac{\mu}{2}\|\nabla\mathbf{u}(t,\cdot)\|^2_{L^2(\Omega)} + \alpha Q^2(t) + \frac{\gamma}{2\tau}V^2(t)$$
$$+ \left(\frac{\eta}{2} - (\eta\mathcal{M} + C_\Omega^{(3)}\mathcal{L}^2)\,\|\nabla\mathbf{u}(t,\cdot)\|_{L^2(\Omega)}\right)\|A_{\mu,\alpha}\mathbf{u}(t,\cdot)\|^2_{\rho,\beta} \le \left(\frac{C_\Gamma^2}{2\mu} + \frac{\eta\kappa^2}{4\delta\rho}\right)\mathcal{P}^2(t).$$

Next we want to make appear some dissipation of

$$\Psi(t) := \frac{\rho}{2}\|\mathbf{u}(t,\cdot)\|^2_{L^2(\Omega)} + \frac{\eta\mu}{2}\|\nabla\mathbf{u}(t,\cdot)\|^2_{L^2(\Omega)} + \frac{\eta\alpha+\beta}{2}Q^2(t) + \frac{\gamma}{2}V^2(t),$$

even in the case $\alpha = 0$ and $\beta > 0$. Since $|Q| \le C_\Gamma\,\|\nabla\mathbf{u}\|_{L^2(\Omega)}$, we have that

$$\frac{\mu}{2}\|\nabla\mathbf{u}(t,\cdot)\|^2_{L^2(\Omega)} \ge \frac{\mu}{4}\|\nabla\mathbf{u}(t,\cdot)\|^2_{L^2(\Omega)} + \frac{\mu}{4C_\Gamma^2}Q^2(t)$$

and thus

$$\frac{\mathrm{d}}{\mathrm{d}t}\left(\frac{\rho}{2}\|\mathbf{u}(t,\cdot)\|^2_{L^2(\Omega)}+\frac{\eta\mu}{2}\|\nabla\mathbf{u}(t,\cdot)\|^2_{L^2(\Omega)}+\frac{\eta\alpha+\beta}{2}Q^2(t)+\frac{\gamma}{2}V^2(t)\right)+\frac{\mu}{4}\|\nabla\mathbf{u}(t,\cdot)\|^2_{L^2(\Omega)}+\left(\alpha+\frac{\mu}{4C_\Gamma^2}\right)Q^2(t)$$
$$+\frac{\gamma}{2\tau}V^2(t)+\left(\frac{\eta}{2}-(\eta\mathcal{M}+C_\Omega^{(3)}\mathcal{L}^2)\|\nabla\mathbf{u}(t,\cdot)\|_{L^2(\Omega)}\right)\|A_{\mu,\alpha}\mathbf{u}(t,\cdot)\|^2_{\rho,\beta}\leq\left(\frac{C_\Gamma^2}{2\mu}+\frac{\eta\kappa^2}{4\delta\rho}\right)\mathcal{P}^2(t).$$

Then, since $\|\mathbf{u}\|_{L^2(\Omega)}\leq C_P\|\nabla\mathbf{u}\|_{L^2(\Omega)}$ by Poincaré inequality,

$$\frac{\mu}{4}\|\nabla\mathbf{u}(t,\cdot)\|^2_{L^2(\Omega)}\geq\frac{\mu}{8}\|\nabla\mathbf{u}(t,\cdot)\|^2_{L^2(\Omega)}+\frac{\mu}{8C_P^2}\|\mathbf{u}(t,\cdot)\|^2_{L^2(\Omega)},$$

we thus obtain

$$\begin{aligned}\frac{\mathrm{d}}{\mathrm{d}t}&\left(\frac{\rho}{2}\|\mathbf{u}(t,\cdot)\|^2_{L^2(\Omega)}+\frac{\eta\mu}{2}\|\nabla\mathbf{u}(t,\cdot)\|^2_{L^2(\Omega)}+\frac{\eta\alpha+\beta}{2}Q^2(t)+\frac{\gamma}{2}V^2(t)\right)\\&+\frac{\mu}{8C_P^2}\|\mathbf{u}(t,\cdot)\|^2_{L^2(\Omega)}+\frac{\mu}{8}\|\nabla\mathbf{u}(t,\cdot)\|^2_{L^2(\Omega)}\\&+\left(\alpha+\frac{\mu}{4C_\Gamma^2}\right)Q^2(t)+\frac{\gamma}{2\tau}V^2(t)+\left(\frac{\eta}{2}-(\eta\mathcal{M}+C_\Omega^{(3)}\mathcal{L}^2)\|\nabla\mathbf{u}(t,\cdot)\|_{L^2(\Omega)}\right)\|A_{\mu,\alpha}\mathbf{u}(t,\cdot)\|^2_{\rho,\beta}\\&\leq\left(\frac{C_\Gamma^2}{2\mu}+\frac{\eta\kappa^2}{4\delta\rho}\right)\mathcal{P}^2(t).\end{aligned}\tag{4.24}$$

Estimate (4.24) can be rewritten as

$$\frac{\mathrm{d}}{\mathrm{d}t}\Psi(t)+\mathcal{D}\Psi(t)+\left(\mathcal{A}-\mathcal{B}\|\nabla\mathbf{u}(t,\cdot)\|_{L^2(\Omega)}\right)\|A_{\mu,\alpha}\mathbf{u}(t,\cdot)\|^2_{\rho,\beta}\leq H(t),\tag{4.25}$$

with

$$\mathcal{A}:=\frac{\eta}{2},\quad\mathcal{B}:=\eta\mathcal{M}+C_\Omega^{(3)}\mathcal{L}^2,\tag{4.26}$$

$$H(t):=\left(\frac{C_\Gamma^2}{2\mu}+\frac{\eta\kappa^2}{4\delta\rho}\right)\mathcal{P}^2(t),\tag{4.27}$$

and a dissipation coefficient defined as

$$\mathcal{D}:=\min\left(\frac{1}{\tau},\frac{\mu}{4\rho C_P^2},\frac{1}{4\eta},\frac{2\alpha+\frac{\mu}{2C_\Gamma^2}}{\eta\alpha+\beta}\right).\tag{4.28}$$

The constant $\mathcal{D}$ stands for the dissipation of the system. In particular, assuming that $\tau<+\infty$ ensures that the 0D model is indeed dissipative with respect to the volume V if the data are small enough. Assuming that $\mathcal{A}-\mathcal{B}\|\nabla\mathbf{u}(t,\cdot)\|_{L^2(\Omega)}\geq 0$, we obtain by Gronwall lemma:

$$\Psi(t)\leq\Psi(0)\mathrm{e}^{-\mathcal{D}t}+\int_0^t|H(s)|\,\mathrm{e}^{\mathcal{D}(s-t)}\,\mathrm{d}s\leq\Psi(0)\mathrm{e}^{-\mathcal{D}t}+\frac{\|H\|_\infty}{\mathcal{D}}(1-\mathrm{e}^{-\mathcal{D}t}).\tag{4.29}$$

Consequently if

$$\Psi(0)\leq\frac{\eta\mu}{8}\frac{\mathcal{A}^2}{\mathcal{B}^2},\qquad\frac{\|H\|_\infty}{\mathcal{D}}\leq\frac{\eta\mu}{8}\frac{\mathcal{A}^2}{\mathcal{B}^2},\tag{4.30}$$

which implies that $\|\nabla\mathbf{u}_0\|_{L^2(\Omega)}\leq\frac{\mathcal{A}}{2\mathcal{B}}$, then we obtain the following estimate for all time:

$$\forall t\geq 0,\qquad\Psi(t)\leq\frac{\eta\mu}{8}\frac{\mathcal{A}^2}{\mathcal{B}^2}.$$

To conclude, provided that the initial data and the source term are small enough (see conditions (4.30)), the solution satisfies a stability estimate in suitable norms, namely

$$\frac{\rho}{2}\|\mathbf{u}(t,\cdot)\|^2_{L^2(\Omega)} + \frac{\eta\mu}{2}\|\nabla\mathbf{u}(t,\cdot)\|^2_{L^2(\Omega)} + \frac{\eta\alpha+\beta}{2}Q^2(t) + \frac{\gamma}{2}V^2(t) \le \mathcal{E} = \frac{\mu\eta^3}{32\left(\eta\mathcal{M} + C^{(3)}_\Omega\mathcal{L}^2\right)^2}.$$

Finally, combining this estimate with (4.25) allows us to conclude that

$$\int_0^t \|A_{\mu,\alpha}\mathbf{u}(s,\cdot)\|^2_{\rho,\beta}\,\mathrm{d}s$$

is also bounded on any time interval $[0,T]$. □

Remark 4.7. *This theorem shows as for the Stokes–Windkessel system that typical 0D models used in blood flows and in airflows modeling behave in a different way. Indeed for the RCR model for instance we obtain global-in-time estimates provided the data are small enough whereas for the RC model we obtain only local-in-time estimates.*

Remark 4.8. *In the dissipative case, parameters δ and η may be specified, for instance as follows:*

$$\delta = \frac{1}{4}, \qquad \eta = \frac{\rho}{2\kappa^2\tau\gamma}.$$

As a consequence, updating the constants and source terms as

$$\mathcal{A} := \frac{\rho}{4\kappa^2\tau\gamma},\ \mathcal{B} := \frac{\rho}{2\kappa^2\tau\gamma}\mathcal{M} + C^{(3)}_\Omega\mathcal{L}^2,\ \mathcal{D} := \min\left(\frac{1}{\tau}, \frac{\kappa^2\tau\gamma}{2\rho}, \frac{\alpha+\frac{\mu}{4C^2_\Gamma}}{\frac{\rho\alpha}{4\kappa^2\tau\gamma}+\frac{\beta}{2}}, \frac{\mu}{4\rho C^2_P}\right), \quad H(t) := \left(\frac{C^2_\Gamma}{2\mu} + \frac{1}{2\tau\gamma}\right)\mathcal{P}^2(t),$$

we deduce that, if

$$\Psi(0) \le \frac{\rho\mu}{16\kappa^2\tau\gamma}\frac{\mathcal{A}^2}{\mathcal{B}^2}, \qquad \frac{\|H\|_\infty}{\mathcal{D}} \le \frac{\rho\mu}{16\kappa^2\tau\gamma}\frac{\mathcal{A}^2}{\mathcal{B}^2},$$

the estimate now reads:

$$\frac{\rho}{2}\|\mathbf{u}(t,\cdot)\|^2_{L^2(\Omega)} + \frac{\rho\mu}{4\kappa^2\tau\gamma}\|\nabla\mathbf{u}(t,\cdot)\|^2_{L^2(\Omega)} + \left(\frac{\beta}{2}+\frac{\rho\alpha}{4\kappa^2\tau\gamma}\right)Q^2(t) + \frac{\gamma}{2}V^2(t) \le \frac{\rho\mu}{64\kappa^2\tau\gamma}\frac{1}{\left(\mathcal{M} + \dfrac{2C^{(3)}_\Omega\mathcal{L}^2\kappa^2\tau\gamma}{\rho}\right)^2}.$$

Note that the behaviour of the required bound on the initial velocity, namely $\frac{\mathcal{A}}{\mathcal{B}}$, as well as the upper bound in the estimate (4.7), namely

$$\mathcal{E} := \frac{\rho\mu}{16\kappa^2\tau\gamma}\frac{\mathcal{A}^2}{\mathcal{B}^2},$$

can be described more precisely with respect to the parameters: $\frac{\mathcal{A}}{2\mathcal{B}}$ and $\mathcal{E}$ tend to 0 when $\mu \to 0$, $\rho \to +\infty$, $\beta \to +\infty$, $\gamma \to +\infty$ or $\tau \to +\infty$. In particular the less the 0D model dissipates energy with respect to the auxiliary volume V, the more restrictive is the smallness condition on the data.

Remark 4.9 (Case $\gamma = 0$)**.** *Note that, in that case, an estimate can be derived by choosing only $A_{\mu,\alpha}\mathbf{u}$ as a test function. Indeed no control on the auxiliary volume $V(t)$ defined by (3.2), is required. More precisely, we easily derive the following estimate*

$$\frac{\mathrm{d}}{\mathrm{d}t}\left(\frac{\mu}{2}\|\nabla\mathbf{u}(t,\cdot)\|^2_{L^2(\Omega)} + \frac{\alpha}{2}Q^2(t)\right) + \left(\frac{1}{2} - \mathcal{M}\|\nabla\mathbf{u}(t,\cdot)\|_{L^2(\Omega)}\right)\|A_{\mu,\alpha}\mathbf{u}(t,\cdot)\|^2_{\rho,\beta} \le \frac{\kappa^2}{2\rho}\mathcal{P}^2(t). \tag{4.31}$$

In this case the dissipation comes from the term $\|A_{\mu,\alpha}\mathbf{u}(t,\cdot)\|^2_{\rho,\beta}$. *Assuming that*

$$\|\nabla\mathbf{u}\|_{L^2(\Omega)} \leq \frac{1}{4\mathcal{M}}$$

and since $\|A_{\mu,\alpha}\mathbf{u}(t,\cdot)\|^2_{\rho,\beta} \geq \rho\,\|A_{\mu,\alpha}\mathbf{u}(t,\cdot)\|^2_{L^2(\Omega)} \geq \frac{\rho}{\mathcal{L}^2}\,\|\nabla\mathbf{u}\|^2_{L^2(\Omega)}$ *estimate* (4.31) *can be rewritten as*

$$\frac{\mathrm{d}}{\mathrm{d}t}\left(\frac{\mu}{2}\,\|\nabla\mathbf{u}(t,\cdot)\|^2_{L^2(\Omega)} + \frac{\alpha}{2}Q^2(t)\right) + \frac{\rho}{4\mathcal{L}^2}\,\|\nabla\mathbf{u}\|^2_{L^2(\Omega)} \leq \frac{\kappa^2}{2\rho}\mathcal{P}^2(t).$$

Moreover since $\|\nabla\mathbf{u}(t,\cdot)\|^2_{L^2(\Omega)} \geq \frac{1}{2}\,\|\nabla\mathbf{u}(t,\cdot)\|^2_{L^2(\Omega)} + \frac{1}{2C_\Gamma^2}Q^2(t)$, *we obtain*

$$\frac{\mathrm{d}}{\mathrm{d}t}\left(\frac{\mu}{2}\,\|\nabla\mathbf{u}(t,\cdot)\|^2_{L^2(\Omega)} + \frac{\alpha}{2}Q^2(t)\right) + \frac{\rho}{8\mathcal{L}^2}\,\|\nabla\mathbf{u}\|^2_{L^2(\Omega)} + \frac{\rho}{8C_\Gamma^2\mathcal{L}^2}Q^2(t) \leq \frac{\kappa^2}{2\rho}\mathcal{P}^2(t). \tag{4.32}$$

Thus the analogue of the dissipation coefficient $\mathcal{D}$ *is, in this case,*

$$\mathcal{D}_0 = \min\left(\frac{\rho}{4\mu\mathcal{L}^2}, \frac{\rho}{4\mu C_\Gamma^2\mathcal{L}^2}\right).$$

Consequently,

$$\frac{\mathrm{d}}{\mathrm{d}t}\left(\frac{\mu}{2}\,\|\nabla\mathbf{u}(t,\cdot)\|^2_{L^2(\Omega)} + \frac{\alpha}{2}Q^2(t)\right) + \mathcal{D}_0\left(\frac{\mu}{2}\,\|\nabla\mathbf{u}(t,\cdot)\|^2_{L^2(\Omega)} + \frac{\alpha}{2}Q^2(t)\right) \leq \frac{\kappa^2}{2\rho}\mathcal{P}^2(t).$$

Proceeding as in the proof of Theorem 4.6, we obtain that if the initial data are small, namely

$$\frac{\mu}{2}\,\|\nabla\mathbf{u}_0\|^2_{L^2(\Omega)} + \frac{\alpha}{2}Q^2(0) \leq \frac{\mu}{32\mathcal{M}^2},$$

and if the external pressure satisfies

$$\frac{\kappa^2}{2\rho}\,\|\mathcal{P}^2\|_\infty \leq \frac{\mathcal{D}_0\mu}{32\mathcal{M}^2},$$

then the solution satisfies the following stability estimate

$$\frac{\mu}{2}\,\|\nabla\mathbf{u}(t,\cdot)\|^2_{L^2(\Omega)} + \frac{\alpha}{2}Q^2(t) \leq \frac{\mu}{32\mathcal{M}^2}. \tag{4.33}$$

Here we recover the results obtained in [31] for the Navier–Stokes system with Neumann boundary conditions as a particular case of this result by setting $\alpha = \beta = 0$. *Note also that the behaviour of the required bound on the initial velocity, namely* $\frac{1}{\mathcal{M}}$, *as well as the upper bound* $\frac{\mu}{\mathcal{M}^2}$ *in estimate* (4.33) *can be described more precisely with respect to the parameters:* $\mathcal{D}_0$, $\frac{1}{\mathcal{M}}$ *and* $\frac{\mu}{\mathcal{M}^2}$ *tend to 0 when* $\mu \to 0$, $\rho \to +\infty$, $\beta \to +\infty$.

Remark 4.10. *We could have kept* (4.9) *instead of* (4.18) *and, following nearly the same lines, obtain a stability estimate for small enough data. But it leads to slightly more tedious calculations we choose not to present here for the sake of simplicity.*

Remark 4.11. *In the case* $\beta > 0$, *estimates* (4.13) *and* (4.20) *can be adapted by using the property* $\|\mathbf{v}\|^2_{\rho,\beta} \geq \beta\left(\int_{\Gamma_W}\mathbf{v}\cdot\mathbf{n}\right)^2$. *In that way similar estimates can be derived by using the 0D inertia instead of the fluid intertia, leading to a possibly less restrictive condition on the smallness assumption on the data.*

As for the Stokes case we can state the following existence result

Theorem 4.12. *Let $T > 0$, $\mathbf{u}_0 \in V$, $\mathcal{P} \in L^2(0,T)$, in the general case there exists a time $T^* \leq T$ and a unique "strong" solution $\mathbf{u} \in L^2(0,T^*; D(A_{\mu,\alpha})) \cap L^\infty(0,T^*;V) \cap H^1(0,T^*;H)$ solution of (2.7) with $\varepsilon = 1$. In the dissipative case ($\tau < \infty$), assuming the data (initial data and applied pressure) to be small enough this solution is global in time.*

Proof. This proof is standard and can be done thanks to a Galerkin approximation with the eigenvectors of operator $A_{\mu,\alpha}$ as a Galerkin basis. The addtional bound on $\partial_t \mathbf{u}$ in $L^2(0,T;L^2(\Omega)$ is obtained by taking $\partial_t \mathbf{u}$ as a test function. The strong convergence in L^2 of the velocity is thus deduced from the Aubin-Lions Lemma and the fact that u is bounded at least in $L^2(0,T;H^1(\Omega))$ and $\partial_t \mathbf{u}$ is bounded in $L^2(0,T;L^2(\Omega))$. We refer to [2,31] for similar proofs. □

4.2. Estimates for the semi-discretized system

4.2.1. Implicit coupling

We now focus on the semi-discrete Navier–Stokes system implicitly coupled to the Windkessel model which corresponds to the variational formulation (2.11) with $\varepsilon = 1$ and $m = n+1$. We consider a semi-implicit treatment of the convective term, namely $I = 0$.

Theorem 4.13 (Implicit coupling with the Navier–Stokes system)**.** *Let $\mu > 0$. Assume that the artificial boundaries Γ_0 and Γ_W meet the lateral boundaries Γ_ℓ at angle $\frac{\pi}{2}$ and that each boundary is smooth enough. Assume that $\alpha \geq 0$, $\beta \geq 0$, $\gamma > 0$.*

- **Dissipative case: global-in-time bound for small data.** *Assume that $\tau < +\infty$. Let us consider the constants δ, η, $\mathcal{D}$ and the function H as in Theorem 4.6. If the initial data and external forces are small enough, namely*

$$\frac{\rho}{2}\|\mathbf{u}^0\|^2_{L^2(\Omega)} + \frac{\eta\mu}{2}\left\|\nabla \mathbf{u}^0\right\|^2_{L^2(\Omega)} + \frac{\eta\alpha+\beta}{2}(Q^0)^2 \leq \widetilde{\mathcal{E}} := \frac{\mu\eta^3}{32\left(\eta C_\Omega^{(7)}\mathcal{M} + C_\Omega^{(3)}\mathcal{L}^2\right)^2},$$

and

$$\|H\|_\infty \leq \mathcal{D}\widetilde{\mathcal{E}},$$

then the solution of (2.11) with $\varepsilon = 1$, $m = n+1$ and $I = 0$ satisfies the following estimate:

$$\frac{\rho}{2}\|\mathbf{u}^n\|^2_{L^2(\Omega)} + \frac{\mu\eta}{2}\|\nabla \mathbf{u}^n\|^2_{L^2(\Omega)} + \left(\frac{\beta}{2} + \frac{\alpha}{2}\eta\right)(Q^n)^2 + \frac{\gamma}{2}(V^n_{\mathrm{imp}})^2 \leq \widetilde{\mathcal{E}}, \tag{4.34}$$

for all $n \in \{0,...,N\}$ Moreover $\Delta t \sum_{n=0}^N \|A_{\mu,\alpha}\mathbf{u}^n\|^2_{\rho,\beta}$ is also bounded independently on N.

- **Case $\tau = +\infty$: local-in-time bound for small data.** *Assume that the time step is such that*

$$\Delta t < \frac{\rho}{8r\kappa^2\gamma} =: \Delta t_r,$$

where r is a positive homogeneity constant. Assume furthermore that the initial data, external forces and final time $T = N\Delta t$ satisfy

$$\frac{\rho}{2}\|\mathbf{u}^0\|^2_{L^2(\Omega)} + \frac{r\mu}{2}\|\nabla \mathbf{u}^0\|^2_{L^2(\Omega)} + \left(\frac{\beta}{2} + \frac{r\alpha}{2}\right)(Q^0)^2 + \left(\frac{C_\Gamma^2}{2\mu} + \frac{2r\kappa^2}{\rho}\right)\Delta t \sum_{k=0}^N (\mathcal{P}^k)^2 \leq \frac{\mu\, \mathrm{e}^{-\frac{T}{\Delta t_r - \Delta t}}}{32\left(C_\Omega^{(3)}\mathcal{L}^2 + rC_\Omega^{(7)}\mathcal{M}\right)^2}, \tag{4.35}$$

then

$$\frac{\rho}{2}\|\mathbf{u}^n\|^2_{L^2(\Omega)} + \frac{r\mu}{2}\|\nabla\mathbf{u}^n\|^2_{L^2(\Omega)} + \left(\frac{\beta}{2}+\frac{r\alpha}{2}\right)(Q^n)^2 + \frac{\gamma}{2}(V^n_{\rm imp})^2 + \frac{r}{4}\Delta t\sum_{k=0}^{n}\left\|A_{\mu,\alpha}\mathbf{u}^k\right\|^2_{\rho,\beta}$$
$$\leq \mathrm{e}^{\frac{T}{\Delta t_r - \Delta t}}\left(\frac{\rho}{2}\|\mathbf{u}^0\|^2_{L^2(\Omega)} + \frac{r\mu}{2}\|\nabla\mathbf{u}^0\|^2_{L^2(\Omega)} + \left(\frac{\beta}{2}+\frac{r\alpha}{2}\right)(Q^0)^2 + \left(\frac{C_\Gamma^2}{2\mu}+\frac{2r\kappa^2}{\rho}\right)\Delta t\sum_{k=0}^{N}(\mathcal{P}^k)^2\right).$$

Proof. All the forthcoming calculations can be rigorously justified by using a Galerkin method with a special basis associated to the Stokes-like operator $A_{\mu,\alpha}$, see Proposition 4.2. Moreover existence of a solution (for which uniqueness could be also proven) can be also derived thanks to the previous estimates by the same Galerkin approximation.

- **Dissipative case: $\tau < +\infty$.**

We consider the system (2.8) with $I = 0$ for which the convection term is semi-explicit. We prove estimate (4.34) by induction. We follow the steps of the continuous case by taking $\mathbf{u}^{n+1}$ and $A_{\mu,\alpha}\mathbf{u}^{n+1}$ as test functions in the variational formulation (2.11). Note that the only difference with the continuous case concerns the estimate of the convection term. The discrete analogue of (4.17) should be read as

$$\left|\rho\int_\Omega(\mathbf{u}^n\nabla)\mathbf{u}^{n+1}\,\mathbf{u}^{n+1}\right| \leq \rho\left\|\mathbf{u}^n\right\|_{L^4(\Omega)}\left\|\nabla\mathbf{u}^{n+1}\right\|_{L^2(\Omega)}\left\|\mathbf{u}^{n+1}\right\|_{L^4(\Omega)}$$
$$\leq C_\Omega^{(3)}\mathcal{L}^2\left\|\nabla\mathbf{u}^n\right\|_{L^2(\Omega)}\left\|A_{\mu,\alpha}\mathbf{u}^{n+1}\right\|^2_{\rho,\beta}.$$

The discrete stability estimate can thus be written as follows

$$\frac{\rho}{2}\|\mathbf{u}^{n+1}\|^2_{L^2(\Omega)} + \frac{\mu}{2}\Delta t\|\nabla\mathbf{u}^{n+1}\|^2_{L^2(\Omega)} + \frac{\beta}{2}(Q^{n+1})^2 + \alpha\Delta t(Q^{n+1})^2 + \frac{\gamma}{2}(V^{n+1}_{\rm imp})^2 + \frac{\gamma\Delta t}{\tau}(V^{n+1}_{imp})^2$$
$$\leq \frac{\rho}{2}\|\mathbf{u}^n\|^2_{L^2(\Omega)} + \frac{\beta}{2}(Q^n)^2 + \frac{\gamma}{2}(V^n_{\rm imp})^2 + \frac{C_\Gamma^2}{2\mu}\Delta t(\mathcal{P}^{n+1})^2 + C_\Omega^{(3)}\mathcal{L}^2\Delta t\left\|\nabla\mathbf{u}^n\right\|_{L^2(\Omega)}\left\|A_{\mu,\alpha}\mathbf{u}^{n+1}\right\|^2_{\rho,\beta}. \quad (4.36)$$

We take $A_{\mu,\alpha}\mathbf{u}^{n+1}$ as a test function in the variational formulation (2.11) for $\varepsilon = 1$, $I = 0$ and $m = n+1$:

$$\rho\int_\Omega(\mathbf{u}^{n+1}-\mathbf{u}^n)\cdot A_{\mu,\alpha}\mathbf{u}^{n+1} + \rho\Delta t\int_\Omega(\mathbf{u}^n\nabla)\mathbf{u}^{n+1}\,A_{\mu,\alpha}\mathbf{u}^{n+1} + \mu\,\Delta t\int_\Omega\nabla\mathbf{u}^{n+1}\cdot\nabla A_{\mu,\alpha}\mathbf{u}^{n+1}$$
$$+\alpha\,\Delta t\,Q^{n+1}\left(\int_{\Gamma_W}A_{\mu,\alpha}\mathbf{u}^{n+1}\cdot\mathbf{n}\right) + \beta\left(Q^{n+1}-Q^n\right)\left(\int_{\Gamma_W}A_{\mu,\alpha}\mathbf{u}^{n+1}\cdot\mathbf{n}\right) + \gamma\Delta t V^{n+1}_{\rm imp}\left(\int_{\Gamma_W}A_{\mu,\alpha}\mathbf{u}^{n+1}\cdot\mathbf{n}\right)$$
$$= -\mathcal{P}^m\,\Delta t\left(\int_{\Gamma_W}A_{\mu,\alpha}\mathbf{u}^{n+1}\cdot\mathbf{n}\right).$$

By definition of operator $A_{\mu,\alpha}$, we have

$$\rho\int_\Omega(\mathbf{u}^{n+1}-\mathbf{u}^n)\cdot A_{\mu,\alpha}\mathbf{u}^{n+1} + \beta\left(Q^{n+1}-Q^n\right)\left(\int_{\Gamma_W}A_{\mu,\alpha}\mathbf{u}^{n+1}\cdot\mathbf{n}\right)$$
$$= a_{\mu,\alpha}(\mathbf{u}^{n+1}-\mathbf{u}^n,\mathbf{u}^{n+1})$$
$$= \frac{\mu}{2}\left\|\nabla\mathbf{u}^{n+1}\right\|^2 + \frac{\mu}{2}\left\|\nabla\mathbf{u}^n\right\|^2 + \frac{\mu}{2}\left\|\nabla\mathbf{u}^{n+1}-\nabla\mathbf{u}^n\right\|^2 + \frac{\alpha}{2}(Q^{n+1})^2 + \frac{\alpha}{2}(Q^n)^2 + \frac{\alpha}{2}(Q^{n+1}-Q^n)^2.$$

Using again the definition of $A_{\mu,\alpha}$, we have also

$$\mu\,\Delta t\int_\Omega\nabla\mathbf{u}^{n+1}\cdot\nabla A_{\mu,\alpha}\mathbf{u}^{n+1} + \alpha\,\Delta t\,Q^{n+1}\left(\int_{\Gamma_W}A_{\mu,\alpha}\mathbf{u}^{n+1}\cdot\mathbf{n}\right) = \Delta t\left\|A_{\mu,\alpha}\mathbf{u}^{n+1}\right\|^2_{\rho,\beta}.$$

Now we have to estimate $\rho \int_\Omega (\mathbf{u}^n \nabla)\mathbf{u}^{n+1}\, A_{\mu,\alpha}\mathbf{u}^{n+1}$. We do not follow exactly the same lines as for the continuous case in particular since the convective term is treated in a semi-implicit way:

$$\begin{aligned}\left|\rho \int_\Omega (\mathbf{u}^n \nabla)\mathbf{u}^{n+1}\, A_{\mu,\alpha}\mathbf{u}^{n+1}\right| &\leq \rho \|\mathbf{u}^n\|_{L^6(\Omega)} \left\|\nabla \mathbf{u}^{n+1}\right\|_{L^3(\Omega)} \left\|A_{\mu,\alpha}\mathbf{u}^{n+1}\right\|_{L^2(\Omega)} \\ &\leq C_\Omega^{(7)} \rho \|\nabla \mathbf{u}^n\|_{L^2(\Omega)} \left\|\mathbf{u}^{n+1}\right\|_{H^{\frac{3}{2}+\epsilon}(\Omega)} \left\|A_{\mu,\alpha}\mathbf{u}^{n+1}\right\|_{L^2(\Omega)} \\ &\leq C_\Omega^{(7)} \mathcal{M} \|\nabla \mathbf{u}^n\|_{L^2(\Omega)} \left\|A_{\mu,\alpha}\mathbf{u}^{n+1}\right\|_{\rho,\beta}^2, \end{aligned} \tag{4.37}$$

where $C_\Omega^{(7)}$ comes from the continuous embeddings $H^{\frac{3}{2}+\epsilon}(\Omega) \hookrightarrow W^{1,3}(\Omega)$ and $H^1(\Omega) \hookrightarrow L^6(\Omega)$. Then using (4.13) for the forcing term, (4.20) for the term involving the volume and estimate (4.37) for the convection term, the discrete analogue of estimate (4.23) reads

$$\begin{aligned}&\frac{\mu}{2}\left\|\nabla \mathbf{u}^{n+1}\right\|_{L^2(\Omega)}^2 + \frac{\alpha}{2}(Q^{n+1})^2 + \frac{\Delta t}{2}\left\|A_{\mu,\alpha}\mathbf{u}^{n+1}\right\|_{\rho,\beta}^2 \\ &\quad\leq \frac{\mu}{2}\|\nabla \mathbf{u}^n\|_{L^2(\Omega)}^2 + \frac{\alpha}{2}(Q^n)^2 + \frac{\gamma}{2\eta\tau}\Delta t (V_{\text{imp}}^{n+1})^2 + \frac{\kappa^2}{4\delta\rho}\Delta t (\mathcal{P}^{n+1})^2 + C_\Omega^{(7)}\mathcal{M}\Delta t \|\nabla \mathbf{u}^n\|_{L^2(\Omega)} \left\|A_{\mu,\alpha}\mathbf{u}^{n+1}\right\|_{\rho,\beta}^2, \end{aligned} \tag{4.38}$$

with (δ, η) satisfying (4.22). By multiplying estimate (4.38) by η and adding (4.36), we obtain

$$\begin{aligned}&\frac{\rho}{2}\|\mathbf{u}^{n+1}\|_{L^2(\Omega)}^2 + \frac{\mu}{2}(\eta + \Delta t)\|\nabla \mathbf{u}^{n+1}\|_{L^2(\Omega)}^2 + \left(\frac{\beta}{2} + \frac{\alpha}{2}\eta + \alpha\Delta t\right)(Q^{n+1})^2 \\ &\qquad + \left(\frac{\gamma}{2} + \frac{\gamma\Delta t}{2\tau}\right)(V_{\text{imp}}^{n+1})^2 + \left(\frac{\eta}{2} - \left(C_\Omega^{(3)}\mathcal{L}^2 + C_\Omega^{(7)}\mathcal{M}\eta\right)\|\nabla \mathbf{u}^n\|_{L^2(\Omega)}\right)\Delta t \left\|A_{\mu,\alpha}\mathbf{u}^{n+1}\right\|_{\rho,\beta}^2 \\ &\quad\leq \frac{\rho}{2}\|\mathbf{u}^n\|_{L^2(\Omega)}^2 + \frac{\mu}{2}\eta\|\nabla \mathbf{u}^n\|_{L^2(\Omega)}^2 + \left(\frac{\beta}{2} + \frac{\alpha}{2}\eta\right)(Q^n)^2 + \frac{\gamma}{2}(V_{\text{imp}}^n)^2 + \left(\frac{C_\Gamma^2}{2\mu} + \frac{\kappa^2}{4\delta\rho}\eta\right)\Delta t(\mathcal{P}^{n+1})^2. \end{aligned} \tag{4.39}$$

Recalling that $\mathcal{A}$ is defined by (4.26) and defining $\tilde{\mathcal{B}}$ by

$$\tilde{\mathcal{B}} = C_\Omega^{(3)}\mathcal{L}^2 + C_\Omega^{(7)}\mathcal{M}\eta, \tag{4.40}$$

since $\left|Q^{n+1}\right| \leq C_\Gamma \left\|\nabla \mathbf{u}^{n+1}\right\|_{L^2(\Omega)}$, and $\left\|\mathbf{u}^{n+1}\right\|_{L^2(\Omega)} \leq C_P \left\|\nabla \mathbf{u}^{n+1}\right\|_{L^2(\Omega)}$ by Poincaré inequality, we proceed as in the continuous case in order to derive the discrete analogue of estimate (4.25):

$$\begin{aligned}&\left(\frac{\rho}{2} + \frac{\mu}{8C_P^2}\Delta t\right)\|\mathbf{u}^{n+1}\|_{L^2(\Omega)}^2 + \left(\frac{\mu\eta}{2} + \frac{\mu}{8}\Delta t\right)\|\nabla \mathbf{u}^{n+1}\|_{L^2(\Omega)}^2 + \left(\frac{\beta}{2} + \frac{\alpha}{2}\eta + \left(\alpha + \frac{\mu}{4C_\Gamma^2}\right)\Delta t\right)(Q^{n+1})^2 \\ &\qquad + \left(\frac{\gamma}{2} + \frac{\gamma\Delta t}{2\tau}\right)(V_{\text{imp}}^{n+1})^2 + \Delta t\left(\mathcal{A} - \tilde{\mathcal{B}}\|\nabla \mathbf{u}^n\|_{L^2(\Omega)}\right)\left\|A_{\mu,\alpha}\mathbf{u}^{n+1}\right\|_{\rho,\beta}^2 \\ &\quad\leq \frac{\rho}{2}\|\mathbf{u}^n\|_{L^2(\Omega)}^2 + \frac{\mu}{2}\eta\|\nabla \mathbf{u}^n\|_{L^2(\Omega)}^2 + \left(\frac{\beta}{2} + \frac{\alpha}{2}\eta\right)(Q^n)^2 + \frac{\gamma}{2}(V_{\text{imp}}^n)^2 + \left(\frac{C_\Gamma^2}{2\mu} + \frac{\kappa^2}{4\delta\rho}\eta\right)\Delta t(\mathcal{P}^{n+1})^2. \end{aligned} \tag{4.41}$$

Recalling the definition of $\mathcal{D}$, see (4.28), and introducing the approximation of $\Psi(t^n)$ defined by

$$\Psi^n := \frac{\rho}{2}\|\mathbf{u}^n\|_{L^2(\Omega)}^2 + \frac{\mu\eta}{2}\|\nabla \mathbf{u}^n\|_{L^2(\Omega)}^2 + \left(\frac{\beta}{2} + \frac{\alpha}{2}\eta\right)(Q^n)^2 + \frac{\gamma}{2}(V_{\text{imp}}^n)^2,$$

we obtain

$$\Psi^{n+1}(1 + \mathcal{D}\Delta t) + \Delta t\left(\mathcal{A} - \tilde{\mathcal{B}}\|\nabla \mathbf{u}^n\|_{L^2(\Omega)}\right)\left\|A_{\mu,\alpha}\mathbf{u}^{n+1}\right\|_{\rho,\beta}^2 \leq \Psi^n + \Delta t H^{n+1},$$

where $H^{n+1} = H(t^{n+1})$, H being defined by (4.27). Then, if $\left\|\nabla \mathbf{u}^k\right\|_{L^2(\Omega)} \leq \frac{\mathcal{A}}{2\tilde{\mathcal{B}}}$, for all $k \in \{0, ..., n\}$, we get

$$\Psi^{n+1} \leq \frac{\Psi^0}{(1+\mathcal{D}\Delta t)^{n+1}} + \frac{\max\limits_{k\in\{0,\dots,n+1\}} H^k}{\mathcal{D}} \left(1 - \frac{1}{(1+\mathcal{D}\Delta t)^{n+1}}\right). \tag{4.42}$$

Assuming that

$$\Psi^0 \leq \frac{\eta\mu}{8}\frac{\mathcal{A}^2}{\tilde{\mathcal{B}}^2}, \qquad \frac{\max\limits_{k\in\{0,\dots,n+1\}} H^k}{\mathcal{D}} \leq \frac{\eta\mu}{8}\frac{\mathcal{A}^2}{\tilde{\mathcal{B}}^2},$$

we conclude that

$$\Psi^{n+1} \leq \frac{\eta\mu}{8}\frac{\mathcal{A}^2}{\tilde{\mathcal{B}}^2}, \quad \text{and} \quad \left\|\nabla \mathbf{u}^{n+1}\right\|_{L^2(\Omega)} \leq \frac{\mathcal{A}}{2\tilde{\mathcal{B}}}. \tag{4.43}$$

Consequently, by induction, we can prove that the solution stays at each time iteration in the same ball defined by estimate (4.43).

- **Case $\tau = +\infty$.**

In this case we cannot take advantage of the dissipitation with respect to the volume V_{imp}^n. Taking $\mathbf{u}^{n+1}$ as a test function, we obtain

$$\begin{aligned}
&\frac{\rho}{2}\|\mathbf{u}^{n+1}\|^2_{L^2(\Omega)} + \frac{\mu}{2}\Delta t\|\nabla \mathbf{u}^{n+1}\|^2_{L^2(\Omega)} + \frac{\beta}{2}(Q^{n+1})^2 + \alpha\Delta t(Q^{n+1})^2 + \frac{\gamma}{2}(V_{\text{imp}}^{n+1})^2 \\
&\quad \leq \frac{\rho}{2}\|\mathbf{u}^{n}\|^2_{L^2(\Omega)} + \frac{\beta}{2}(Q^{n})^2 + \frac{\gamma}{2}(V_{\text{imp}}^{n})^2 + \frac{C_\Gamma^2}{2\mu}\Delta t(\mathcal{P}^{n+1})^2 + C_\Omega^{(3)}\mathcal{L}^2\Delta t\left\|\nabla \mathbf{u}^n\right\|_{L^2(\Omega)}\left\|A_{\mu,\alpha}\mathbf{u}^{n+1}\right\|^2_{\rho,\beta}.
\end{aligned} \tag{4.44}$$

Next, once again we take $A_{\mu,\alpha}\mathbf{u}^{n+1}$ as a test function. Here we have to control the term

$$\gamma\Delta t\left|V_{\text{imp}}^{n+1}\int_{\Gamma_W} A_{\mu,\alpha}\mathbf{u}^{n+1}\cdot\mathbf{n}\right|$$

without using the dissipative term $\frac{\gamma\Delta t}{\tau}(V_{\text{imp}}^{n+1})^2$ of (4.36) that is equal to zero in the case $\tau = +\infty$. We have, by using Lemma 2.4 and the definition of $\|\cdot\|_{\rho,\beta}$:

$$\gamma\Delta t\left|V_{\text{imp}}^{n+1}\int_{\Gamma_W} A_{\mu,\alpha}\mathbf{u}^{n+1}\cdot\mathbf{n}\right| \leq \frac{\gamma\kappa}{\sqrt{\rho}}\Delta t|V_{\text{imp}}^{n+1}|\left\|A_{\mu,\alpha}\mathbf{u}^{n+1}\right\|_{\rho,\beta} \leq \frac{\kappa^2\gamma^2}{\delta\rho}\Delta t(V_{\text{imp}}^{n+1})^2 + \delta\Delta t\left\|A_{\mu,\alpha}\mathbf{u}^{n+1}\right\|^2_{\rho,\beta}, \tag{4.45}$$

for $\delta > 0$ that will be chosen latter. Remembering estimate (4.13) of the linear forcing terms and estimate (4.37) of the convection term, we obtain

$$\begin{aligned}
&\frac{\mu}{2}\left\|\nabla \mathbf{u}^{n+1}\right\|^2_{L^2(\Omega)} + \frac{\alpha}{2}(Q^{n+1})^2 + \Delta t\left\|A_{\mu,\alpha}\mathbf{u}^{n+1}\right\|^2_{\rho,\beta} \\
&\leq \frac{\mu}{2}\left\|\nabla \mathbf{u}^{n}\right\|^2_{L^2(\Omega)} + \frac{\alpha}{2}(Q^{n})^2 + \frac{\kappa^2\gamma^2}{\delta\rho}\Delta t(V_{\text{imp}}^{n+1})^2 + \frac{\kappa^2}{4\delta\rho}\Delta t(\mathcal{P}^{n+1})^2 + \left(2\delta\Delta t + C_\Omega^{(7)}\mathcal{M}\Delta t\left\|\nabla \mathbf{u}^n\right\|_{L^2(\Omega)}\right)\left\|A_{\mu,\alpha}\mathbf{u}^{n+1}\right\|^2_{\rho,\beta}.
\end{aligned}$$

Consequently by choosing $2\delta = \frac{1}{2}$, we have

$$\begin{aligned}
&\frac{\mu}{2}\left\|\nabla \mathbf{u}^{n+1}\right\|^2_{L^2(\Omega)} + \frac{\alpha}{2}(Q^{n+1})^2 + \left(\frac{1}{2} - C_\Omega^{(7)}\mathcal{M}\left\|\nabla \mathbf{u}^n\right\|_{L^2(\Omega)}\right)\Delta t\left\|A_{\mu,\alpha}\mathbf{u}^{n+1}\right\|^2_{\rho,\beta} \\
&\qquad \leq \frac{\mu}{2}\left\|\nabla \mathbf{u}^{n}\right\|^2_{L^2(\Omega)} + \frac{\alpha}{2}(Q^{n})^2 + 4\frac{\kappa^2\gamma^2}{\rho}\Delta t(V_{\text{imp}}^{n+1})^2 + \frac{\kappa^2}{\rho}\Delta t(\mathcal{P}^{n+1})^2.
\end{aligned} \tag{4.46}$$

Multiplying (4.46) by a homogeneity coefficient r and adding (4.44) yields

$$\begin{aligned}\frac{\rho}{2}\|\mathbf{u}^{n+1}\|^2_{L^2(\Omega)} + \frac{\mu}{2}(r+\Delta t)\|\nabla\mathbf{u}^{n+1}\|^2_{L^2(\Omega)} + \left(\frac{\beta}{2}+\frac{r\alpha}{2}+\alpha\Delta t\right)(Q^{n+1})^2 + \left(\frac{\gamma}{2} - 4\frac{r\kappa^2\gamma^2}{\rho}\Delta t\right)(V_{\mathrm{imp}}^{n+1})^2 \\ + \left(\frac{r}{2} - \left(C_\Omega^{(3)}\mathcal{L}^2 + rC_\Omega^{(7)}\mathcal{M}\right)\|\nabla\mathbf{u}^n\|_{L^2(\Omega)}\right)\Delta t\left\|A_{\mu,\alpha}\mathbf{u}^{n+1}\right\|^2_{\rho,\beta} \\ \leq \frac{\rho}{2}\|\mathbf{u}^n\|^2_{L^2(\Omega)} + \frac{r\mu}{2}\|\nabla\mathbf{u}^n\|^2_{L^2(\Omega)} + \left(\frac{\beta}{2}+\frac{r\alpha}{2}\right)(Q^n)^2 + \frac{\gamma}{2}(V_{\mathrm{imp}}^n)^2 + \left(\frac{C_\Gamma^2}{2\mu}+\frac{r\kappa^2}{\rho}\right)\Delta t(\mathcal{P}^{n+1})^2. \quad (4.47)\end{aligned}$$

Thus, if we impose

$$\Delta t < \frac{\rho}{8r\kappa^2\gamma} = \Delta t_r,$$

and assuming that

$$\left\|\nabla\mathbf{u}^k\right\|_{L^2(\Omega)} \leq \frac{r}{4\left(C_\Omega^{(3)}\mathcal{L}^2 + rC_\Omega^{(7)}\mathcal{M}\right)}, \quad \forall k\in\{0,\dots,n\}, \quad (4.48)$$

we obtain, thanks to discrete Gronwall Lemma, the following discrete stability estimate

$$\begin{aligned}\frac{\rho}{2}\|\mathbf{u}^{n+1}\|^2_{L^2(\Omega)} + \frac{r\mu}{2}\|\nabla\mathbf{u}^{n+1}\|^2_{L^2(\Omega)} + \left(\frac{\beta}{2}+\frac{r\alpha}{2}\right)(Q^{n+1})^2 + \frac{\gamma}{2}(V_{\mathrm{imp}}^{n+1})^2 + \frac{r}{4}\Delta t\sum_{k=0}^{n+1}\left\|A_{\mu,\alpha}\mathbf{u}^k\right\|^2_{\rho,\beta} \\ \leq \mathrm{e}^{\frac{T}{\Delta t_r-\Delta t}}\left(\frac{\rho}{2}\|\mathbf{u}^0\|^2_{L^2(\Omega)} + \frac{r\mu}{2}\|\nabla\mathbf{u}^0\|^2_{L^2(\Omega)} + \left(\frac{\beta}{2}+\frac{r\alpha}{2}\right)(Q^0)^2 + \left(\frac{C_\Gamma^2}{2\mu}+\frac{r\kappa^2}{\rho}\right)\Delta t\sum_{k=0}^{N}(\mathcal{P}^k)^2\right). \quad (4.49)\end{aligned}$$

Consequently to satisfy (4.48) for $k = n+1$ and obtain the desired result by induction, the data have to verify

$$\begin{aligned}\mathrm{e}^{\frac{T}{\Delta t_r-\Delta t}}\left[\frac{\rho}{2}\|\mathbf{u}^0\|^2_{L^2(\Omega)} + \frac{r\mu}{2}\|\nabla\mathbf{u}^0\|^2_{L^2(\Omega)} + \left(\frac{\beta}{2}+\frac{r\alpha}{2}\right)(Q^0)^2 + \left(\frac{C_\Gamma^2}{2\mu}+\frac{r\kappa^2}{\rho}\right)\Delta t\sum_{k=0}^{N}(\mathcal{P}^k)^2\right] \\ \leq \frac{r^3\mu}{32\left(C_\Omega^{(3)}\mathcal{L}^2 + rC_\Omega^{(7)}\mathcal{M}\right)^2}. \quad (4.50)\end{aligned}$$

The above condition requires that the initial conditions, the forcing term as well as the final time T are small enough. □

Note that a standard fixed point argument [31, 49] allows us to obtain the same kind of stability bound for the solution of system (2.11) with $I = 1$ together with the existence of a strong solution.

Remark 4.14. *Let us comment the dependency on the homogeneity constant r. The upper bounds defined by (4.48) and (4.50) are increasing with respect to r, are equal to zero for $r = 0$ and have a finite limit as r goes to $+\infty$. Moreover, at the same time, the critical time step Δt_r goes to zero as r goes to $+\infty$ and so does the exponential growth. Thus, large values for r induce restrictive smallness conditions on the time step and on the data. For small values for r the condition on the time step is dropped but the upper bound on the data goes to 0.*

Remark 4.15. *We can already note that for typical Windkessel model in blood flow for which $\tau < +\infty$, we can ensure global-in-time stability of the semi-discrete solution for small enough initial data and external forces, whereas for typical Windkessel model in airflow for which $\tau = +\infty$ we exhibit restrictive sufficient conditions on the time step and on the data (initial data, external forces, final time). In this case, the restriction on the time step writes $\Delta t < \frac{\rho}{8r\kappa^2\gamma}$. In particular the smaller the Windkessel compliance is, the more restrictive the conditions on the data and the time step are. Thus when ρ goes to zero or when γ goes to infinity the time step goes to zero.*

Remark 4.16. *Note that we cannot extend easily the proof of Theorem 4.13 to the fully-discretized system, unlike for the Stokes system. To do so one should introduce the finite element discrete analogue of $A_{\mu,\alpha}$, see [29] in which this type of analysis is done for the Navier–Stokes system with homogeneous Dirichlet boundary conditions.*

Remark 4.17 (Case $\gamma = 0$)**.** *As for the continuous case, it is sufficient to choose $A_{\mu,\alpha}\mathbf{u}^{n+1}$ as a test function in order to derive a stability estimate, as in Remark 4.9. In this case the system is also dissipative and no condition on the time step is required for the stability.*

4.2.2. Explicit coupling

We now focus on the semi-discretized Navier–Stokes–Windkessel model with explicit coupling. More precisely, as for the Stokes–Windkessel model with explicit coupling, the inertia of the 0D model associated to the parameter β is treated implicitly whereas the terms related to the parameters α and γ are treated explicitly. Moreover we consider a semi-implicit treatment of the convective term. It thus corresponds to the problem (2.11) with $\varepsilon = 1$, $m = n$ and $I = 0$. We have all the ingredients to study this case, since it will be a mix of the study done for the Stokes system with explicit coupling and the study of the Navier–Stokes system.

Theorem 4.18. *Let $\mu > 0$. Assume that the artificial boundaries Γ_0 and Γ_W meet the lateral boundaries Γ_ℓ at angle $\frac{\pi}{2}$ and that each boundary is smooth enough. Assume that $\alpha \geq 0$, $\beta \geq 0$, $\gamma > 0$ and $0 < \tau \leq +\infty$. The discrete solution of (2.11) with $\varepsilon = 1$, $I = 0$ and $m = n$ satisfies a discrete stability estimate, under restrictive condition on the data (final time, initial data and external forces) and on the time step. More precisely, let r be a positive homogeneity constant, assuming that $\Delta t < \lambda_1$ (where λ_1 is defined by (3.20)) and that*

$$\frac{\rho}{2}\|\mathbf{u}^0\|^2_{L^2(\Omega)} + \frac{r\mu}{2}\|\nabla\mathbf{u}^0\|^2_{L^2(\Omega)} + \frac{\gamma}{\delta_{\Delta t}}\frac{(V^1_{\mathrm{exp}})^2}{2} + \frac{\beta}{2}(Q^0)^2 + \Delta t\left(\frac{C_\Gamma^2}{2\mu} + \frac{2r\kappa^2}{\rho}\right)\sum_{k=0}^{N}(\mathcal{P}^k)^2 \leq \frac{r^3\mu \mathrm{e}^{-C^{\mathrm{NS}}_{\Delta t,r}T}\mathrm{e}^{-\frac{T}{\lambda_1-\Delta t}}}{32\left(C^{(3)}_\Omega\mathcal{L}^2 + rC^{(7)}_\Omega\mathcal{M}_0\right)^2}$$

with

$$C^{\mathrm{NS}}_{\Delta t,r} = C^{\mathrm{S}}_{\Delta t} + r\left(\frac{2\alpha^2\kappa^4}{\rho^2} + \frac{8\kappa^2\gamma\delta_{\Delta t}}{\rho}\right), \tag{4.51}$$

(the constant $C^{\mathrm{S}}_{\Delta t}$ being defined in Thm. 3.9) and

$$\mathcal{M}_0 := C^{(2)}_\Omega\left(\frac{\rho}{\mu} + C^{(1)}_\Omega\kappa\frac{\beta}{\mu}\right), \tag{4.52}$$

then the following discrete estimate holds true

$$\begin{aligned}
&\frac{\rho}{2}\|\mathbf{u}^{n+1}\|^2_{L^2(\Omega)} + \frac{r\mu}{2}\|\nabla\mathbf{u}^{n+1}\|^2_{L^2(\Omega)} + \frac{\gamma}{\delta_{\Delta t}}\frac{(V^{n+2}_{\mathrm{exp}})^2}{2} + \frac{\beta}{2}(Q^{n+1})^2 + \frac{r}{4}\Delta t\sum_{k=0}^{n+1}\left\|A_{\mu,0}\mathbf{u}^k\right\|^2_{\rho,\beta}\\
&\leq \mathrm{e}^{C^{\mathrm{NS}}_{\Delta t,r}T}\mathrm{e}^{\frac{T}{\lambda_1-\Delta t}}\left(\frac{\rho}{2}\|\mathbf{u}^0\|^2_{L^2(\Omega)} + \frac{r\mu}{2}\|\nabla\mathbf{u}^0\|^2_{L^2(\Omega)} + \frac{\gamma}{\delta_{\Delta t}}\frac{(V^1_{\mathrm{exp}})^2}{2} + \frac{\beta}{2}(Q^0)^2 + \left(\frac{C_\Gamma^2}{2\mu} + \frac{2r\kappa^2}{\rho}\right)\Delta t\sum_{k=0}^{n}(\mathcal{P}^k)^2\right).
\end{aligned}$$

Note that here the discrete estimates are derived on the system with a semi-implicit treatment of the convection term. Nevertheless a fixed point procedure could enable to prove a similar estimate in the case of an implicit treatment of this term, namely in the case $I = 1$.

Proof. By taking $\mathbf{u}^{n+1}$ as a test function in the variational formulation (2.11) with $\varepsilon = 1$, $I = 0$ and $m = n$ following the same lines as in the proof of Theorem 3.9 in the case $\beta \geq 0$ and using moreover the following estimate of the convection term

$$\left|\rho\int_\Omega(\mathbf{u}^n\nabla)\mathbf{u}^{n+1}\,\mathbf{u}^{n+1}\right| \leq \rho\left\|\mathbf{u}^n\right\|_{L^4(\Omega)}\left\|\nabla\mathbf{u}^{n+1}\right\|_{L^2(\Omega)}\left\|\mathbf{u}^{n+1}\right\|_{L^4(\Omega)} \leq C^{(3)}_\Omega\mathcal{L}^2\left\|\nabla\mathbf{u}^n\right\|_{L^2(\Omega)}\left\|A_{\mu,0}\mathbf{u}^{n+1}\right\|^2_{\rho,\beta},$$

we get

$$\begin{aligned}
&\frac{\rho}{2}\left(1-\frac{\alpha\kappa^2}{\rho}\Delta t-\frac{2\gamma\kappa^2}{\rho}\Delta t^2\right)\|\mathbf{u}^{n+1}\|^2_{L^2(\Omega)}+\frac{\mu\Delta t}{2}\|\nabla\mathbf{u}^{n+1}\|^2_{L^2(\Omega)}+\frac{\gamma}{\delta_{\Delta t}}\frac{(V_{\rm exp}^{n+2})^2}{2}+\frac{\gamma\Delta t}{\tau}(V_{\rm exp}^{n+1})^2+\frac{\beta}{2}(Q^{n+1})^2\\
&\leq\frac{\rho}{2}\left(1+\frac{\alpha\kappa^2}{\rho}\Delta t\right)\|\mathbf{u}^{n}\|^2_{L^2(\Omega)}+\frac{\gamma}{\delta_{\Delta t}}\left(1+\frac{2\Delta t^2}{\tau^2}\right)\frac{(V_{\rm exp}^{n+1})^2}{2}\\
&\quad+\frac{\beta}{2}(Q^{n})^2+\frac{C_\Gamma^2}{2\mu}\Delta t(\mathcal{P}^n)^2+C_\Omega^{(3)}\mathcal{L}^2\|\nabla\mathbf{u}^n\|_{L^2(\Omega)}\left\|A_{\mu,0}\mathbf{u}^{n+1}\right\|^2_{\rho,\beta},
\end{aligned}\tag{4.53}$$

where $\delta_{\Delta t}$ have been previously defined in the proof of Theorem 3.9 (see (3.12)). As the coupling is explicit the next test function to consider is $A_{\mu,0}\mathbf{u}^{n+1}$. Note that the constant $\mathcal{L}$ appearing in the previous estimate (4.53) does not depend on the parameter α. Following the same lines as in the proof of Theorem 4.13 leads to

$$\begin{aligned}
\frac{\mu}{2}\left\|\nabla\mathbf{u}^{n+1}\right\|^2_{L^2(\Omega)}+\Delta t\left\|A_{\mu,0}\mathbf{u}^{n+1}\right\|^2_{\rho,\beta}&\leq\frac{\mu}{2}\|\nabla\mathbf{u}^n\|^2_{L^2(\Omega)}+\frac{\kappa^2}{4\delta\rho}\Delta t(\mathcal{P}^{n+1})^2+C_\Omega^{(7)}\mathcal{M}_0\Delta t\|\nabla\mathbf{u}^n\|_{L^2(\Omega)}\left\|A_{\mu,0}\mathbf{u}^{n+1}\right\|^2_{\rho,\beta}\\
&\quad+\alpha\Delta t\left|Q^n\int_{\Gamma_W}A_{\mu,0}\mathbf{u}^{n+1}\cdot\mathbf{n}\right|+\gamma\Delta t\left|V_{\rm exp}^{n+1}\int_{\Gamma_W}A_{\mu,0}\mathbf{u}^{n+1}\cdot\mathbf{n}\right|.
\end{aligned}\tag{4.54}$$

Here the constant $\mathcal{M}_0$ is associated to the operator $A_{\mu,0}$ and thus is defined by (4.3) with $\alpha=0$ (see (4.52)). We next have to estimate the last two terms of the right hand side of (4.54) corresponding to the explicit coupling. Let us first consider $\alpha\Delta t\left|Q^n\int_{\Gamma_W}A_{\mu,0}\mathbf{u}^{n+1}\cdot\mathbf{n}\right|$. By Lemma 2.4 and Young's inequality, we have

$$\begin{aligned}
\alpha\Delta t\left|Q^n\int_{\Gamma_W}A_{\mu,0}\mathbf{u}^{n+1}\cdot\mathbf{n}\right|&\leq\frac{\alpha\kappa^2}{\sqrt{\rho}}\Delta t\|\mathbf{u}^n\|_{L^2(\Omega)}\left\|A_{\mu,0}\mathbf{u}^{n+1}\right\|_{\rho,\beta}\\
&\leq\frac{\alpha^2\kappa^4}{4\delta\rho}\Delta t\|\mathbf{u}^n\|^2_{L^2(\Omega)}+\delta\Delta t\left\|A_{\mu,0}\mathbf{u}^{n+1}\right\|^2_{\rho,\beta},
\end{aligned}\tag{4.55}$$

where $\delta>0$ will be chosen later. Next we estimate $\gamma\Delta t\left|V_{\rm exp}^{n+1}\int_{\Gamma_W}A_{\mu,0}\mathbf{u}^{n+1}\cdot\mathbf{n}\right|$ using once again Lemma 2.4:

$$\gamma\Delta t\left|V_{\rm exp}^{n+1}\int_{\Gamma_W}A_{\mu,0}\mathbf{u}^{n+1}\cdot\mathbf{n}\right|\leq\frac{\gamma\kappa}{\sqrt{\rho}}\Delta t\left|V_{\rm exp}^{n+1}\right|\left\|A_{\mu,0}\mathbf{u}^{n+1}\right\|_{\rho,\beta}$$

At this stage we do not distinghish two cases as we did previoulsly. In the general case we can not take advantage of the dissipation of the volume, thus we estimate $\gamma\Delta t\left|V_{\rm exp}^{n+1}\int_{\Gamma_W}A_{\mu,0}\mathbf{u}^{n+1}\cdot\mathbf{n}\right|$ as we did in the implicit coupling, see (4.45):

$$\gamma\Delta t\left|V_{\rm exp}^{n+1}\int_{\Gamma_W}A_{\mu,0}\mathbf{u}^{n+1}\cdot\mathbf{n}\right|\leq\frac{\kappa^2\gamma^2}{\delta\rho}\Delta t(V_{\rm exp}^{n+1})^2+\delta\Delta t\left\|A_{\mu,0}\mathbf{u}^{n+1}\right\|^2_{\rho,\beta}.\tag{4.56}$$

Thus from (4.54) multiplied by a homogeneity coefficient $r>0$, using (4.55), choosing $\delta=\frac{1}{4}$, and adding (4.53) we obtain

$$\begin{aligned}
&\frac{\rho}{2}\left(1-\frac{\alpha\kappa^2}{\rho}\Delta t-\frac{2\gamma\kappa^2}{\rho}\Delta t^2\right)\frac{\rho}{2}\|\mathbf{u}^{n+1}\|^2_{L^2(\Omega)}+\frac{\mu}{2}(r+\Delta t)\|\nabla\mathbf{u}^{n+1}\|^2_{L^2(\Omega)}+\frac{\gamma}{\delta_{\Delta t}}\frac{(V_{\rm exp}^{n+2})^2}{2}+\frac{\gamma\Delta t}{\tau}(V_{\rm exp}^{n+1})^2+\frac{\beta}{2}(Q^{n+1})^2\\
&\quad+\left(\frac{r}{2}-\left(C_\Omega^{(3)}\mathcal{L}^2+rC_\Omega^{(7)}\mathcal{M}_0\right)\|\nabla\mathbf{u}^n\|_{L^2(\Omega)}\right)\Delta t\left\|A_{\mu,0}\mathbf{u}^{n+1}\right\|^2_{\rho,\beta}\\
&\quad\leq\frac{\rho}{2}\left(1+\left(\frac{\alpha\kappa^2}{\rho}+\frac{2r\alpha^2\kappa^4}{\rho^2}\right)\Delta t\right)\|\mathbf{u}^n\|^2_{L^2(\Omega)}+\frac{r\mu}{2}\|\nabla\mathbf{u}^n\|^2_{L^2(\Omega)}\\
&\quad+\frac{\gamma}{\delta_{\Delta t}}\left(1+\frac{8r\kappa^2\gamma\delta_{\Delta t}}{\rho}\Delta t+\frac{2}{\tau^2}\Delta t^2\right)\frac{(V_{\rm exp}^{n+1})^2}{2}+\frac{\beta}{2}(Q^n)^2+\left(\frac{C_\Gamma^2}{2\mu}+\frac{2r\kappa^2}{\rho}\right)\Delta t(\mathcal{P}^n)^2.
\end{aligned}\tag{4.57}$$

Next remembering the definition of the polynomial function P (see (3.19)) and its positive root λ_1 (see (3.20)) and using the lower bound (3.21), we have

$$\begin{aligned}\frac{\rho}{2}\left(1-\frac{\Delta t}{\lambda_1}\right)\|\mathbf{u}^{n+1}\|^2_{L^2(\Omega)}+\frac{\mu}{2}(r+\Delta t)\|\nabla\mathbf{u}^{n+1}\|^2_{L^2(\Omega)}+\frac{\gamma}{\delta_{\Delta t}}\frac{(V^{n+2}_{\exp})^2}{2}+\frac{\gamma\Delta t}{\tau}(V^{n+1}_{\exp})^2+\frac{\beta}{2}(Q^{n+1})^2\\ +\left(\frac{r}{2}-\left(C^{(3)}_\Omega\mathcal{L}^2+rC^{(7)}_\Omega\mathcal{M}_0\right)\|\nabla\mathbf{u}^n\|_{L^2(\Omega)}\right)\Delta t\left\|A_{\mu,0}\mathbf{u}^{n+1}\right\|^2_{\rho,\beta}\\ \leq\frac{\rho}{2}\left(1+\left(\frac{\alpha\kappa^2}{\rho}+\frac{2r\alpha^2\kappa^4}{\rho^2}\right)\Delta t\right)\|\mathbf{u}^n\|^2_{L^2(\Omega)}+\frac{r\mu}{2}\|\nabla\mathbf{u}^n\|^2_{L^2(\Omega)}\\ +\frac{\gamma}{\delta_{\Delta t}}\left(1+\frac{8r\kappa^2\gamma\delta_{\Delta t}}{\rho}\Delta t+\frac{2}{\tau^2}\Delta t^2\right)\frac{(V^{n+1}_{\exp})^2}{2}+\frac{\beta}{2}(Q^n)^2+\left(\frac{C^2_\Gamma}{2\mu}+\frac{2r\kappa^2}{\rho}\right)\Delta t(\mathcal{P}^n)^2.\end{aligned}\tag{4.58}$$

Thus assuming that

$$\left\|\nabla\mathbf{u}^k\right\|_{L^2(\Omega)}\leq\frac{r}{4\left(C^{(3)}_\Omega\mathcal{L}^2+rC^{(7)}_\Omega\mathcal{M}_0\right)},\quad\forall k\in\{0,...,n\},\tag{4.59}$$

and if we moreover impose $\Delta t<\lambda_1$, we obtain thanks to the discrete Gronwall Lemma that

$$\begin{aligned}&\frac{\rho}{2}\|\mathbf{u}^{n+1}\|^2_{L^2(\Omega)}+\frac{r\mu}{2}\|\nabla\mathbf{u}^{n+1}\|^2_{L^2(\Omega)}+\frac{\gamma}{\delta_{\Delta t}}\frac{(V^{n+2}_{\exp})^2}{2}+\frac{\beta}{2}(Q^{n+1})^2+\frac{r}{4}\Delta t\sum_{k=0}^{n+1}\left\|A_{\mu,0}\mathbf{u}^k\right\|^2_{\rho,\beta}\\ &\leq\mathrm{e}^{C^{\mathrm{NS}}_{\Delta t,r}T}\mathrm{e}^{\frac{T}{\lambda_1-\Delta t}}\left(\frac{\rho}{2}\|\mathbf{u}^0\|^2_{L^2(\Omega)}+\frac{r\mu}{2}\|\nabla\mathbf{u}^0\|^2_{L^2(\Omega)}+\frac{\gamma}{\delta_{\Delta t}}\frac{(V^1_{\exp})^2}{2}+\frac{\beta}{2}(Q^0)^2+\left(\frac{C^2_\Gamma}{2\mu}+\frac{2r\kappa^2}{\rho}\right)\Delta t\sum_{k=0}^{n}(\mathcal{P}^k)^2\right),\end{aligned}$$

with $C^{\mathrm{NS}}_{\Delta t,r}$ defined by (4.51). Consequently if the data satisfy

$$\frac{\rho}{2}\|\mathbf{u}^0\|^2_{L^2(\Omega)}+\frac{r\mu}{2}\|\nabla\mathbf{u}^0\|^2_{L^2(\Omega)}+\frac{\gamma}{\delta_{\Delta t}}\frac{(V^1_{\exp})^2}{2}+\frac{\beta}{2}(Q^0)^2+\Delta t\left(\frac{C^2_\Gamma}{2\mu}+\frac{2r\kappa^2}{\rho}\right)\sum_{k=0}^{N}(\mathcal{P}^k)^2\leq\frac{r^3\mu\mathrm{e}^{-C^{\mathrm{NS}}_{\Delta t,r}T}\mathrm{e}^{-\frac{T}{\lambda_1-\Delta t}}}{32\left(C^{(3)}_\Omega\mathcal{L}^2+rC^{(7)}_\Omega\mathcal{M}_0\right)^2},$$

we obtain the desired result by induction. □

Remark 4.19. *Let us discuss the* so called *dissipative case, namely $\tau<+\infty$ for which we could have tried to take advantage of the volume dissipation. In this case we can reproduce* (4.20) *to obtain*

$$\gamma\Delta t\left|V^{n+1}_{\exp}\int_{\Gamma_W}A_{\mu,0}\mathbf{u}^{n+1}\cdot\mathbf{n}\right|\leq\frac{\gamma}{2\eta\tau}\Delta t(V^{n+1}_{\exp})^2+\frac{\eta\tau\kappa^2\gamma}{2\rho}\Delta t\left\|A_{\mu,0}\mathbf{u}^{n+1}\right\|^2_{\rho,\beta}\tag{4.60}$$

Thus by (4.55) *and* (4.60)*, the bound* (4.54) *becomes*

$$\begin{aligned}\frac{\mu}{2}\left\|\nabla\mathbf{u}^{n+1}\right\|^2_{L^2(\Omega)}+\Delta t\left\|A_{\mu,0}\mathbf{u}^{n+1}\right\|^2_{\rho,\beta}\leq\frac{\mu}{2}\left\|\nabla\mathbf{u}^n\right\|^2_{L^2(\Omega)}+\frac{\kappa^2}{4\delta\rho}\Delta t(\mathcal{P}^{n+1})^2+C^{(7)}_\Omega\mathcal{M}_0\Delta t\left\|\nabla\mathbf{u}^n\right\|_{L^2(\Omega)}\left\|A_{\mu,0}\mathbf{u}^{n+1}\right\|^2_{\rho,\beta}\\ +\frac{\alpha^2\kappa^4}{4\delta\rho}\Delta t\left\|\mathbf{u}^n\right\|^2_{L^2(\Omega)}+\frac{\gamma}{2\eta\tau}\Delta t(V^{n+1}_{\exp})^2+\left(\delta+\frac{\eta\tau\kappa^2\gamma}{2\rho}\right)\Delta t\left\|A_{\mu,0}\mathbf{u}^{n+1}\right\|^2_{\rho,\beta}.\end{aligned}\tag{4.61}$$

By choosing δ and η satisfying (4.22)*, the previous estimate* (4.61) *writes*

$$\begin{aligned}&\frac{\mu}{2}\left\|\nabla\mathbf{u}^{n+1}\right\|^2_{L^2(\Omega)}+\left(\frac{1}{2}-C^{(7)}_\Omega\mathcal{M}_0\left\|\nabla\mathbf{u}^n\right\|_{L^2(\Omega)}\right)\Delta t\left\|A_{\mu,0}\mathbf{u}^{n+1}\right\|^2_{\rho,\beta}\\ &\leq\frac{\mu}{2}\left\|\nabla\mathbf{u}^n\right\|^2_{L^2(\Omega)}+\frac{\kappa^2}{4\delta\rho}\Delta t(\mathcal{P}^{n+1})^2+\frac{\alpha^2\kappa^4}{4\delta\rho}\Delta t\left\|\mathbf{u}^n\right\|^2_{L^2(\Omega)}+\frac{\gamma}{2\eta\tau}\Delta t(V^{n+1}_{\exp})^2\end{aligned}\tag{4.62}$$

By multiplying (4.62) *by* η *and adding* (4.53)*, leads to*

$$\begin{aligned}\frac{\rho}{2}\left(1-\frac{\alpha\kappa^2}{\rho}\Delta t-\frac{2\gamma\kappa^2}{\rho}\Delta t^2\right)\|\mathbf{u}^{n+1}\|^2_{L^2(\Omega)}+\frac{\mu}{2}(\eta+\Delta t)\|\nabla\mathbf{u}^{n+1}\|^2_{L^2(\Omega)}+\frac{\gamma}{\delta_{\Delta t}}\frac{(V_{\rm exp}^{n+2})^2}{2}+\frac{\gamma\Delta t}{2\tau}(V_{\rm exp}^{n+1})^2+\frac{\beta}{2}(Q^{n+1})^2\\ +\left(\frac{\eta}{2}-\left(C_\Omega^{(3)}\mathcal{L}^2+C_\Omega^{(7)}\eta\mathcal{M}_0\right)\|\nabla\mathbf{u}^n\|_{L^2(\Omega)}\right)\Delta t\left\|A_{\mu,0}\mathbf{u}^{n+1}\right\|^2_{\rho,\beta}\\ \leq\frac{\rho}{2}\left(1+\left(\frac{\alpha\kappa^2}{\rho}+\frac{\eta\alpha^2\kappa^4}{8\delta\rho^2}\right)\Delta t\right)\|\mathbf{u}^n\|^2_{L^2(\Omega)}+\frac{\mu\eta}{2}\|\nabla\mathbf{u}^n\|^2_{L^2(\Omega)}+\frac{\gamma}{\delta_{\Delta t}}\left(1+\frac{2\Delta t^2}{\tau^2}\right)\frac{(V_{\rm exp}^{n+1})^2}{2}+\frac{\beta}{2}(Q^n)^2\\ +\left(\frac{C_\Gamma^2}{2\mu}+\frac{\eta\kappa^2}{4\delta\rho}\right)\Delta t(\mathcal{P}^n)^2.\end{aligned}$$

Let us define $\mathcal{B}_0$ *by*

$$\mathcal{B}_0=C_\Omega^{(3)}\mathcal{L}^2+C_\Omega^{(7)}\eta\mathcal{M}_0. \tag{4.63}$$

Note that $\mathcal{B}_0$ *corresponds to the constant* $\tilde{\mathcal{B}}$ *defined by* (4.40) *with* $\alpha=0$*. Next remembering the definition of the polynomial function* P *(see* (3.19)*) and its positive root* λ_1 *(see* (3.20)*) and using the the lower bound* (3.21)*, remembering also the definitions of* $\mathcal{A}$ *defined by* (4.26) *and of* H *defined by* (4.27)*, we have*

$$\begin{aligned}\frac{\rho}{2}\left(1-\frac{\Delta t}{\lambda_1}\right)\|\mathbf{u}^{n+1}\|^2_{L^2(\Omega)}+\frac{\mu}{2}(\eta+\Delta t)\|\nabla\mathbf{u}^{n+1}\|^2_{L^2(\Omega)}+\frac{\gamma}{\delta_{\Delta t}}\frac{(V_{\rm exp}^{n+2})^2}{2}+\frac{\gamma\Delta t}{2\tau}(V_{\rm exp}^{n+1})^2+\frac{\beta}{2}(Q^{n+1})^2\\ +\left(\mathcal{A}-\mathcal{B}_0\|\nabla\mathbf{u}^n\|_{L^2(\Omega)}\right)\Delta t\left\|A_{\mu,0}\mathbf{u}^{n+1}\right\|^2_{\rho,\beta}\\ \leq\frac{\rho}{2}\left(1+\left(\frac{\alpha\kappa^2}{\rho}+\frac{\eta\alpha^2\kappa^4}{8\delta\rho^2}\right)\Delta t\right)\|\mathbf{u}^n\|^2_{L^2(\Omega)}+\frac{\mu\eta}{2}\|\nabla\mathbf{u}^n\|^2_{L^2(\Omega)}+\frac{\gamma}{\delta_{\Delta t}}\left(1+\frac{2\Delta t^2}{\tau^2}\right)\frac{(V_{\rm exp}^{n+1})^2}{2}+\frac{\beta}{2}(Q^n)^2+\Delta t H^n.\end{aligned}$$

Thus, if $\left\|\nabla\mathbf{u}^k\right\|_{L^2(\Omega)}\leq\frac{\mathcal{A}}{2\mathcal{B}_0}$*, for all* $k\in\{0,\dots,n\}$*, and assuming that* $\Delta t<\lambda_1$*, we obtain thanks to the discrete Gronwall Lemma*

$$\begin{aligned}\frac{\rho}{2}\|\mathbf{u}^{n+1}\|^2_{L^2(\Omega)}+\frac{\mu\eta}{2}\|\nabla\mathbf{u}^{n+1}\|^2_{L^2(\Omega)}+\frac{\gamma}{\delta_{\Delta t}}\frac{(V_{\rm exp}^{n+2})^2}{2}+\frac{\gamma\Delta t}{2\tau}(V_{\rm exp}^{n+1})^2+\frac{\beta}{2}(Q^{n+1})^2+\frac{\mathcal{A}}{2}\Delta t\sum_{k=0}^{n+1}\left\|A_{\mu,0}\mathbf{u}^k\right\|^2_{\rho,\beta}\\ \leq\mathrm{e}^{C_{\Delta t}^{\rm NS}T}\mathrm{e}^{\frac{T}{\lambda_1-\Delta t}}\left(\frac{\rho}{2}\|\mathbf{u}^0\|^2_{L^2(\Omega)}+\frac{\mu\eta}{2}\|\nabla\mathbf{u}^0\|^2_{L^2(\Omega)}+\frac{\gamma}{\delta_{\Delta t}}\frac{(V_{\rm exp}^1)^2}{2}+\frac{\beta}{2}(Q^0)^2+\Delta t\sum_{k=0}^{n}H^k\right),\end{aligned} \tag{4.64}$$

where

$$C_{\Delta t}^{\rm NS}=C_{\Delta t}^{\rm S}+\frac{\eta\alpha^2\kappa^4}{8\delta\rho^2}.$$

Consequently the desired discrete stability estimate can be proven by induction assuming that the data of the problem satisfy

$$\mathrm{e}^{C_{\Delta t}^{\rm NS}T}\mathrm{e}^{\frac{T}{\lambda_1-\Delta t}}\left(\frac{\rho}{2}\|\mathbf{u}^0\|^2_{L^2(\Omega)}+\frac{\mu\eta}{2}\|\nabla\mathbf{u}^0\|^2_{L^2(\Omega)}+\frac{\gamma}{\delta_{\Delta t}}\frac{(V_{\rm exp}^1)^2}{2}+\frac{\beta}{2}(Q^0)^2+\Delta t\sum_{k=0}^{N}H^k\right)\leq\frac{\eta\mu}{8}\frac{\mathcal{A}^2}{\mathcal{B}_0^2}.$$

As a conclusion, in the case of the semi-discrete Navier–Stokes system coupled explicitly to the 0D model, the obtained stability estimates are quite similar in both considered cases. In both proofs, we exhibit a similar sufficient condition on the time step (which is the same as for the Stokes system) and restrictive assumptions on the data imposing smallness of the initial data as well as on the applied forces but also on the global time T. In particular in the *so called* dissipative case, when explicitly coupled to the Navier–Stokes equation, the system does not dissipate energy anymore.

Remark 4.20. *As in the proof of Theorem 3.9 we can adapt the previous calculations to the case where $\beta > 0$ and take advantage of the inertia of the 0D model. For the sake of simplicity we do not reproduce the calculations here.*

Remark 4.21. *For the case where $\tau < +\infty$ in order to control the exponential growth $\mathrm{e}^{\frac{2\Delta t}{\tau^2}T}$ one could impose to the time step to satisfy $\Delta t \leq \frac{2\tau^2}{T}$ which could be a rather restrictive condition in particular for large time T or small relaxation time τ.*

5. Numerical results

5.1. Numerical method for the implicit coupling

In this section we numerically illustrate some of the previous theoretical results. First, let us present the way we choose to solve the Navier–Stokes–Windkessel model with the implicit coupling, since this case involves all the numerical difficulties of the problems we are interested in. We focus on a 2D/0D coupled problem, for the sake of simplicity and we use the software `FreeFem++` which is a programming language and a free software focused on solving PDEs using the finite element method, see https://freefem.org/.

Basically `FreeFem++` is a finite element library which contains basic solvers for linear problems such as Stokes problems (actually it builds the resulting linear system based upon the finite element approximation of a linear variational problem and, if well-posed, proposes associated numerical solvers). The resolution of the Stokes problems is done with classical inf-sup stable $P_2 - P_1$ finite elements. The scheme we use allows us to deal with the nonlocal boundary condition by solving only standard Stokes problems with mixed Dirichlet–Neumann boundary conditions. The method relies on a superposition principle that is proposed in [14] and which is similar to what is proposed in [50]. It has the advantage not to alter the conditioning of the resulting matrix with respect to the parameters of the 0D model. The main drawback of the method is its computational cost in the case of a large number of outlets. The semi-discretized problem takes the following form:

$$\begin{cases} \dfrac{\rho}{\Delta t}\mathbf{u}^{n+1} + \varepsilon(\mathbf{u}^n \cdot \nabla)\mathbf{u}^{n+1} - \mu\Delta\mathbf{u}^{n+1} + \nabla p^{n+1} = \dfrac{\rho}{\Delta t}\mathbf{u}^n, & \text{on } \Omega, \\ \operatorname{div}(\mathbf{u}^{n+1}) = 0, & \text{on } \Omega, \\ \mathbf{u}^{n+1} = 0, & \text{on } \Gamma_\ell \\ -\mu\nabla\mathbf{u}^{n+1}\cdot\mathbf{n} + p^{n+1}\mathbf{n} = g_0\,\mathbf{n}, & \text{on } \Gamma_0 \\ -\mu\nabla\mathbf{u}^{n+1}\cdot\mathbf{n} + p^{n+1}\mathbf{n} = \alpha Q^{n+1}\,\mathbf{n} + g_1\,\mathbf{n}, & \text{on } \Gamma_1 \end{cases} \tag{5.1}$$

where $g := g_i$ denote source terms that may depend to the solution at previous time steps. All the systems we are interested in (such as R, RC, RCL, RCRL models) fall into the scope of this formalism, by choosing or updating in a suitable manner the generalized parameters or functions α and g_i.

The main difficulty relies on the nonlocal boundary condition located at Γ_1 since

$$Q^{n+1} = \int_{\Gamma_1} \mathbf{u}^{n+1}\cdot\mathbf{n}.$$

We propose the following strategy, which allows us not to build the contribution of the nonlocal term in the resulting matrix. The method is based on the construction of the solution of two linear systems at each time step:

1. Define $(\mathbf{w}^0, \pi^0)$ as the solution of

$$\begin{cases} \dfrac{\rho}{\Delta t}\mathbf{w}^0 + \varepsilon(\mathbf{u}^n \cdot \nabla)\mathbf{w}^0 - \mu\Delta\mathbf{w}^0 + \nabla\pi^0 = \dfrac{\rho}{\Delta t}\mathbf{u}^n, & \text{on } \Omega, \\ \operatorname{div}(\mathbf{w}^0) = 0, & \text{on } \Omega, \\ \mathbf{w}^0 = 0, & \text{on } \Gamma_\ell \\ -\mu\nabla\mathbf{w}^0\cdot\mathbf{n} + \pi^0\mathbf{n} = g_0\,\mathbf{n}, & \text{on } \Gamma_0 \\ -\mu\nabla\mathbf{w}^0\cdot\mathbf{n} + \pi^0\mathbf{n} = g_1\,\mathbf{n}, & \text{on } \Gamma_1 \end{cases} \tag{5.2}$$

TABLE 2. Stability results for the (Navier–)Stokes-R model with applied pressure $g_0 = 5\times10^{+2}$. Symbol $\square$ means that the simulation is stable whereas $\boxtimes$ means that it is unstable.

Time step Δt	0.05	0.10	0.20	0.40
Stokes (implicit)	$\square$	$\square$	$\square$	$\square$
Stokes (explicit)	$\square$	$\square$	$\boxtimes$	$\boxtimes$
Navier–Stokes (implicit)	$\boxtimes$	$\boxtimes$	$\boxtimes$	$\boxtimes$
Navier–Stokes (explicit)	$\boxtimes$	$\boxtimes$	$\boxtimes$	$\boxtimes$

2. Define $(\mathbf{w}^1, \pi^1)$ as the solution of

$$\begin{cases} \dfrac{\rho}{\Delta t}\mathbf{w}^1 + \varepsilon(\mathbf{u}^n\cdot\nabla)\mathbf{w}^1 - \mu\Delta\mathbf{w}^1 + \nabla\pi^1 = \mathbf{0}, & \text{on } \Omega, \\ \operatorname{div}(\mathbf{w}^1) = 0, & \text{on } \Omega, \\ \mathbf{w}^1 = 0, & \text{on } \Gamma_\ell \\ -\mu\nabla\mathbf{w}^1\cdot\mathbf{n} + \pi^1\mathbf{n} = 0, & \text{on } \Gamma_0 \\ -\mu\nabla\mathbf{w}^1\cdot\mathbf{n} + \pi^1\mathbf{n} = 1\,\mathbf{n}, & \text{on } \Gamma_1 \end{cases} \tag{5.3}$$

3. By linearity, define

$$(\mathbf{u}^{n+1}, p^{n+1}) = (\mathbf{w}^0, \pi^0) + k(\mathbf{w}^1, \pi^1),$$

where k has to be fixed. By means of construction, we have

$$\begin{aligned} -\mu\nabla\mathbf{w}^0\cdot\mathbf{n} + \pi^0\mathbf{n} + k(-\mu\nabla\mathbf{w}^1\cdot\mathbf{n} + \pi^1\mathbf{n}) &= g_0\,\mathbf{n}, && \text{on } \Gamma_0, \\ -\mu\nabla\mathbf{w}^0\cdot\mathbf{n} + \pi^0\mathbf{n} + k(-\mu\nabla\mathbf{w}^1\cdot\mathbf{n} + \pi^1\mathbf{n}) &= (k+g_1)\,\mathbf{n}, && \text{on } \Gamma_1, \end{aligned}$$

and k has to be chosen such that $k = \alpha\left(\int_{\Gamma_1}\mathbf{w}^0\cdot\mathbf{n} + k\int_{\Gamma_1}\mathbf{w}^1\cdot\mathbf{n}\right)$ *i.e.*

$$k = \frac{\alpha\int_{\Gamma_1}\mathbf{w}^0\cdot\mathbf{n}}{1-\alpha\int_{\Gamma_1}\mathbf{w}^1\cdot\mathbf{n}}.$$

Note that if $\varepsilon = 0$ (in the case of the Stokes–Windkessel system), the computation of $\mathbf{w}^1$ is required only once (this computation can be made offline).

5.2. Numerical results for the R model

We focus on a simple tubular geometry. The data are built upon some analogy in cgs units. The tubular dimensions are set to $L_x = 2$ and $L_y = 12$ and the computational mesh is generated with 20×120 nodes. Computations have been led for the R model with the following parameters:

$$\rho = 1.2\times10^{-3}, \quad \mu = 2\times10^{-4}, \quad \alpha = 1\times10^{-1}.$$

The initial velocity field is set to 0. Let Δt be the computational time step and let us recall that g_0 which represents the applied pressure and it has still to be prescribed.

- *Experiment 1.* Results summarized in Table 2 correspond to an applied pressure g_0 which is taken as a constant function, *i.e.* $g_0 = 5\times10^{+2}$.
  For $\Delta t = 0.10$, the numerical solution of the *Stokes-R model* with the *explicit* scheme is stable and the solution converges to a stationary Poiseuille profile, see Figure 4. Note that the stationary Poiseuille profile corresponds to the stationary flow obtained in a tube whose length is equal to the sum of the length of the original (truncated) tube plus the one corresponding to the resistive 0D model.

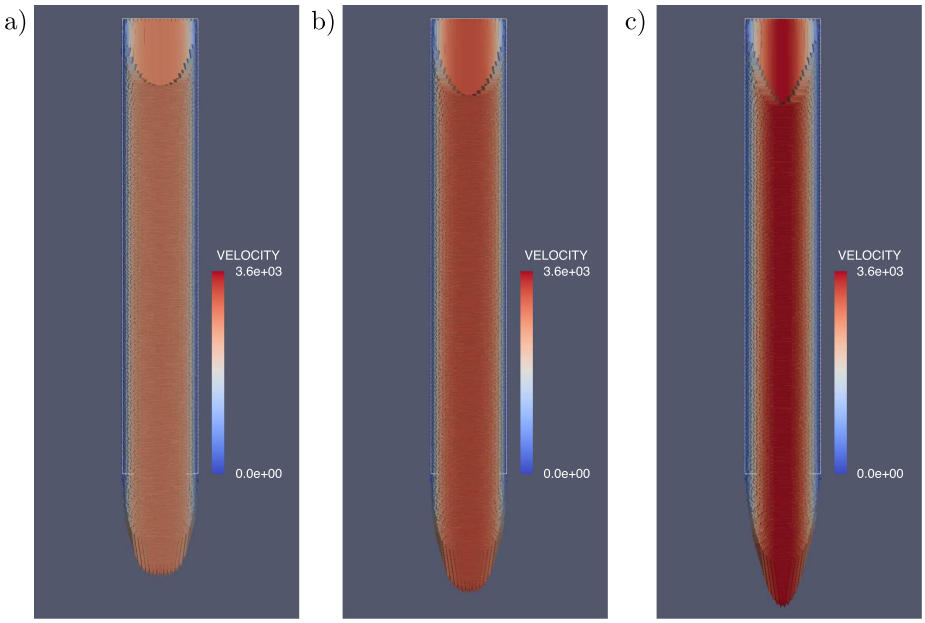

FIGURE 4. Simulation of the Stokes-R model with explicit coupling with "small" time-step ($\Delta t = 0.10$). Velocity field at time $i\Delta t$ (for $i = 1, 2, 10$).

For $\Delta t = 0.20$, the numerical solution of the *Stokes-R model* with the *explicit* scheme is unstable: instability is observed with spontaneous unphysical inversions of the flow between two time steps: flow reversal is observed at each time step and the magnitude of the flux (at the inlet) exponentially increases, through the analysis of the flux at the inlet (upper boundary), see Figure 5. This illustrates how the stability for the simulation of the Stokes-R model with explicit coupling depends on the distance of the value of the time step from the critical value $\frac{\rho}{\alpha\kappa^2}$.

The numerical solution of the *Stokes-R model* with the *implicit* scheme is unconditionally stable for any value of the time step and it converges to the stationary Poiseuille profile that was previously observed with the explicit coupling (stable case).

Then when considering the convective terms, the observations are quite different: the numerical solution of the *Navier–Stokes-R model* is unstable for both *implicit* and *explicit* schemes, whatever the value of the time-step is: blow up phenomena appear, see Figure 6. Instabilities presumably come from the smallness assumption on the data which is not satisfied: this will be confirmed in the next series of numerical results.

- *Experiment 2.* In order to verify the argument related to the smallness assumption, we perform the very same simulations as before except for the value of g_0 which is now set to $g_0 = 5 \times 10^{+0}$ (*i.e.* the applied pressure is 100 times smaller as in the previous cases). Results are summarized in Table 3.

  As expected, the stability results of the Stokes-R model are not affected by the modification of the applied pressure. When focusing on the Navier–Stokes-R model with the *implicit* coupling, the results have turned out to be stable due to the data reduction, as no restriction on the time step is required, see Remark 4.17. When focusing on the Navier–Stokes-R model with the *explicit* coupling, the conditional stability ensured by the smallness of the data (due to the convective term in the Navier–Stokes system) and time step restriction (due to the explicit coupling) is illustrated by the numerical results.
- *Experiment 3.* Let us highlight the role of the threshold value $\frac{\rho}{\alpha\kappa^2}$ for the time step on the stability of the explicit scheme in the Stokes-R model. Fixing the fluid viscosity at $\mu = 2 \times 10^{-4}$ and the applied pressure at $g^0 = 5 \times 10^{+2}$, we exhibit the constraint on the time step in Table 4:

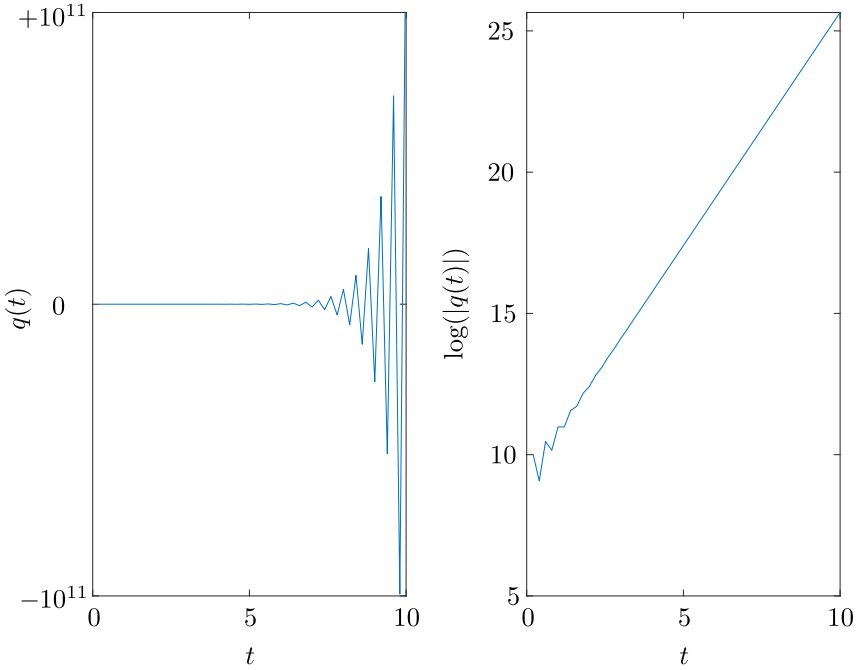

FIGURE 5. Simulation of the Stokes-R model with explicit coupling with "large" time-step ($\Delta t = 0.20$). Evolution of the flux at the upper boundary: $t \mapsto q(t) := L_x \int_{\Gamma_0} \mathbf{u}(t,\cdot) \cdot \mathbf{n}$. Oscillations are observed at each time step and the magnitude has an exponential behaviour.

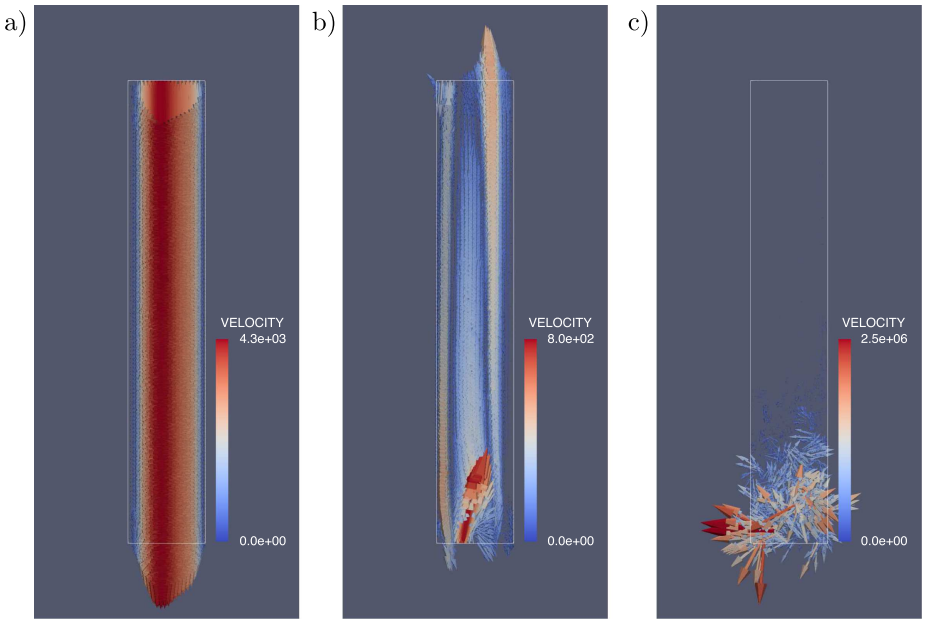

FIGURE 6. Simulation of the Navier–Stokes-R model with explicit coupling with time-step $\Delta t = 0.10$. Velocity field at time $i\Delta t$ (for $i = 2, 6, 10$). The numerical solution is unstable as blow up occurs.

TABLE 3. Stability results for the (Navier–)Stokes-R model with applied pressure $g_0 = 5 \times 10^{+0}$. Symbol ☐ means that the simulation is stable whereas ☒ means that it is unstable.

Time step Δt	0.05	0.10	0.20	0.40
Stokes (implicit)	☐	☐	☐	☐
Stokes (explicit)	☐	☐	☒	☒
Navier–Stokes (implicit)	☐	☐	☐	☐
Navier–Stokes (explicit)	☐	☐	☒	☒

TABLE 4. Stability results for the Stokes-R model with explicit coupling with applied pressure $g^0 = 5 \times 10^{+2}$. Symbol ☐ means that the simulation is stable whereas ☒ means that it is unstable.

	Time step Δt	0.05	0.10	0.20	0.40
(*)	$\rho = 1.2 \times 10^{-3},\ \alpha = 1 \times 10^{-1}$	☐	☐	☒	☒
(a)	$\rho = 2.4 \times 10^{-3},\ \alpha = 2 \times 10^{-1}$	☐	☐	☒	☒
(b)	$\rho = 2.4 \times 10^{-3},\ \alpha = 1 \times 10^{-1}$	☐	☐	☐	☒
(c)	$\rho = 1.2 \times 10^{-3},\ \alpha = 2 \times 10^{-1}$	☐	☒	☒	☒

We may observe that, for the tubular geometry under consideration, for $\rho = 1.2 \times 10^{-3}$ and $\alpha = 1 \times 10^{-1}$, the critical value of the time step lies between 0.10 and 0.20, see Table 4 (*). From this situation,

- multiplying both the fluid density and the model resistance by a factor 2, see Table 4 (a), does not alter this observation, which is expected since the critical time step $\frac{\rho}{\alpha\kappa^2}$ is not modified;
- multiplying only the fluid density by a factor 2, see Table 4 (b), allows us to choose a time step which is twice bigger as before: this is confirmed by the numerical simulations, as the critical time step now lies between 0.20 and 0.40 (instead of 0.10 and 0.20);
- multiplying only the resistance by a factor 2, see Table 4 (c), reduces the stability region by a factor 2: this is confirmed by the numerical simulations, as the critical time step now lies between 0.05 and 0.10 (instead of 0.10 and 0.20).

As a concluding remark, the previous observations do not depend on the applied pressure g^0: the stability results remain the same when considering $g^0 = 5 \times 10^{+4}$ instead of $g^0 = 5 \times 10^{+2}$, as the stability of the explicit scheme for the Stokes-R model is not affected by the magnitude of the data g^0.

5.3. Influence of the 0D inertance parameter on the numerical stability

We focus on the influence of the 0D inertance parameter β on the stability results.

First we illustrate in *Experiment 4* the instability occurring when the 0D inertia is treated explicitly and is large enough compared to the fluid inertia in the linear regime. Second, In *Experiments 5* and *6* we investigate the stabilization effect of the 0D inertia when treated implicitly in the nonlinear regime.

5.3.1. In the Stokes regime

In *Experiment 4*, we consider the Stokes system coupled to a resistance and an inductance. We consider the same parameter values as in Experiment 1 (with, in particular, a resistance value which is set to $\alpha = 1 \times 10^{-1}$) and we add some inductance 0D model (thus considering a RCL model with $C^{-1} = 0$). Parameter β is identified to L and we solve the Stokes-RL system with an implicit coupling for the resistance and an implicit or explicit coupling for the inductance. The time step is set to $\Delta t = 0.05$ and the applied pressure is set to $g_0 = 5 \times 10^{+0}$.

When considering the *implicit coupling* for the inductance (with values $L = 10^{-1}$, 10^{+0}, 10^{+1}), numerical simulations are stable, even if the time step and the applied pressure are increased.

TABLE 5. Blow up of the numerical solution with respect to the 0D inertance parameter β (all other data taken from Experiment 1, in the Navier–Stokes regime with the implicit coupling).

β	$T_{\text{blow up}}$
0	0.05
1×10^{-1}	0.10
$1 \times 10^{+0}$	0.30
$1 \times 10^{+1}$	2.80

TABLE 6. Stability of the numerical solution with respect to the applied pressure g^0 and the 0D inertance parameter β (all other data taken from Experiment 1, in the Navier–Stokes regime with the implicit coupling). Symbol ☐ means that the simulation is stable whereas ☒ means that it is unstable.

	$\beta = 0.0$	$\beta = 10.0$
$g^0 = 5.0 \times 10^{+2}$	☒	☒
$g^0 = 1.5 \times 10^{+1}$	☒	☐
$g^0 = 5.0 \times 10^{+0}$	☐	☐

When considering the *explicit coupling* for the inductance (with $L = 10^{-1}$), numerical simulations are unconditionnally unstable: we observe some unphysical flow reversal at each numerical time step along with a velocity magnitude which tends to explode. Instability is unconditional as smaller values of the time step or applied pressure lead to the very same phenomenon. Stable simulations are recovered for sufficiently small values of L as, for $L = 10^{-2}$, an oscillatory phenomenon is observed but no flow reversal occurs: in this regime the added-mass effect is negligible with respect to the inertia of the fluid.

5.3.2. In the Navier–Stokes regime

In *Experiment 5*, we consider the Navier–Stokes system coupled to a resistance and an inductance. We consider the same parameter values as in Experiment 1, and we add some inductance 0D model (thus considering a RCL model with $C^{-1} = 0$). We solve the implicit coupling (for both α and β) for the Navier–Stokes regime, with $\Delta t = 0.05$. We observe, see Table 5, that the existence time increases with β.

In *Experiment 6*, we investigate the numerical stability with respect to the applied pressure g^0 and the 0D inertance parameter β, see Table 6. Let us recall that the small data assumption is necessary for the global existence in the Navier–Stokes-R model (see Experiments 1 and 2 for the Navier–Stokes regime with the implicit coupling, while choosing either $g^0 = 5 \times 10^{+2}$ or $g^0 = 5 \times 10^{+0}$). Selecting an intermediate applied pressure, namely $g^0 = 1.5 \times 10^{+1}$ still leads to instabilities with the R model; but introducing some 0D inertance in the system provides numerical stabilisation. Taking into account inertia in the 0D model may allow us to increase the magnitude of the applied pressure in the simulations.

5.4. Influence of the geometry

Estimates that have been derived involve constants that depend on the geometry (such as Poincaré constant, for instance). In this subsection we illustrate the influence of the domain on the stability issue. In *Experiment 7*, we consider the Navier–Stokes system with

$$\rho = 1.2 \times 10^{-3}, \quad \mu = 0.5 \times 10^{-3}, \quad \alpha = \beta = \gamma = 0.$$

We report several simulations with the following domains:

TABLE 7. Influence of the geometry on the stability results for the Navier–Stokes system.

	T_1	T_2	B_{1-2}	T_1	T_5	B_{1-5}
$g^0 = +2.0$	□	□	⊠	□	⊠	⊠
$g^0 = -2.0$	□	□	□	□	⊠	□

- tubular domains (for which $|\Gamma_0| = |\Gamma_1|$) with dimensions

$$|\Gamma_0| = |\Gamma_1| = L_x = 1,\ 2 \text{ or } 5, \qquad L_y = 12$$

  respectively denoted T_1, T_2, T_5.
- bottle-like domains (for which $|\Gamma_0| < |\Gamma_1|$) with $L_y = 12$ and "upper" width $|\Gamma_0| = 1$ and "lower" width $|\Gamma_1| = 2$ or 5; these domains are respectively denoted B_{1-2} and B_{1-5}.

In each simulation the computational mesh is generated with 20 nodes per unit length and the time-step is set to $\Delta t = 0.1$. The boundary condition at Γ_1 reduces to a free outlet condition (as the 0D model parameters are set to 0) and the applied pressure at Γ_0 is (still) denoted g^0.

As expected $\mathbf{A}_1$ and $\mathbf{A}_2$ (resp.: $\mathbf{B}_1$ and $\mathbf{B}_2$; $\mathbf{C}_1$ and $\mathbf{C}_2$) give the very same results (Fig. 7). We see that increasing the radius of the tube leads to instable Navier–Stokes simulations for the same applied pressure. This is due to the fact that resistance of the tube T_5 is much smaller than the one of T_1 T_2 and thus the Reynolds number is higher in this case. When considering a bottle, even for small values of the in/outlet surfaces (which provides stable simulations in the case of a tube), instabilities appear but only when the flow enters through the smaller inlet. It shows the influence of the ratio $\frac{\Gamma_0}{\Gamma_1}$ and more generally of the geometry on the stability for the Navier–Stokes system with Neumann boundary conditions (and incoming flows) (Fig. 8).

5.5. On the backflow in the RCR model

In this subsection we illustrate the emergence of backflows in the context of RCR or RC models. In *Experiment 8*, we consider the Stokes system with

$$\rho = 1.2 \times 10^{-3}, \quad \mu = 2 \times 10^{-5}, \quad \alpha = \beta = \gamma = 0.$$

We report several simulations in a tubular domain with dimensions $L_x = 2$ and $L_y = 12$. The boundary condition at Γ_1 is associated to a RCR model and the applied pressure at Γ_0 is (still) denoted $g^0 = +1$. The RCR model is obtained with

$$\alpha = R_p \cdot L_x, \quad \beta = 0, \quad \gamma = C^{-1} \cdot L_x, \quad \tau = R_d \cdot C$$

and we will use the following values for R_p and C

$$R_p = 5 \times 10^{-2}, \quad C = 0.2,$$

whereas we will make the magnitude of R_d varies.

First let us deal with the *implicit scheme*. Using a time step $\Delta t = 0.1$ and a distal resistance $R_d = 5$ provides a stable simulation which reveals at the beginning the emergence of a backflow phenomenon which vanishes as the solution relaxes to steady state velocity. The backflow phenomenon is characterized at the boundaries by a normal velocity distribution which is not signed. Several observations can be made:

- From the reference situation we increase the value of the distal resistance. We observe that the backflow is enhanced by increasing values of R_d, see Figure 9 (actually, at $t = 0.5$, the backflow phenomenon has nearly

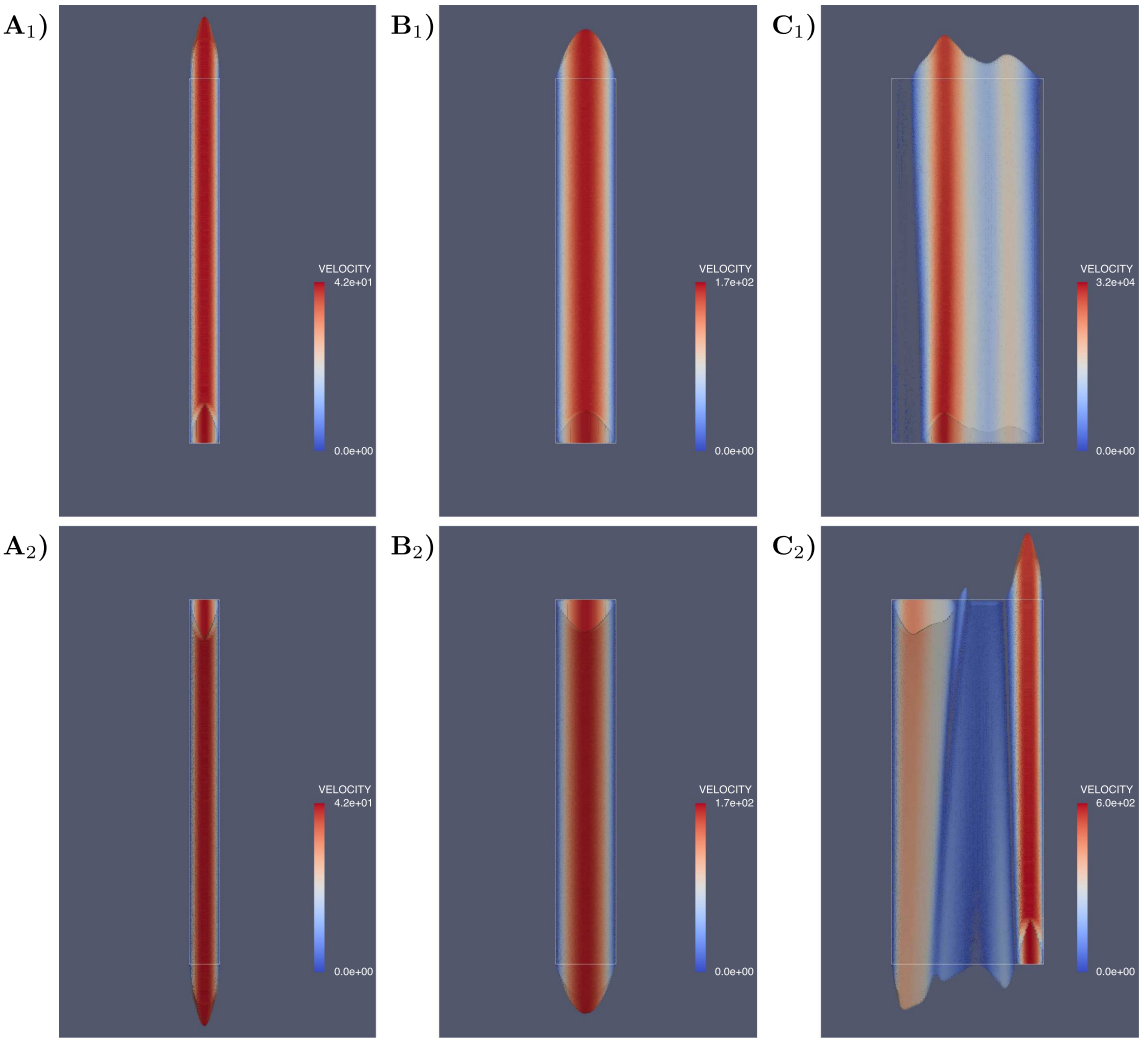

FIGURE 7. Velocity field for the Navier–Stokes model in a tube. **A$_1$)** in the domain T_1 with pressure drop $g^0 = -2$ at time $t = 15$ (distribution close to a steady state). **B$_1$)** in the domain T_2 with pressure drop $g^0 = -2$ at time $t = 15$ (distribution close to a steady state). **C$_1$)** in the domain T_5 with pressure drop $g^0 = -2$ at time $t = 5$ (the numerical solution is unphysical). **A$_2$)** in the domain T_1 with pressure drop $g^0 = +2$ at time $t = 15$ (distribution close to a steady state). **B$_2$)** in the domain T_2 with pressure drop $g^0 = +2$ at time $t = 15$ (distribution close to a steady state). **C$_2$)** in the domain T_5 with pressure drop $g^0 = +2$ at time $t = 5$ (the numerical solution is unstable).

vanished for $R_d = 5$). In particular, the simulation remains stable even for large values of R_d (including the RC model for which $R_d = +\infty$) and the persistence time of the phenomenon is increased with increasing values of R_d until reaching a limit regime (which is rapidly obtained, as only minor distribution differences are observed between $R_d = 50$ and $R_d = 500$).

Figure 10 presents a series of temporal snapshots exhibiting the backflow phenomenon for $R_d = 50$.

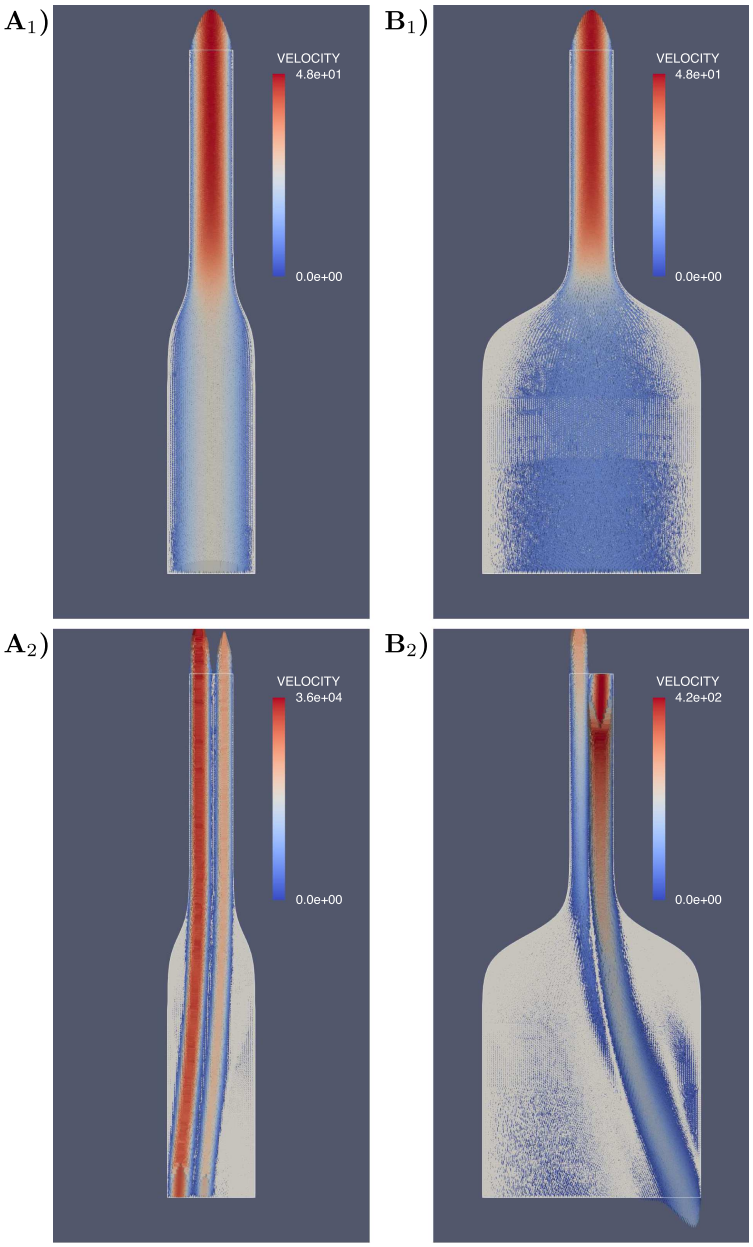

FIGURE 8. Velocity field for the Navier–Stokes model in a bottle-like geometry. **$\mathbf{A}_1$)** in the domain B_{1-2} with pressure drop $g^0 = -2$ at time $t = 15$ (distribution close to a steady state). **$\mathbf{B}_1$)** in the domain B_{1-5} with pressure drop $g^0 = -2$ at time $t = 15$ (distribution close to a steady state). **$\mathbf{A}_2$)** in the domain B_{1-2} with pressure drop $g^0 = +2$ at time $t = 12$ (the numerical solution is unphysical). **$\mathbf{B}_2$)** in the domain B_{1-5} with pressure drop $g^0 = +2$ at time $t = 10$ (the numerical solution is unstable).

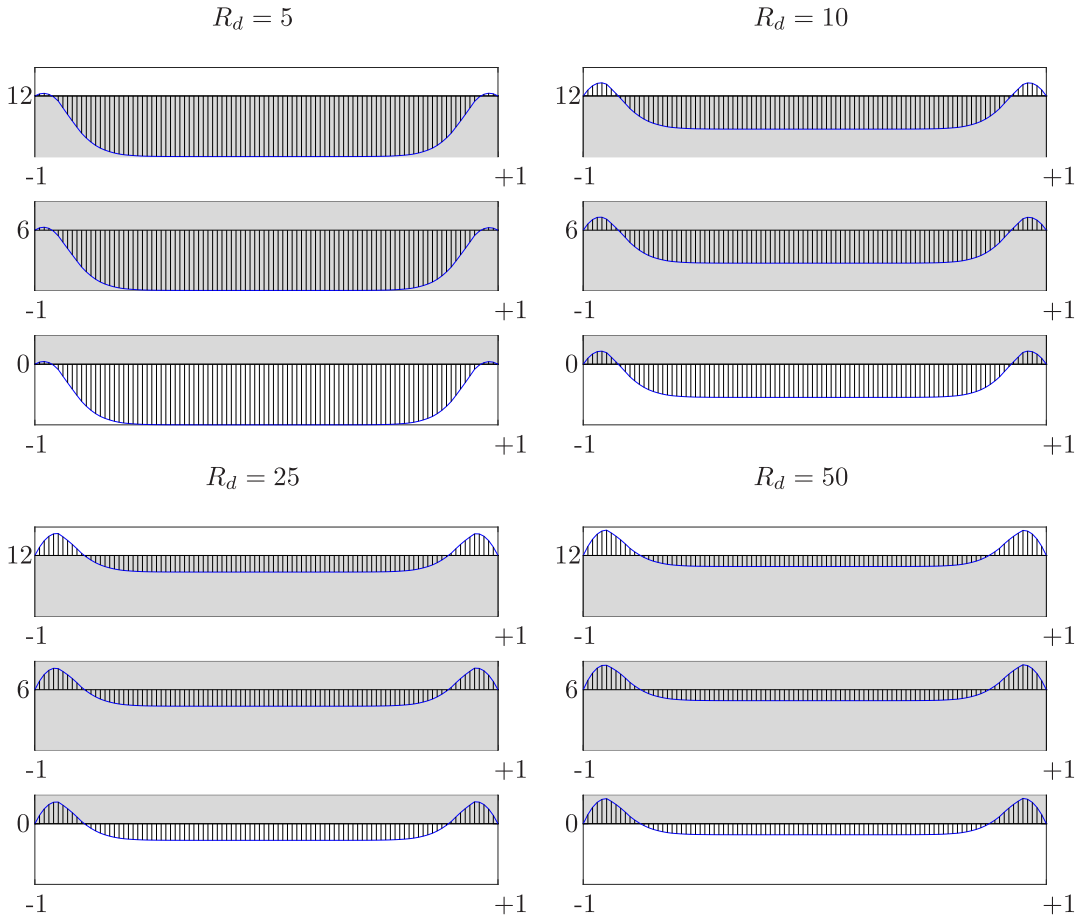

FIGURE 9. Numerical solution for the Stokes-RCR model with implicit coupling. Backflow phenomenon at time $t = 0.5$ for different values of the distal resistance: $R_d = 5$, 10, 25, 50. The velocity field is represented at different altitudes of the tube: $y = 0$ (lower outlet), $y = 6$ and $y = 12$ (upper outlet) all over the width of the tube, *i.e.* $x \in (-1, 1)$.

- The previous simulation with $R_d = 50$ and $\Delta t = 0.1$ has led to the backflow phenomenon. If we now reduce the distal resistance (e.g $R_d = 0.5$) with the same time step $\Delta t = 0.1$, then the backflow is skipped and not observed anymore; if, in turn, we divide the time step (e.g $R_d = 0.5$ with $\Delta t = 0.01$), then the backflow phenomenon is recovered: this illustrates the fact that the backflow is physically relevant and it is numerically captured provided $\Delta t < \tau$.

Now let us deal with the *explicit* scheme. Simulation with $\Delta t = 0.1$ and $R_d = 5$ reveals unphysical oscillations and it is to be noticed that these oscillations do not blow up but rather exponentially grow up in time (in a similar way as what is described in Fig. 5). The oscillations are unphysical as they are directly driven by the time step (flow reversal occurs at each numerical time step). For the same data except the time step, which is now $\Delta t = 0.01$ we observe that the numerical solution exhibits an oscillatory phenomenon (with a characteristic time which is much greater than the time step) along with a backflow phenomenon; moreover the magnitude of the oscillations tends to damp with time, see Figure 11.

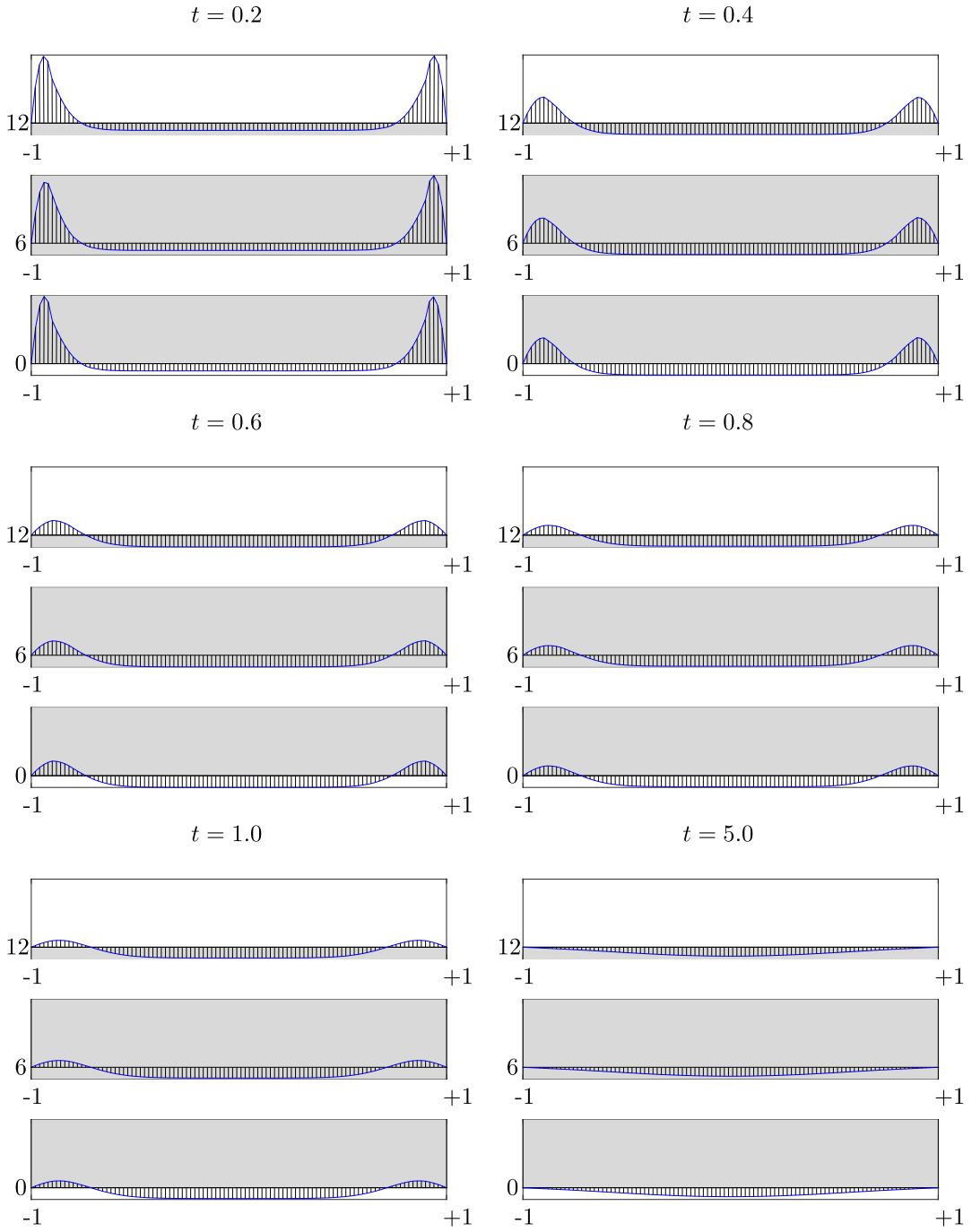

FIGURE 10. Numerical solution for the Stokes-RCR model with implicit coupling. Backflow phenomenon at time $t = 0.2$, 0.4, 0.6, 0.8, 1.0 and relaxation of the phenomenon at a longer time $t = 5$ for $R_d = 50$ and $\Delta t = 0.1$. The velocity field is represented at different altitudes of the tube: $y = 0$ (lower outlet), $y = 6$ and $y = 12$ (upper outlet) all over the width of the tube, *i.e.* $x \in (-1, 1)$.

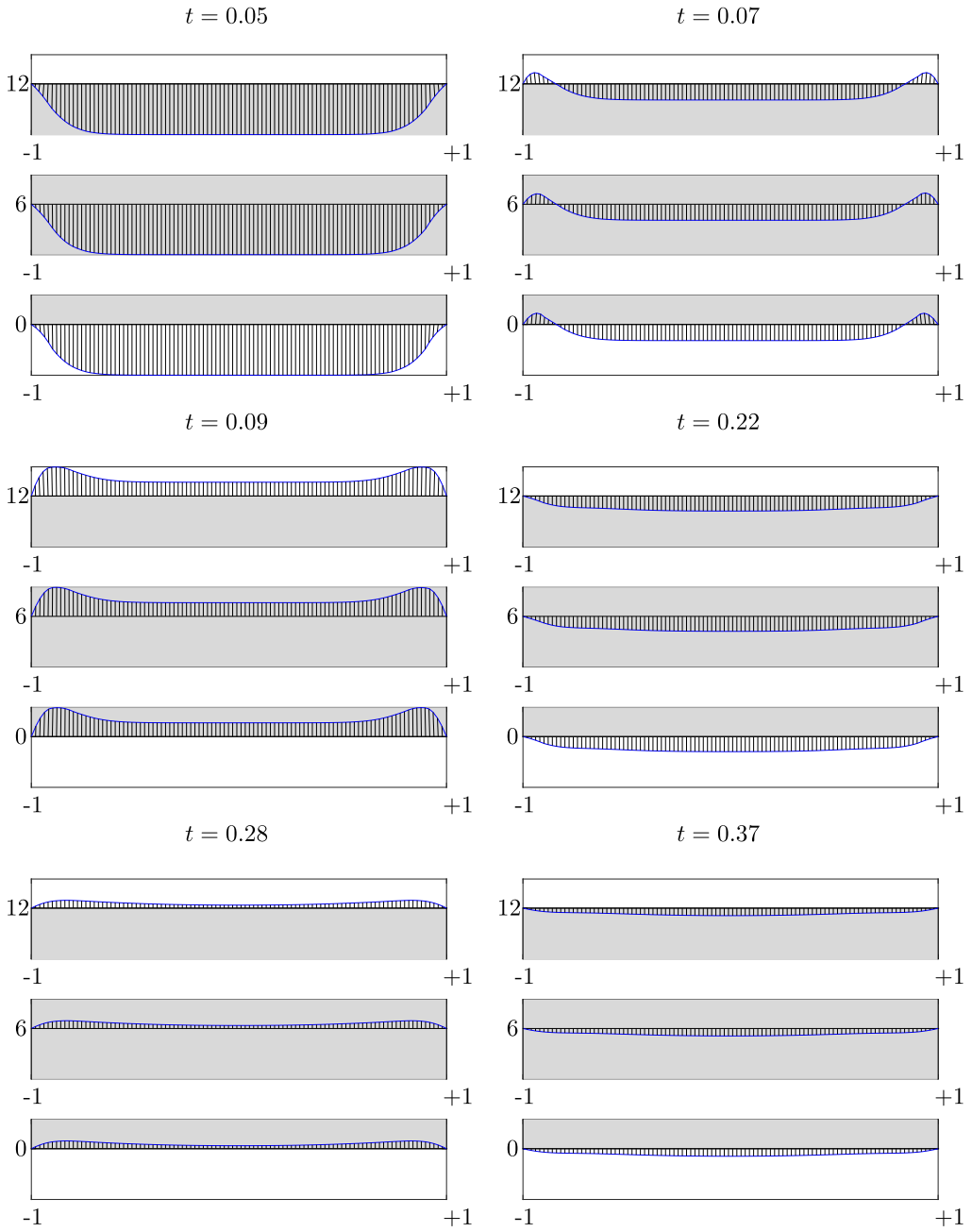

FIGURE 11. Numerical solution for the Stokes-RCR model with explicit coupling at time $t = 0.05$, 0.07, 0.09, 0.22, 0.28, 0.37 (with $R_d = 5$ and $\Delta t = 0.01$). At $t = 0.07$, the backflow phenomenon has appeared; at $t = 0.09$, the compliance of the 0D model has led to a reversal flow; at $t = 0.22$, the flow has gone back to a classical Poiseuille-like situation; at $t = 0.28$, a backflow phenomenon has appeared again leading to a reversal flow (with smaller amplitude than before); at $t = 0.37$, the Poiseuille-like situation is recovered with a velocity magnitude which is smaller than before.

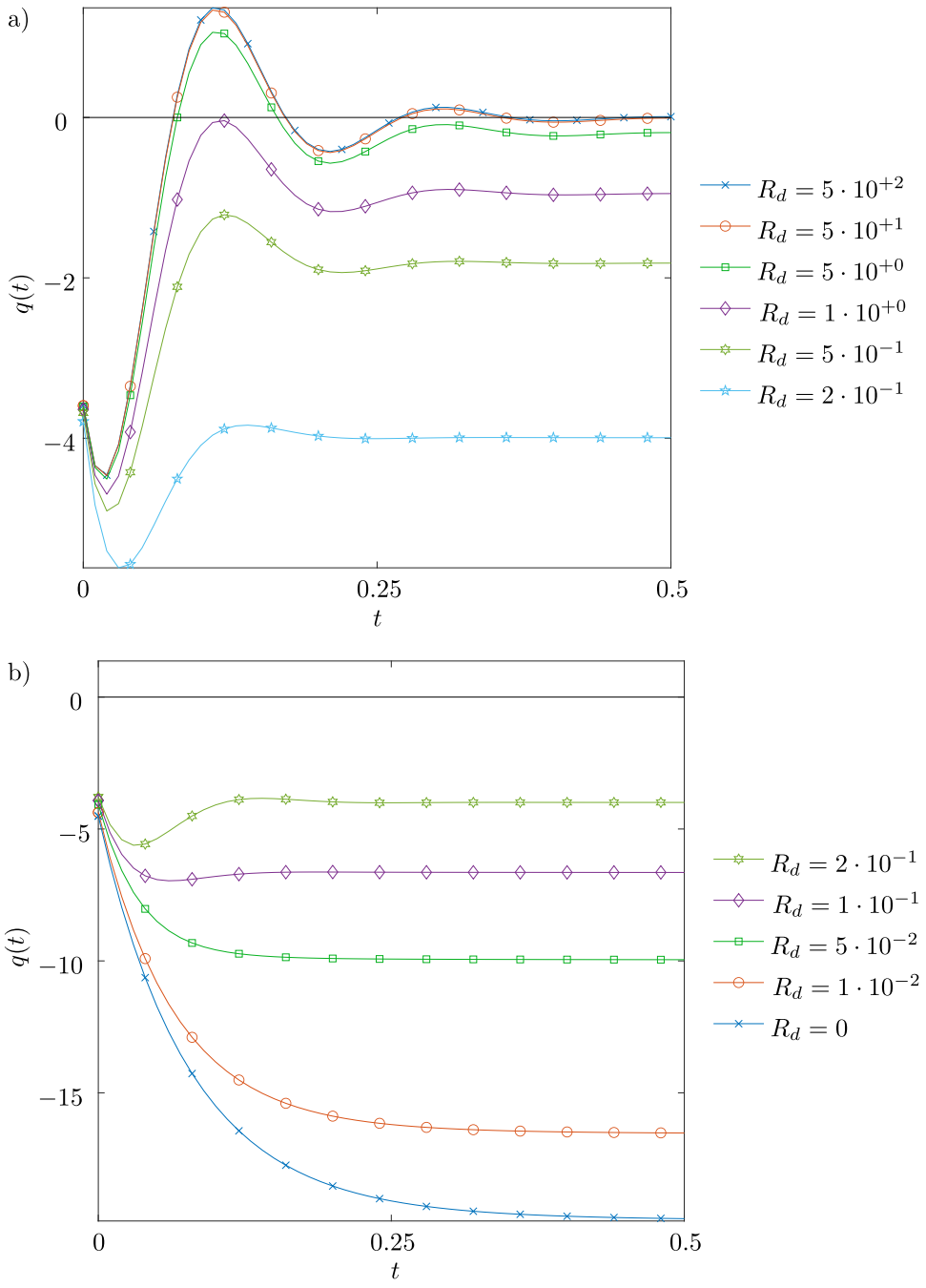

FIGURE 12. Simulation of the Stokes-RCR model with implicit coupling and a time-step $\Delta t = 0.01$. Evolution of the flux at the upper boundary: $t \mapsto q(t) := L_x \int_{\Gamma_0} \mathbf{u}(t, \cdot) \cdot \mathbf{n}$. a) for moderate to large values of R_d; b) for small to moderate values of R_d.

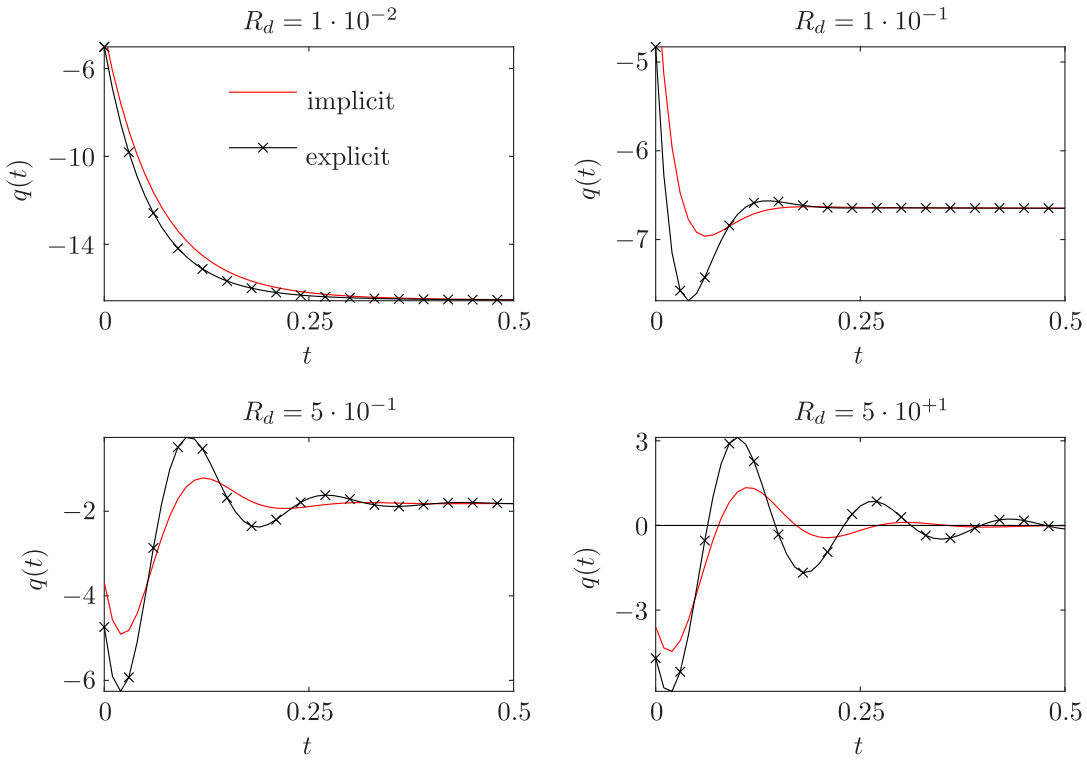

FIGURE 13. Simulation of the Stokes-RCR model with a time-step $\Delta t = 0.01$ with the explicit and implicit schemes. Evolution of the flux at the upper boundary: $t \mapsto q(t) := L_x \int_{\Gamma_0} \mathbf{u}(t,\cdot)\cdot\mathbf{n}$ for different values of the distal resistance R_d.

Now let us investigate the influence of the distal resistance R_d over the magnitude of the backflow phenomenon and the flow reversals. Figure 12, obtained using the *implicit* coupling, shows that the distal resistance has an impact on the phenomenon by focusing on the flux at the inlet with respect to time:

- for small values of R_d (from 0 to 5×10^{-2} in the experiment), no flow reversal is observed as the flux is negative, monotonic in time and converges in time to a stationary value.
- for moderate values of R_d (from 1×10^{-1} to $1 \times 10^{+0}$ in the experiment), the flux is not monotonic: backflow phenomenon is identified even if it is not sufficient to generate flow reversal.
- for large values of R_d (from $5 \times 10^{+0}$ to $5 \times 10^{+2}$ in the experiment), flow reversal is observed as the the flux may become positive. Actually oscillations may occur, with damped amplitude and it is to be noticed that both the (finite) number and the magnitude of flow reversals depend on the value of the distal resistance R_d.

Note that the asymptotic regime ($R_d \to +\infty$) corresponding to the RC model is nearly reached for $R_d = 50$ or 500, as the two situations cannot be really distinguished in Figure 12a: flow reversal occurs around the asymptotic flux whereas, for finite values of R_d, oscillations do not occur when time increases.

Finally let us observe how the scheme (implicit or explicit) captures the backflow phenomenon. Using a small time-step $\Delta t = 0.01$ (that guarantees the stability of the explicit scheme) for both schemes, Figure 13 presents the evolution of the flux at the inlet for different values of R_d with both schemes. It is to be noticed that the backflow phenomenon is overestimated by the explicit scheme.

Concluding remarks can be done from simulations that are not presented here:

- As a concluding observation with respect to the distal resistance for the explicit scheme, using $R_d \in \{0.5 - 500\}$ with $\Delta t = 0.01$ provides stable simulations leading to relaxation that may include both physical oscillations and backflow phenomena whereas $\Delta t = 0.1$ leads to unphysical oscillations with exponential growth. Thus for the RCR model, the distal resistance does not seem to play a role in the stability of the simulation with the explicit scheme.
- As a concluding observation with respect to C for the explicit scheme (in the stable simulations), the higher the compliance value is, the later the backflow phenomenon occurs. Note that this is conform with the fact that, when C increases, the relaxation time $\tau = R_d C$ also increases.

Finally note that test cases where the physical behaviour underlying 0D models has been investigated. In particular some backflows have been obtained. Remark that we we not able to get simulations with backflows which could induce instabilities for the Navier–Stokes system. Yet using stabilization techniques as in [1, 3, 4, 12, 28] may kill these backflow phenomena which are however contained in the 0D model.

6. Conclusion

In this paper we derived energy or stability estimates and existence results for Stokes–Windkessel and Navier–Stokes–Windkessel models, both in the continuous setting and in the semi-discrete one with implicit or explicit coupling. One of the key ingredients in the derivation is the control of an auxiliary volume associated to the 0D model. This property is obtained by taking the velocity field $\mathbf{u}$ as a test function in the variational formulation for both Stokes and Navier–Stokes regimes. Nevertheless in the Navier–Stokes regime, it is not sufficient to obtain a stability estimate; in this case we have to consider a combination of the previous estimate with another one in which $A_{\mu,\alpha}\mathbf{u}$ is used as a test function, where $A_{\mu,\alpha}$ is a new Stokes-like operator adapted to our coupled system. This enables us to control both the convective term and the auxiliary volume.

In particular, we have shown that for the standard Windkessel model used in blood flow modeling, namely the RCR model (for which $\alpha > 0$, $\beta = 0$, $\gamma > 0$ and $0 < \tau < +\infty$), "energy" dissipation holds true and can be also derived when considering the Navier–Stokes system under smallness assumptions on the data. Meanwhile the standard Windkessel model used in airflow modeling (for which $\alpha > 0$, $\beta = 0$, $\gamma > 0$ and $\tau = +\infty$) is not dissipative, leading to restrictive conditions – on the time step, on the data, on the final time – for the stability of the Navier–Stokes system even for the implicit coupling; this echoes the numerical simulations of such coupled problems for which instabilities arise leading to the use of stabilization techniques that make it possible to get away from smallness conditions on the data or, at least, give access to a larger range of data, see [5] where benchmark tests are performed for various stabilization methods. When considering an explicit coupling for the Navier–Stokes system, in both cases (RCR and RC models), "energy" dissipation does not hold anymore; stability estimates are derived but they require the same type of restrictive conditions.

We also paid attention to the dependency on the various physical parameters. Even if some of these constants are not explicit and depend on the geometry (such as the Poincaré constant, for instance) and thus on the considered test case, the derived estimates and their related validity conditions give a good insight into the behaviour of coupled systems according to the underlying fluid involved. For instance increasing the inertance in the 0D model (namely taking greater values for β) which is always treated in an implicit way stabilizes the semi-discretized system for the Stokes regime whereas it leads to a more restrictive smallness condition on the data in the Navier–Stokes regime.

References

[1] G. Arbia, I.E. Vignon-Clementel, T.-Y. Hsia and J.-F. Gerbeau. Modified Navier-Stokes equations for the outflow boundary conditions in hemodynamics. *Eur. J. Mech. B Fluids* **60** (2016) 175–188.

[2] L. Baffico, C. Grandmont and B. Maury. Multiscale modeling of the respiratory tract. *Math. Models Methods Appl. Sci.* **20** (2010) 59–93.

[3] Y. Bazilevs, J.R. Gohean, T.J.R. Hughes, R.D. Moser and Y. Zhang. Patient-specific isogeometric fluid-structure interaction analysis of thoracic aortic blood flow due to implantation of the Jarvik 2000 left ventricular assist device. *Comput. Methods Appl. Mech. Engrg.* **198** (2009) 3534–3550.

[4] C. Bertoglio and A. Caiazzo. A Stokes-residual backflow stabilization method applied to physiological flows. *J. Comput. Phys.* **313** (2016) 260–278.

[5] C. Bertoglio, A. Caiazzo, Y. Bazilevs, M. Braack, M. Esmaily, V. Gravemeier, A. Marsden, O. Pironneau, I.E. Vignon-Clementel and W.A. Wall. Benchmark problems for numerical treatment of backflow at open boundaries. *Int. J. Numer. Meth. Biomed. Engng.* **34** (2017) e2918.

[6] C. Bertoglio, A. Caiazzo and M.A. Fernández. Fractional-step schemes for the coupling of distributed and lumped models in hemodynamics. *SIAM J. Sci. Comput.* **35** (2013) B551–B575.

[7] P.J. Blanco, S. Deparis and A.C.I. Malossi. On the continuity of mean total normal stress in geometrical multiscale cardiovascular problems. *J. Comput. Phys.* **251** (2013) 136–155.

[8] P.J. Blanco, M. Discacciati and A. Quarteroni. Modeling dimensionally-heterogeneous problems: analysis, approximation and applications. *Numer. Math.* **119** (2011) 299–335.

[9] P.J. Blanco, R.A. Feijóo and S.A. Urquiza. A unified variational approach for coupling 3D-1D models and its blood flow applications. *Comput. Methods Appl. Mech. Engrg.* **196** (2007) 4391–4410.

[10] H. Brezis. Analyse fonctionnelle. Collection Mathématiques Appliquées pour la Maîtrise. Masson, Paris (1983).

[11] C.-H. Bruneau and P. Fabrie. Effective downstream boundary conditions for incompressible Navier-Stokes equations. *Int. J. Numer Meth. Fluids* **19** (1994) 693–705.

[12] C.-H. Bruneau and P. Fabrie. New efficient boundary conditions for incompressible Navier-Stokes equations: a well-posedness result. *RAIRO Modél. Math. Anal. Numér.* **30** (1996) 815–840.

[13] A. Comerford, C. Forster and W.A. Wall. Structured tree impedance outflow boundary conditions for 3D lung simulations. *J. Biomech. Eng.* **132** (2010) 081002.

[14] A. Devys, C. Grandmont, B. Grec, B. Maury and D. Yakoubi. Numerical method for the 2D simulation of the respiration. In: *CEMRACS 2008 – Modelling and numerical simulation of complex fluids*. Vol. 28 of *ESAIM Proc.* EDP Sciences, Les Ulis (2009) 162–181.

[15] M. Esmaily Moghadam, Y. Bazilevs, T.-Y. Hsia, I.E. Vignon-Clementel, A.L. Marsden and Modeling of Congenital Hearts Alliance (MOCHA) Investigators. A comparison of outlet boundary treatments for prevention of backflow divergence with relevance to blood flow simulations. *Comput. Mech.* **48** (2011) 277–291.

[16] M. Esmaily Moghadam, F. Migliavacca, I.E. Vignon-Clementel, T.-Y. Hsia, A. Marsden and Modeling of Congenital Hearts Alliance (MOCHA) Investigators. Optimization of shunt placement for the Norwood surgery using multi-domain modeling. *J. Biomech. Eng.* **134** (2012) 051002.

[17] M. Esmaily Moghadam, I.E. Vignon-Clementel, R. Figliola and A.L. Marsden. A modular numerical method for implicit 0D/3D coupling in cardiovascular finite element simulations. *J. Comput. Phys.* **244** (2012) 63–79.

[18] L. Formaggia, A. Moura and F. Nobile. On the stability of the coupling of 3D and 1D fluid-structure interaction models for blood flow simulations. *ESAIM: M2AN* **41** (2007) 743–769.

[19] L. Formaggia, A. Quarteroni and A. Veneziani. Cardiovascular Mathematics Modeling and simulation of the circulatory system. Springer-Verlag, Milan (2009).

[20] L. Formaggia, A. Quarteroni and C. Vergara. On the physical consistency between three-dimensional and one-dimensional models in haemodynamics. *J. Comput. Phys.* **244** (2013) 97–112.

[21] J. Fouchet-Incaux. Artificial boundaries and formulations for the incompressible Navier–Stokes equations: applications to air and blood flows. *SeMA J.* **64** (2014) 1–40.

[22] J. Fouchet-Incaux. *Modélisation, analyse numérique et simulations autour de la respiration*. Ph.D. thesis, Université Paris-Sud (2015).

[23] J. Fouchet-Incaux, C. Grandmont and S. Martin. Numerical stability of coupling schemes in the 3d/0d modelling of airflows and blood flows (2014). Preprint available at https://hal.inria.fr/hal-01095960/document

[24] T. Gengenbach, V. Heuveline and M. J. Krause. Numerical simulation of the human lung: A two-scale approach. *EMCL 45 Preprint Ser.* **29** 2011–11 (2011).

[25] J.-F. Gerbeau, M. Vidrascu and P. Frey. Fluid-structure interaction in blood flows on geometries based on medical imaging. *Comput. Struct.* **83** (2005) 155–165.

[26] C. Grandmont, Y. Maday and B. Maury. A multiscale/multimodel approach of the respiration tree. New trends in continuum mechanics. In: Vol. 3 of *Theta Series in Advanced Mathematics*. Theta, Bucharest (2005) 147–157.

[27] C. Grandmont and A. Soualah. Solutions fortes des équations de Navier-Stokes avec conditions dissipatives naturelles. *ESAIM Proc.* **25** (2008) 1–18.

[28] V. Gravemeier, A. Comerford, L. Yoshihara, M. Ismail and W.A. Wall. A novel formulation for Neumann inflow boundary conditions in biomechanics. *Int. J. Numer. Methods Biomed. Eng.* **28** (2012) 560–573.

[29] J.G. Heywood and R. Rannacher. Finite element approximation of the nonstationary Navier-Stokes problem. I. Regularity of solutions and second-order error estimates for spatial discretization. *SIAM J. Numer. Anal.* **19** (1982) 275–311.

[30] J.G. Heywood and R. Rannacher. Finite-element approximations of the nonstationary Navier–Stokes problem. part IV: Error estimates for second-order time discretization. *SIAM J. Numer. Anal.* **27** (1990) 353–384.

[31] J.G. Heywood, R. Rannacher and S. Turek. Artificial boundaries and flux and pressure conditions for the incompressible Navier–Stokes equations. *Int. J. Numer. Methods Eng.* **22** (1996) 325–352.

[32] M. Ismail, A. Comerford and W.A. Wall. Coupled and reduced dimensional modeling of respiratory mechanics during spontaneous breathing. *Int. J. Numer. Methods Biomed. Eng.* **29** (2013) 1285–1305.

[33] M. Ismail, V. Gravemeier, A. Comerford and W.A. Wall. A stable approach for coupling multidimensional cardiovascular and pulmonary networks based on a novel pressure-flow rate or pressure-only Neumann boundary condition formulation. *Int. J. Numer. Methods Biomed. Eng.* **4** (2014) 447–469.
[34] C. Kleinstreuer, Z. Zhang, Z. Li, W.L. Roberts and C. Rojas. A new methodology for targeting drug-aerosols in the human respiratory system. *Int. J. Heat Mass Transfer* **51** (2008) 5578–5589.
[35] A.P. Kuprat, S. Kabilan, J.P. Carson, R.A. Corley and D.R. Einstein. A bidirectional coupling procedure applied to multiscale respiratory modeling. *J. Comput. Phys.* **244** (2013) 148–167.
[36] J.S. Leiva, P.J. Blanco and G.C. Buscaglia. Iterative strong coupling of dimensionally heterogeneous models. *Internat. J. Numer. Methods Engrg.* **81** (2010) 1558–1580.
[37] J.S. Leiva, P.J. Blanco and G.C. Buscaglia. Partitioned analysis for dimensionally-heterogeneous hydraulic networks. *Multiscale Model. Simul.* **9** (2011) 872–903.
[38] A.C.I. Malossi, P.J. Blanco, P. Crosetto, S. Deparis and A. Quarteroni. Implicit coupling of one-dimensional and three-dimensional blood flow models with compliant vessels. *Multiscale Model. Simul.* **11** (2013) 474–506.
[39] A.C.I. Malossi, P.J. Blanco, S. Deparis and A. Quarteroni. Algorithms for the partitioned solution of weakly coupled fluid models for cardiovascular flows. *Int. J. Numer. Methods Biomed. Eng.* **27** (2011) 2035–2057.
[40] B. Maury. The respiratory system in equations. In: Vol. 7 of *MS&A: Modeling, Simulation and Applications*. Springer-Verlag Italia, Milan (2013).
[41] V. Maz'ya and J. Rossmann. Point estimates for Green's matrix to boundary value problems for second order elliptic systems in a polyhedral cone. *ZAMM: Z. Angew. Math. Mech.* **82** (2002) 291–316.
[42] V. Maz'ya and J. Rossmann. L_p estimates of solutions to mixed boundary value problems for the Stokes system in polyhedral domains. *Math. Nachr.* **280** (2007) 751–793.
[43] J.M. Oakes, A.L. Marsden, C. Grandmont, S.C. Shadden, C. Darquenne and I.E. Vignon-Clementel. Airflow and particle deposition simulations in health and emphysema: From in vivo to in silico animal experiments. *Ann. Biomed. Eng.* **42** (2014) 899–914.
[44] A. Porpora, P. Zunino, C. Vergara and M. Piccinelli. Numerical treatment of boundary conditions to replace lateral branches in hemodynamics. *Int. J. Numer. Methods Biomed. Eng.* **28** (2012) 1165–1183.
[45] A. Quarteroni, S. Ragni and A. Veneziani. Coupling between lumped and distributed models for blood flow problems. *Comput. Visual Sci.* **4** (2001) 111–124.
[46] A. Quarteroni and A. Veneziani. Modeling and simulation of blood flow problems, edited by M.-O. Bristeau, G. Etgen, W. Fitzgibbon, J.-L. Lions, Periaux J. and M.F. Wheeler. In: *Computational Science for the 21st Century*. J. Wiley and Sons (1997) 369–379.
[47] A. Quarteroni and A. Veneziani. Analysis of a geometrical multiscale model based on the coupling of ODEs and PDEs for blood flow simulations. *Multiscale Model. Simul.* **1** (2003) 173–195.
[48] A. Quarteroni, A. Veneziani and C. Vergara. Geometric multiscale modeling of the cardiovascular system, between theory and practice. *Comput. Methods Appl. Mech. Engrg.* **302** (2016) 193–252.
[49] R. Temam. Navier-Stokes equations: theory and numerical analysis, Vol. 2. American Mathematical Society (2001).
[50] A. Veneziani and C. Vergara. Flow rate defective boundary conditions in haemodynamics simulations. *Inter. J. Numer. Methods Fluids* **47** (2005) 803–816.
[51] I.E. Vignon-Clementel, C.A. Figueroa, K.E. Jansen and C.A. Taylor. Outflow boundary conditions for three-dimensional finite element modeling of blood flow and pressure in arteries. *Comput. Methods Appl. Mech. Engrg.* **195** (2006) 3776–3796.
[52] W.A. Wall, L. Wiechert, A. Comerford and S. Rausch. Towards a comprehensive computational model for the respiratory system. *Int. J. Numer. Methods Biomed. Eng.* **26** (2010) 807–827.